

In presenting the dissertation as a partial fulfillment of the requirements for an advanced degree from the Georgia Institute of Technology, I agree that the Library of the Institute shall make it available for inspection and circulation in accordance with its regulations governing materials of this type. I agree that permission to copy from, or to publish from, this dissertation may be granted by the professor under whose direction it was written, or, in his absence, by the Dean of the Graduate Division when such copying or publication is solely for scholarly purposes and does not involve potential financial gain. It is understood that any copying from, or publication of, this dissertation which involves potential financial gain will not be allowed without written permission.

*John M. D.*  
*John M. D.*

3/17/65

b

A STUDY OF THE MECHANISM BY WHICH BIOAEROSOLS  
ARE GENERATED WHEN LIQUIDS CONTAINING  
MICROORGANISMS ARE AERATED

A THESIS

Presented to

The Faculty of the Graduate Division

by

Benjamin Michael Smith

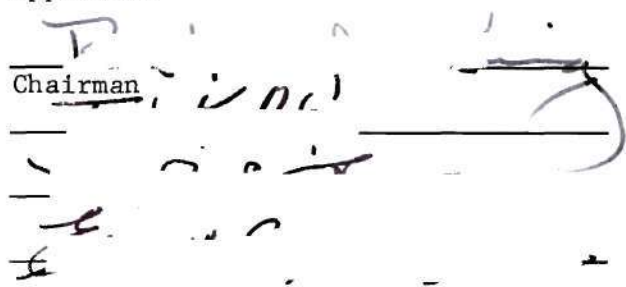
In Partial Fulfillment  
of the Requirements for the Degree  
Doctor of Philosophy  
in the School of Civil Engineering

Georgia Institute of Technology

June, 1968

A STUDY OF THE MECHANISM BY WHICH BIOAEROSOLS  
ARE GENERATED WHEN LIQUIDS CONTAINING  
MICROORGANISMS ARE AERATED

Approved:

  
Chairman

Date approved by Chairman: May 21, 1968

## ACKNOWLEDGEMENTS

My sincere thanks and appreciation are extended to the members of my Reading Committee, Professors Richard King (Chairman), M.R. Carstens, T.W. Kethley, and E.C. Tsivoglou, for their advice, technical assistance, and encouragement during the conduct and presentation of this research. The efforts of other faculty members who rendered assistance are also greatly appreciated.

I thank my wife, Carolyn, for her patience and encouragement and for typing the several drafts of this dissertation.

This study was conducted at the Georgia Institute of Technology in conjunction with "Outside-the-Service" training sponsored by the U.S. Public Health Service.



## TABLE OF CONTENTS

	Page
ACKNOWLEDGEMENTS . . . . .	ii
LIST OF TABLES . . . . .	v
LIST OF FIGURES . . . . .	vii
SUMMARY . . . . .	ix
GLOSSARY OF ABBREVIATIONS . . . . .	xiii
Chapter	
I. INTRODUCTION . . . . .	1
Statement of the Problem	
Background	
Bioaerosols from Bursting Bubbles	
Aerosol Generation by Bursting Bubbles	
II. EXPERIMENTAL EQUIPMENT . . . . .	18
Experimental System	
Conditioning Column Design	
Bubbler Design	
Bioaerosol Sampler	
III. EXPERIMENTAL TECHNIQUES . . . . .	43
Microorganisms	
Bacteriological Assay	
Test Liquid Composition	
Experimental Procedures	
IV. RESULTS AND DISCUSSION . . . . .	53
General	
Bioparticle Size Distribution	
Effect of Spore Concentration on Bioparticle Production	
Initial Droplet Size Distribution	
Effect of Bubble Size on Bioparticle Production	
Effect of Test Liquid Composition on Bioparticle Production	
V. SUMMARY AND CONCLUSIONS . . . . .	93
Conclusion	

## TABLE OF CONTENTS (Continued)

Chapter	Page
VI. RECOMMENDATIONS . . . . .	96
APPENDIX A. BASIC EXPERIMENTAL DATA . . . . .	98
APPENDIX B. EXPERIMENTAL SAMPLE DATA . . . . .	109
APPENDIX C. SUMMARY OF DATA COMPUTATIONS . . . . .	120
APPENDIX D. BACKGROUND SAMPLE DATE . . . . .	131
APPENDIX E. STATISTICAL COMPUTATIONS . . . . .	134
APPENDIX F. MISCELLANEOUS DATA AND COMPUTATIONS . . . . .	145
LITERATURE CITED . . . . .	149
OTHER REFERENCES . . . . .	155
VITA . . . . .	161

## LIST OF TABLES

Table	Page
1. Large Droplets from Air Bubbles Rising in Water at the Rate of 60 Bubbles per Minute and Bursting at the Surface . . . . .	14
2. Small Droplets from Air Bubbles Rising in Water at the Rate of 60 Bubbles per Minute and Bursting at the Surface . . . . .	17
3. Definition of Test Liquid Symbols . . . . .	55
4. Initial Count Median Diameters of Droplets Containing Spores . . . . .	63
5. Experimental vs. Theoretical Droplet Sizes . . . . .	65
6. Comparison Among Observed and Calculated Droplet and Particle Sizes . . . . .	66
7. Effect of Test Liquid on Bioparticle Distribution Characteristics . . . . .	83
8. Comparison of Bioparticle Production Rates . . . . .	92
9. Basic Experimental Data . . . . .	99
10. Experimental Sample Data . . . . .	110
11. Summary of Data Computations . . . . .	121
12. Background Sample Data . . . . .	132
13. Chi Square Verification of Poisson Distribution . . . . .	136
14. Statistical Data: $D_a/D_{a0.5}$ vs. $D_b$ . . . . .	138
15. Analysis of Variance: $D_a/D_{a0.5}$ vs. $D_b$ . . . . .	139
16. Statistical Data: (No. Bioparticles/Bubble)/ (No. Bioparticles/0.5 mm Bubble) vs. $D_b$ . . . . .	140
17. Analysis of Variance: (No. Bioparticles/Bubble)/ (No. Bioparticles/0.5 mm Bubble) vs. $D_b$ . . . . .	141
18. Statistical Data: $\sigma_g/\sigma_{g0.5}$ vs. $D_b$ . . . . .	142

## LIST OF TABLES (Continued)

Table	Page
19. Analysis of Variance: $\sigma_g / \sigma_{g_{0.5}}$ vs. $D_b$ . . . . .	142
20. Analysis of Variance: $\sigma_g / \sigma_{g_{0.5}}$ vs. $D_b$ for $D_b = 1.1$ mm and 0.5 mm . . . . .	143
21. Surface Tension and Viscosity Measurements . . . . .	146
22. Calculation of Initial Droplet Size Distribution . . . . .	147

## LIST OF FIGURES

Figure	Page
1. Mechanism of Bubble Burst at Water Surface . . . . .	10
2. Jet Droplet Distribution Above Water Surface . . . . .	13
3. Flow Diagram - Experimental Bioaerosol System . . . . .	19
4. Schematic Diagram - Experimental Bioaerosol System . . . . .	20
5. Photograph of Experimental Bioaerosol System . . . . .	22
6. Isometric Sketch - Aeration Chamber Details . . . . .	24
7. Photograph of Aeration Chamber . . . . .	25
8. Isometric Sketch - Sampling Mechanism Details . . . . .	27
9. Photograph of Sampling Mechanism . . . . .	28
10. Bubbler Calibration System . . . . .	38
11. Schematic Diagram - Andersen Sampler . . . . .	39
12. Photograph of Andersen Sampler . . . . .	40
13. Total and Regional Deposition of Inhaled Particles in the Human Lung . . . . .	57
14. Bioparticle Production Rate in Relation to Test Liquid Spore Concentration for 0.5 mm Bubbles . . . . .	59
15. Bioparticle Production Rate in Relation to Test Liquid Spore Concentration for 2.2 mm Bubbles . . . . .	60
16. Log Probability Plot of Calculated Initial Droplet Size Distribution for 0.5, 0.9, 1.1, and 2.2 mm Bubbles . . . . .	68
17. Bioparticle Size Frequency Curves for 0.5, 0.9, 1.1, 2.2, 3.7, and 5.7 mm Bubbles . . . . .	70
18. Log Probability Plot of Bioparticle Size Distributions for 0.5, 0.9, 1.1, 2.2, 3.7, and 5.7 mm Bubbles . . . . .	71

## LIST OF FIGURES (Continued)

Figure		Page
19.	Ratio of Mean Bioparticle Size to Mean Size for 0.5 mm Bubbles versus Bubble Diameter . . . . .	72
20.	Ratio of Bioparticle Production Rate to Production Rate for 0.5 mm Bubbles versus Bubble Diameter . . . . .	74
21.	Ratio of Geometric Standard Deviation of Bioparticle Size Distribution to Geometric Standard Deviation for 0.5 mm Bubbles versus Bubble Diameter . . . . .	75
22.	Bioparticle Production per Liter of Aeration Air in Relation to Bubble Diameter . . . . .	77
23.	Log Probability Plot of Bioparticle Size Distributions for DM and G-150 Test Liquids and 0.9 mm Bubbles . . . . .	79
24.	Log Probability Plot of Bioparticle Size Distributions for DM and S-400 Test Liquids and 0.8 mm Bubbles . . . . .	80
25.	Log Probability Plot of Bioparticle Size Distributions for DM and G-150 Test Liquids and 3.7 mm Bubbles . . . . .	81
26.	Log Probability Plot of Bioparticle Size Distributions for DM and S-400 Test Liquids and 3.7 mm Bubbles . . . . .	82
27.	Bioparticle Production Rate for Various Test Liquids in Relation to Bubble Diameter . . . . .	88
28.	Comparison of Bioparticle Production Rates for Various Test Liquids and Bubble Sizes in Relation to Production Rates for DM Test Liquid . . . . .	90



## SUMMARY

The bursting of gas bubbles at a liquid surface creates liquid droplets which are ejected into the space above the liquid. If the liquid contains microorganisms, it is possible that the ejected droplets will also contain microorganisms. The purpose of this research was to determine if bioaerosols are created when bubbles burst at the surface of liquids containing microorganisms, and if so, to relate the mechanism of droplet production to the production of bioaerosols (aerosols in which the disperse phase contains microorganisms). The findings of this study should be particularly applicable to the evaluation and control of the possible hazard of airborne infection which might be associated with the treatment of domestic wastes by aeration.

The basic components of the experimental equipment used in this study were: (1) a dilution air chamber to provide control of temperature, relative humidity, and bioaerosol content of the major fraction of air used to condition and transport bioparticles (aerosol particles containing microorganisms); (2) an aeration chamber in which liquids containing microorganisms were aerated; (3) a dilution and conditioning column for conditioning and transporting the bioparticles; and (4) a semiautomatic sampling mechanism utilizing an Andersen-type bioaerosol sampler. In order to provide a means of effectively studying the aerosolization of microorganisms by bursting bubbles, spores of Bacillus subtilis var. niger, were employed as tracers. Several types of liquids were used to study the effects of liquid composition on bioaerosol production and to

demonstrate production mechanisms. Seven different liquids in varying concentrations were employed: (1) inert liquids, demineralized water and hydrophilic sols of gelatin and peptone employed for their solids concentrations; (2) electrolyte solutions of sodium chloride and dibasic potassium phosphate to facilitate reduction of spore surface charges and thus enhance spore association with the air-liquid interface; and (3) organic "collector" solutions, octanoic acid and dipentylamine, to render spore surfaces more hydrophobic and allow greater association of spores with the air-liquid interface.

The major goals of this study were achieved. Bioaerosols were found to be produced by the bursting of 0.5 mm to 5.7 mm diameter bubbles (the range of bubble sizes studied) at the surface of liquids containing tracer spores. Jet droplets formed by the collapse of bubble craters were observed to provide a mode of bioaerosol generation from bubbles of 0.5 mm to approximately 1.0 mm diameter. Film droplets created by the rupture of bubble films were found to supply a means of bioaerosol generation from bubbles of approximately 1.0 mm to 5.7 mm diameter.

Other findings of importance were also made. Bioparticle production rate varied in direct proportion to the spore concentration of the test liquid to a concentration at which each droplet contained at least one spore. With further increases in spore concentration, production rate remained essentially constant. For a mean spore concentration comparable with microorganism concentrations found in domestic wastes, mean bioparticle production was observed to range from a maximum of approximately three million bioparticles per liter of aeration air for 0.5 mm diameter bubbles to a minimum of approximately five thousand per liter



for 5.7 mm diameter bubbles. Bioparticle size distribution in air varied with the spore concentration of the liquid. Increases in spore concentration resulted in decreased mean bioparticle size and increased dispersion of size distribution as the chance for smaller and smaller droplets to contain at least one spore increased.

Bioparticle size distribution characteristics were found to vary with bubble size. Median bioparticle size increased with bubble size to a maximum for bubbles of approximately 0.9 mm diameter and then decreased to a minimum for 5.7 mm bubbles. Dispersion of size distribution increased with bubble size from a minimum for bubbles of 0.5 mm diameter to a maximum for 1.1 mm bubbles and then decreased to an intermediate value for 5.7 mm bubbles. Bioparticle production per bubble burst increased with bubble size.

Bioparticle production varied with the composition of the liquid being aerated. Bioparticle production was from two to five times greater for gelatin and peptone sols than for demineralized water. Although essentially the same for bubbles of from 0.5 to 1.0 mm diameter, production for larger bubbles ranged up to three times greater for sodium chloride, dibasic potassium phosphate, octanoic acid, and dipentylamine solutions than for demineralized water. Water sols of gelatin and peptone affected the size distribution of bioparticles over the entire range of bubble sizes studied by increasing the median bioparticle size without significantly affecting dispersion. Water solutions of sodium chloride and dibasic potassium phosphate and collector solutions of octanoic acid and dipentylamine affected bioparticle size distribution by increasing the median size without significantly affecting dispersion for bubbles up to

approximately one mm diameter. However, the electrolyte and collector solutions were observed to decrease median bioparticle size and increase dispersion for bubbles larger than approximately one mm diameter.

The median bioparticle sizes produced under the conditions of this study were generally small enough to remain airborne and to permit lung penetration with the larger sizes capable of being retained in the upper regions of the human respiratory system.

It was concluded within the limits of this research that: (1) bioaerosols are produced by bubbles bursting at the surface of liquids containing microorganisms; (2) that both the rupture of bubble films as well as the subsequent collapse of bubble craters provide mechanisms for the production of bioaerosols; (3) that bubble size and the composition and microorganism concentration of the liquid being aerated significantly affect bioparticle size distribution and production rate; and (4) that aeration of contaminated wastes and other liquids could be responsible for the production of hazardous aerosols.

## GLOSSARY OF ABBREVIATIONS

A	-	DM plus octanoic acid
CMD	-	Count median diameter
C <sub>s</sub>	-	Test liquid solids concentration
C <sub>sp</sub>	-	Test liquid spore concentration
D <sub>a</sub>	-	Bioparticle CMD (Bioparticle = particle containing one or more microorganisms)
D <sub>d</sub>	-	Droplet CMD
D <sub>d<sub>o</sub></sub>	-	Initial Droplet CMD
D <sub>p</sub>	-	Pipe diameter
DA	-	DM plus dipentylamine
DF	-	Degrees of freedom
DM	-	Demineralized water
E	-	Experiment
F	-	Variance ratio
G	-	DM plus gelatin
g	-	Gravitational constant
H	-	Vertical distance
H <sub>T</sub>	-	Vertical distance traveled in time t
H <sub>T<sub>e</sub></sub>	-	Vertical distance traveled in time t <sub>e</sub>
k	-	Coefficient of diffusion of water vapor in air
MS	-	Mean square (variance estimate)
N	-	Number of items, number of bioparticles
N <sub>m</sub>	-	Number of items in a particular sample
P	-	DM plus peptone

$\Delta p$	-	Pressure differential
PH	-	DM plus dibasic potassium phosphate
R	-	Radius
r	-	Depth of bubble base below liquid surface
S	-	DM plus sodium chloride
SS	-	Sum of squares
T	-	$\Sigma x$ , the grand total
$T_m$	-	$\Sigma x_m$ , the total for a particular sample
t	-	Time
$t_e$	-	Time required for complete evaporation
$\bar{V}$	-	Mean velocity
$V_a$	-	Velocity of air
$V_c$	-	Centerline velocity
$V_{sp}$	-	Volume of one spore
x	-	Any item
$\gamma$	-	Surface tension
$\mu$	-	Micron
$\mu_a$	-	Dynamic viscosity of air
$\nu_a$	-	Kinematic viscosity of air
$\omega$	-	Fall velocity or terminal settling velocity
$\pi$	-	Constant = 3.14159
$\rho_a$	-	Density of air
$\rho_d$	-	Density of droplet
$\rho_e$	-	Vapor density of the environment
$\rho_s$	-	Vapor density of water at the surface of a droplet
$\rho_w$	-	Density of liquid
$\sigma_g$	-	Geometric standard deviation

## CHAPTER I

### INTRODUCTION

#### Statement of the Problem

When gas bubbles burst at a liquid surface, droplets of the liquid are ejected into the space above the liquid. If the liquid contains microorganisms, the possibility exists that the ejected liquid droplets will also contain microorganisms. Specifically, the purpose of this investigation is to determine if indeed bioaerosols are created when bubbles burst at the surface of liquids containing microorganisms, and if so, to relate the mechanism of droplet generation to the generation of bioaerosols (aerosols in which the disperse phase contains microorganisms). The findings of this research should be particularly applicable to the evaluation and control of the possible hazard of airborne infection which might be associated with the treatment of domestic wastes by aeration. The findings should also be of interest to laboratories and industries which aerate liquids containing microorganisms in their experiments or processes and to those concerned with contamination control and the microbiology of the air.

#### Background

There is an increasing interest in bioaerosols and the role which they may play in disease transmission. Airborne infection as an important concept of disease transmission existed as early as 1600 B.C. (1) and was promoted by Hippocrates, the "Father of Medicine," with his writing that



men were attacked by fevers when they inhaled air containing hostile pollutants (2). Miasmas, meaning noxious vapors, and malaria, meaning bad air, illustrate this point. Once almost universally accepted, the concept of airborne infection was then rejected. With the establishment of the germ theory of disease, and particularly with the work of Lister, the concept of contact infection became dominant (3). Airborne infection was discarded as a significant mode of spread of disease for almost fifty years. In the past thirty years, however, a resurgence of interest and a more sophisticated scientific evaluation of evidence have lead to the establishment of a sound theory of airborne infection of great importance to public health.

In the 1930's William F. Wells (1,4-11) an engineer at Harvard University, introduced the modern concept of airborne infection (3) both with laboratory demonstrations of the survival of bioaerosols in exposure chambers and with practical field trials of ultraviolet irradiation for the control of measles in schools. Wells (5) demonstrated that a variety of pathogens, including streptococci, pneumococci, and influenza virus, could be atomized into a chamber and remain viable as bioaerosols for hours or even days. Additional importance is placed on the theory of airborne infection by the fact that there is now a series of diseases in which the airborne route of infection has been well substantiated (12). These include: psittacosis, histoplasmosis, coccidioidomycosis, inhalation anthrax, brucellosis, and primary pulmonary tuberculosis (3). Subsequent studies have shown that the number of bioaerosols necessary to infect through the alveoli of the human lung is very small, often ten organisms or less (3,12). Steere, in the Handbook of Laboratory Safety (13),

points out that inhalation of infectious aerosols is by far the most frequent mode of laboratory infection.

Toward the end of the nineteenth century, Miguel observed up to 900 bacteria per cubic meter of air in Paris sewers; however, he found like numbers in the air of city streets (14). Similar counts were obtained by Carnelly and Haldame (2) and Horrocks (15) in London sewers. Winslow was concerned about the possible transmission of enteric fever through the inhalation of sewer gas (16). He showed that the splashing of sewage liberated organisms into the air where they could be borne considerable distances, but concluded that infection from sewer gas was remote.

In 1934, Fair and Wells (17) made the first study of bacteria emitted to the atmosphere by sewage disposal processes. Their very brief study concluded that the atmosphere can be contaminated by those sewage treatment processes in which small droplets are discharged into the air and evaporate. Apparently, the next actual study of bacterial air pollution from waste treatment plants was conducted in 1958. In that year, Albrecht (18) performed a limited study of bacterial air pollution in the vicinity of a trickling filter sewage treatment plant. He concluded that significant bacterial air contamination can occur through the agitation of sewage.

Prior to Albrecht's studies, Jensen (19) in 1954 had observed the presence and survival of the tubercle bacillus in the liquid phases of sewage treatment processes. From these results, he surmised that there is a real danger of tuberculosis infection, especially to operating and supervisory personnel, from droplets injected into the air by activated

sludge units, by trickling filters, by spray irrigation with sewage effluent, and by wind action on wastewater surfaces. Added importance is placed on Jensen's observations by Langmuir's (3) statements that undoubtedly the most important naturally acquired airborne infection is primarily pulmonary tuberculosis, that the pathogenesis of the disease clearly points to the alveolus of the human lung as the portal of entry, and that the only reasonable route whereby the tubercle bacillus can reach the alveolus is by inhalation.

Several investigators have shown that many human pathogens may be present in various stages of the sewage treatment process (20,21). Because known pathogens may be present in the wastes being treated, some initial attempts have been made to determine whether the incidence of infection among sewage plant workers is increased, but have resulted in findings that were inconclusive because of incomplete employee medical records (22).

In 1955, Woodcock (23) proposed that aerosols arising from bursting bubbles in contaminated waters might carry microorganisms into the air. Employing a wind tunnel in a laboratory study, Higgins (24) in 1964 observed bioaerosols in the air following the aeration of contaminated water; however, he found that recovery of viable airborne organisms was highly dependent upon species and the composition of the aeration liquid. He did not, however, attempt to define the mechanism(s) by which the bioaerosols were produced or the basis of the effect of liquid composition on the production of the bioaerosols.

The latest study was a field study by Ledbetter and Randall (25-28) in 1965. They obtained significant data on the emission of bacteria to



the atmosphere from an activated sludge sewage treatment unit. They found only about eight bacteria per cubic foot upwind of the unit but up to 1170 per cubic foot on the downwind side. Despite a rapid die-off of bacteria during the first three seconds of being airborne, the investigators observed the increase in bacterial population to persist for a considerable time and distance from the unit.

Bacteria of the family Enterobacteriaceae, including species of known pathogenicity, were observed in large numbers. Klebsiella, proven pathogens of the respiratory tract, were the most numerous of the Enterobacteriaceae. The members of the family that are potential pathogens of the respiratory tract were found to be far more numerous than the enteric pathogens. About 70 per cent of the viable bacteria found 20 feet downwind of the unit were of a size that permits lung penetration. Ledbetter and Randall concluded that a definite possibility of airborne infection from activated sludge units exists.

#### Bioaerosols from Bursting Bubbles

With the notable exception of Higgins' work (24), no controlled, laboratory study of the ejection of bacteria into the air by the aeration of liquids containing suspended bacteria has been made.

In his study, Higgins utilized a wind tunnel fitted with an aeration tank containing fritted glass bubblers. Samples of bioaerosols were collected by means of slit (29-30) and Andersen (30-31) samplers. Only non-pathogenic microorganisms were used in the study. They included strains of Escherichia coli, Escherichia freundii, Escherichia aurescens, Aerobacter aerogenes, Serratia marcescens, Streptococcus durans, and Streptococcus salivarius, and Bacillus subtilis spores.

Higgins' conclusions concerning mechanisms of bioaerosol generation by aeration were simply that "The production of viable aerosols by bursting bubbles is highly dependent upon species... and composition of the aeration liquid" and that "Calculated original diameters of droplets produced by bursting bubbles indicated that many particles were too small to have originated through the jet-droplet mechanism".

No attempt was made by Higgins to define accurately the influence of bubble size on the aerosolization of bacteria. The system which he used was designed only to produce a range of bubble sizes that might be expected to be present in an activated sludge unit. He noted that the generation of bioaerosols was found to be highly dependent upon the concentration of organisms in the test liquid. Data indicated that bioaerosols generated were proportional to organism concentration in the liquid. It should be noted that the organism concentration in the aeration liquid was in every reported case less than the number necessary to allow at least one organism to be contained in each droplet of the median size produced during aeration.

The production of bioaerosols was found to depend a great deal upon the composition of the aeration liquid. The only conjecture concerning composition was that production seemed to depend upon bubble stability; however, no conclusion was offered.

The primary result of Higgins' limited data on droplet sizes produced by aeration of liquids concerned original droplet sizes. Assuming complete evaporation of water and unit density of solids, he observed the measured diameter of droplet residues to vary with the solids content of

the liquids indicating that the size distribution of droplets before evaporation was reasonably independent of type of liquid. Count median diameters of evaporated droplets were found to vary from about 4.6 to 5.6 microns. Calculated median diameters of droplets before evaporation were observed to vary from about 70 to 110 microns.

#### Aerosol Generation by Bursting Bubbles

As very little work has been concerned with the aerosolization of microorganisms by aeration, an understanding of related studies which have been performed on the ejection of liquid droplets into the air by aeration is appropriate.

Almost as soon as it leaves the place in a liquid where it is formed, a bubble reaches a terminal velocity (32). When the bubble reaches the liquid surface, it usually rebounds back and forth with decreasing amplitude until it comes to rest with its upper part projecting above the surface in the form of a hemispherical dome (33). The walls of the dome become extremely thin at the apex but thicken toward the base. The time-lag between the bubble reaching the surface and its bursting depends upon the state of the interface. If stabilizing agents are present at the interface, the bubble may remain on the surface for an appreciable time. Even in pure water, the time-lag at the surface before film rupture is of the order of one-hundredth of a second (33).

As long as the bubble is intact, the pressure inside is greater than the surrounding pressure by an amount  $\Delta p$  depending upon the curvature of the bubble film and the surface tension,  $\gamma$ , of the liquid (34).

$$\Delta p = 2\gamma[(1/R_1) + (1/R_2)] \quad (1)$$



where  $R_1$  and  $R_2$  are the principal radii of curvature. As the upper dome is nearly a hemisphere,  $R_1 \cong R_2$  and :

$$\Delta p \cong 4\gamma/R_1. \quad (2)$$

The liquid level at the base of the bubble may be depressed below the liquid surface by an amount  $r$  given approximately by the equation:

$$r \cong (2\gamma/g\rho_w)[(2/R_1) - (1/R_3)] \quad (3)$$

Where:

$g$  = gravitational constant

$\rho_w$  = density of liquid

$R_3$  = radius of curvature of crater.

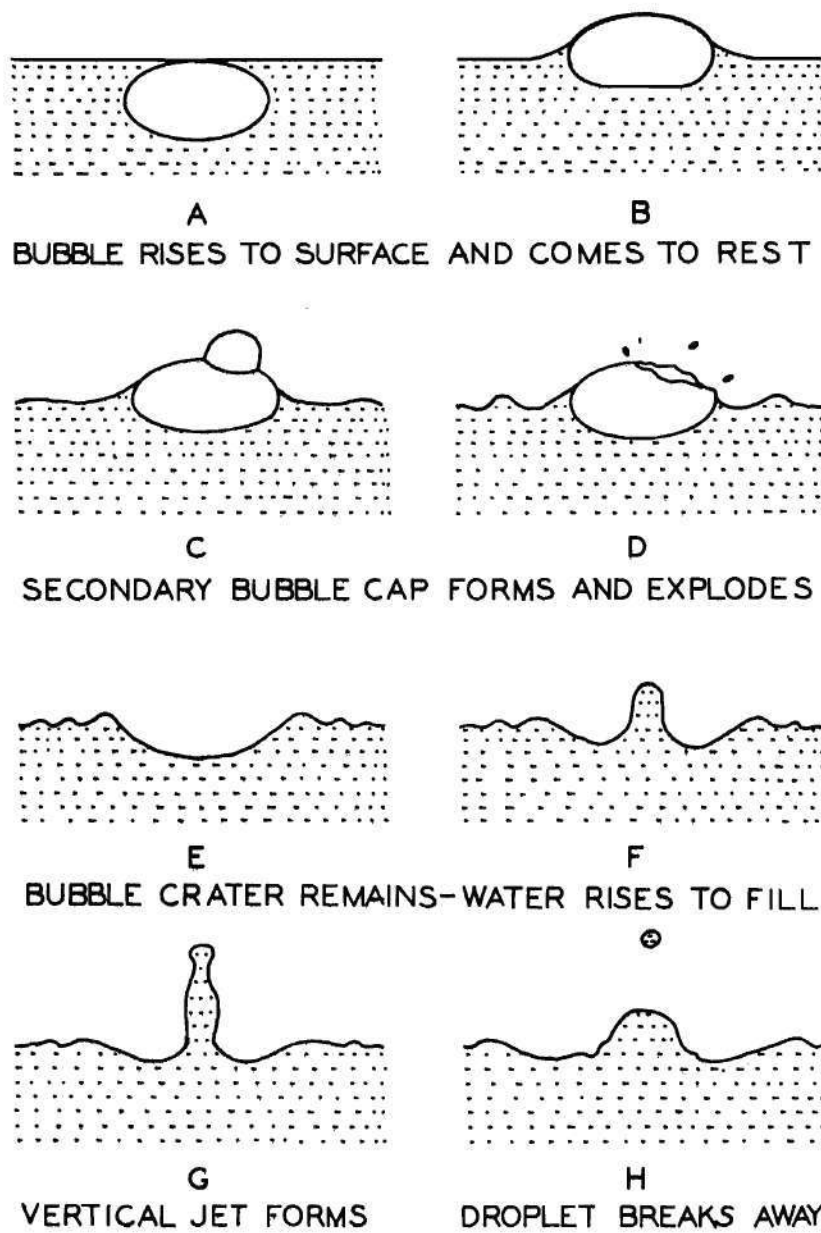
As may be seen from the above, the bursting of a bubble at a liquid surface occurs with the release of energy which may be sufficient to create and eject liquid droplets into the surrounding air.

In water for example, a bubble which has a hemispherical dome with a radius of about 1.0 mm will release about 9.1 ergs of surface free energy from the rupture and withdrawal of its film. The minimum energy required to create a droplet 100  $\mu$  diameter is approximately 0.09 erg, discounting viscous forces. The  $\Delta p$  of such a bubble is about 2880 dynes/cm<sup>2</sup>, sufficient to impart an initial velocity of about 880 cm/sec to a droplet 100  $\mu$  diameter assuming the mean pressure force acts over a time interval of approximately 10 microseconds. Assuming a hemispherical bubble crater of radius 1.0 mm in water, an impulse force of about 314 dynes is

available for the creation of a jet and jet droplets. It is, therefore, important to consider by what mechanism the bubble breaks up and the origin of any droplets which may be formed.

In separate investigations, Kientzler, et al. (35) and Newitt, et al. (33) in 1954 applied high-speed photographic techniques to observe the bursting of bubbles in water. Kientzler's studies were an effort to determine the origin of sea-salt condensation nuclei found throughout the earth's atmosphere and which give rise to cloud formation. Facy (36,37) in 1951 had suggested that the rupturing of bubble films on the ocean surface might produce droplets which upon evaporation would produce such sea-salt nuclei. Stuhlman (32) in 1932 had previously observed that the bursting of bubbles in water produced water jets similar to "Worthington's Splashes" (38-40), which subsequently broke into small droplets. Kientzler proved photographically that jets are produced when small bubbles (0.2 to 1.8 mm diameter) burst at the surface of fresh and sea water. He showed that such jets give rise to droplets that are ejected vertically upward to heights large compared to the bubble size. The size of the droplets were of the order of one-tenth of the size bubble producing them. He concluded that the energy associated with the jet formation and break-up is principally derived from the collapse of the bubble cavity after the initial film rupture. Kientzler observed no droplets being formed from the ruptures bubble film of the bubbles he studied.

Newitt (33) photographed the bursting of bubbles of a somewhat larger size (3.1 to 5.3 mm diameter). He observed the burst mechanism to be as follows (see Figure 1). The bubble, Figure 1 (a) comes to rest at the liquid surface and forms a hemispherical dome, Figure 1 (b).



REF. (33)

Figure 1. Mechanism of Bubble Burst at Water Surface

Its internal pressure produces a depression of the air-liquid interface. Liquid drains from the dome until the upper part is so weakened that the internal pressure causes the formation of a secondary cap (c). This cap subsequently explodes, (d), and under certain circumstances gives rise to droplets of a few microns in diameter. These droplets are carried away by the rush of gas issuing from the perforated dome. The results of these events are a system of standing waves and a well defined crater, (e), at the interface. As the crater fills in, the momentum of the inflowing liquid produces a jet, (f), which rises vertically and in certain instances detaches one or more comparatively large drops, (g), (h), from its apex. The jet then retracts and the surface of the liquid returns to rest.

As the liquid jet approaches its maximum height, it forms an unstable column (32). As early as 1873, Plateau (41) had demonstrated that a liquid cylinder is not a figure of stability if its length exceeds  $\pi$  times its diameter, i.e., its circumference. Lord Rayleigh (42) observed this length to be about 4.5 times the diameter of the jet. Under these conditions, the detached masses can reform into droplets which have less surface area than the liquid cylinder from which they came (43). The most likely droplet diameter can be computed to be slightly less than twice the diameter of the jet (43). For low-viscosity, high-interfacial tension liquids, interfacial tension forces alone account for such jet break-up (43).

Worthington and Cole (39) were first to observe the liquid jet. They, in 1897, photographed jets and jet droplets produced by the collapse of surface cavities created in liquids as a result of objects being dropped into the liquids. Stuhlman (32) in 1932 investigated the number and ejection heights of jet droplets created by the collapse of a bubble cavity.



His bubbles ranged in size from 0.3 to 3.6 mm in diameter. He observed that as many as seven droplets are produced by bubbles of about 0.75 mm in diameter bursting at the surface of freshly-surfaced water. Figure 2 shows the distribution of jet-droplets observed by Stuhlman. As may be seen, droplets were found to be projected as high as 14 cm into the air by the bursting of 1.2 mm bubbles. For bubble diameters greater than 2.4 mm, the ejection of droplets was not of sufficient regularity to warrant quantitative interpretation. Benzene, with a lower surface tension, projected droplets only about one-half as high as did water and produced a maximum of only four droplets. Stuhlman also observed that the jet-droplet process is greatly affected by the presence of surface films or contamination.

The observations of Newitt, et al. (33) are presented in Table 1. From the tabulated results it may be seen that in all cases the droplet diameter decreases nearly linearly and the number of droplets increases with decreasing bubble diameter. Furthermore, both diameter and number decrease with rising temperature, and the number of droplets produced by large bubbles decrease markedly as the temperature is raised. At the lower temperatures, a relatively longer jet is formed than at higher temperatures. This is a result of the initial resistance to break-up at the higher viscosity. Thus, there is a longer time for a drop to detach before the jet is drawn back to the surface. This tendency for drop formation is further aided by the higher surface tension.

In general, over the bubble range 3.1 to 5.3 mm diameter, less than one droplet per bubble is produced. As the bubble diameter is reduced, its internal pressure rises and the energy available for jet and



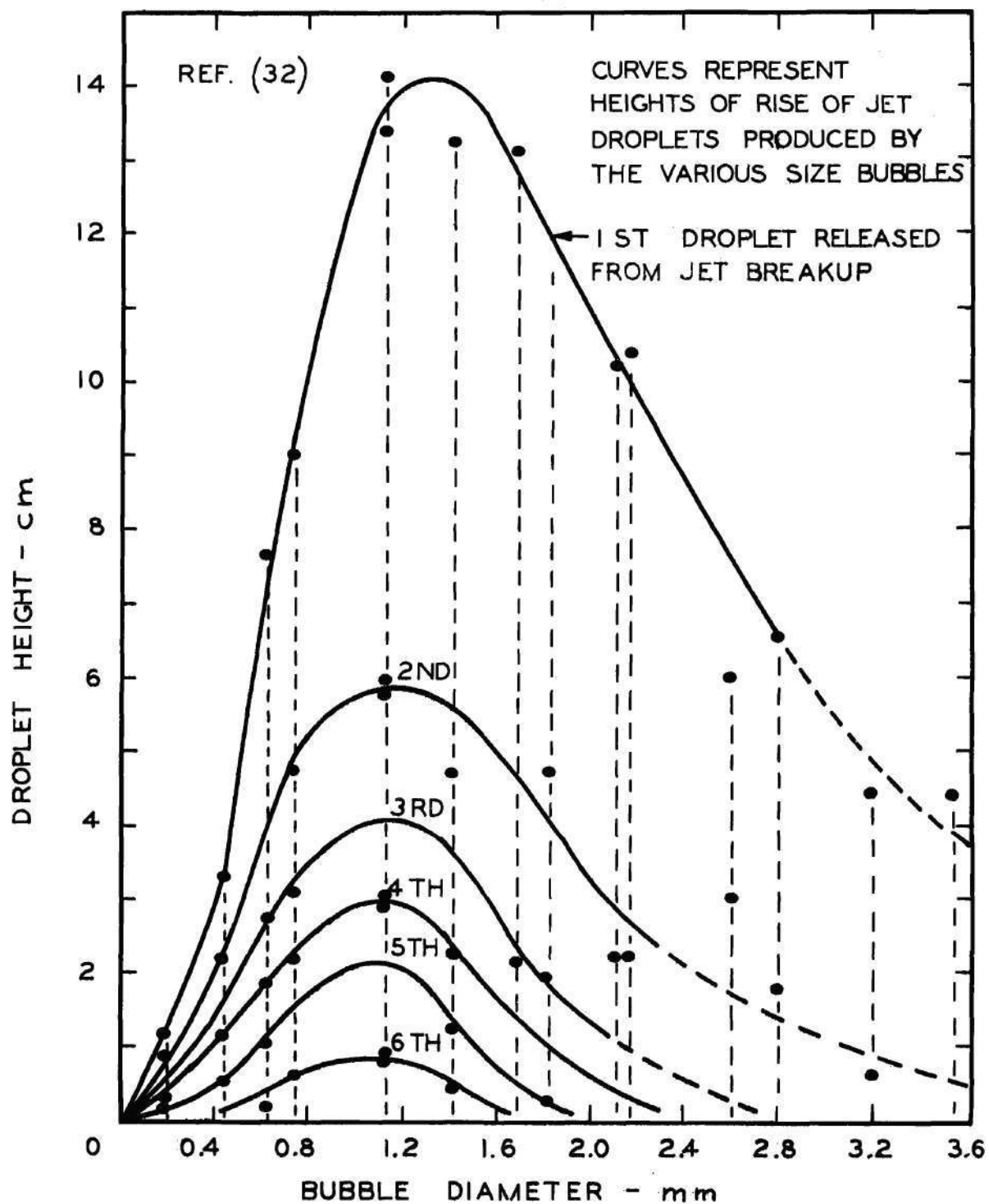


Figure 2. Jet Droplet Distribution Above Water Surface

Table 1. Large Droplets from Air Bubbles Rising in Water  
at the Rate of 60 Bubbles per Minute and  
Bursting at the Surface (33)

Bubble diameter (mm)	Height above Surface (cm)	Sauter mean Diameter*			No. of drops/min.		
		(microns)					
		25°C	35°C	45°C	25°C	35°C	45°C
5.30	0.64	1000	989	905	10.75	6.30	2.60
	1.91	965	955	879	5.72	2.53	1.09
	3.17	949	899	840	2.50	1.07	0.44
	4.44	858	831	790	0.68	0.42	0.14
	5.71	788	750	720	0.17	0.07	
4.65	0.64	920	915	860	25.80	16.00	9.80
	1.91	905	890	838	21.00	11.60	7.00
	3.17	865	845	803	15.00	7.50	4.50
	4.44	815	793	760	8.25	3.50	2.04
	5.71	755	735	707	2.90	0.90	0.25
4.10	0.64	870	855	830	35.80	25.80	17.30
	1.91	847	830	805	32.00	20.50	13.80
	3.17	815	795	775	26.30	15.00	9.45
	4.44	775	760	731	19.20	9.50	5.10
	5.71	725	710	670	10.75	3.60	1.60
3.60	0.64	805	799	775	46.40	35.00	24.80
	1.91	790	775	758	43.00	30.50	20.95
	3.17	762	751	730	37.60	24.80	16.30
	4.44	735	710	695	29.80	17.50	10.00
	5.71	690	665	644	18.70	9.90	4.70
3.11	0.64	740	728	725	58.60	45.00	37.40
	1.91	730	712	710	56.00	41.70	33.00
	3.17	710	693	688	50.80	36.60	27.40
	4.44	693	663	660	43.00	27.50	18.30
	5.71	650	630	613	28.00	18.00	11.00

$$* \text{Sauter mean diameter} = \frac{\sum (\Delta \text{no. droplets}) (\text{droplet dia.})^3}{\sum (\Delta \text{no. droplets}) (\text{droplet dia.})^2}$$

droplet formation increases. Stuhlman (32), as discussed above, observed more than one droplet per bubble burst for bubbles less than about two mm diameter.

Plateau (41) demonstrated that the break-up of a liquid cylinder results in the formation of much smaller satellite droplets. Kientzler, et al. (35) photographically demonstrated the production of such droplets from the break-up of a liquid jet. They also observed larger droplets to reduce their mass upon rebound from the liquid surface.

Kientzler, et al. (35) observed that bubbles larger than about two mm in diameter produce droplets smaller than those occurring from jet break-up. Plateau (41) had proposed in the nineteenth century that the rupture of bubble films creates ligaments which subsequently break into droplets.

The work of Dombrowski and Frazer (44) affords strong evidence that a thin liquid film such as a bubble film breaks up by the initial formation of a number of perforations which subsequently expand to give a lace-like structure. The liquid ligaments so formed are unstable and break into small drops of varying size.

Moore and Mason (45) in 1954 determined that droplets smaller than the comparatively large spray droplets produced by disruption of a liquid jet are produced by disintegration of bubble films. They found in their experiments that the great majority of droplets formed by film rupture had diameters between 5 and 30 microns. Larger bubbles tended to produce larger numbers of rather smaller droplets. In addition to droplets of greater than ten microns in diameter, Mason, in a later study (46), demonstrated droplets of less than ten microns using a cloud chamber technique.

He determined jet droplets produced by bubbles of from 0.3 to 4.3 mm in diameter to have diameters of roughly 15 per cent of the bubble size. However, as many as 200 droplets per bubble burst were demonstrated to have diameters ranging from 0.4 to 1.0 micron in diameter.

Newitt, et al. (33) also observed film droplets to be produced from water by bubbles of three to five mm diameter. Their observations are presented in Table 2. An inspection of the tabulated data reveals a decrease in mean droplet diameter with increasing bubble diameter according to a power function of the bubble diameter and with increasing temperature by a linear relationship. The number of droplets is shown to increase with bubble diameter. Although as many as ten droplets per bubble burst were observed, most remained very near the water surface.

Table 2. Small Droplets from Air Bubbles Rising in Water  
at the Rate of 60 Bubbles per Minute and  
Bursting at the Surface (33)

Bubble diameter (mm)	Height above Surface (cm)	Sauter mean diameter (microns)			No. of drops/min.		
		25°C	35°C	45°C	25°C	35°C	45°C
5.30	0.64	22	20	18	718	490	260
	1.91	32	28	24	24.3	20.7	17.5
	3.17	41	37	33	17.8	16.3	14.7
	4.44	54	54	45	14.7	13.3	12.2
4.65	0.65	26	24	22	306	260	122
	1.91	39	36	34	19.3	15.9	13.7
	3.17	54	55	50	12.7	11.6	11.3
	4.44	70	67	63	10.1	10.3	10.2
4.10	0.64	34	32	30	201	170	77.1
	1.91	51	49	45	14.8	12.5	10.8
	3.17	68	65	58	9.8	8.8	9.1
	4.44	92	87	81	7.7	8.7	8.3
3.60	0.64	45	42	40	120	90.0	49.0
	1.91	61	67	63	11.7	10.3	8.5
	3.17	92	85	83	7.5	7.5	7.7
	4.44	108	109	105	6.0	6.5	7.0
3.11	0.64	58	56	57	93.8	76	41
	1.91	87	80	80	8.8	8.1	7.4
	3.17	118	112	109	6.2	6.1	6.7
	4.44	133	130	129	4.9	5.5	6.3



## CHAPTER II

### EXPERIMENTAL EQUIPMENT

#### Experimental System

The experimental equipment was assembled in the Air Pollution Laboratory of the School of Civil Engineering at the Georgia Institute of Technology. Figure 3 presents a flow diagram of the experimental system used in this research. The equipment is schematically described in Figure 4. The basic components of the system were (1) a dilution air conditioning chamber (A), (See Figure 4), (2) an aeration chamber (B), (3) a bioaerosol dilution and conditioning column (C), and (4) a sampling mechanism (D).

Dilution air entered the system through the dilution air conditioning chamber (A). The chamber volume was about 1.2 cubic meters and contained two dehumidifiers\* (E) for humidity control and a water cooler radiator (F) for temperature control. The water cooler\*\* (G) was equipped with a thermostat and a pump to circulate cooling water through the radiator.

Dilution air was withdrawn from the conditioning chamber through four high efficiency aerosol filters\*\*\* (H) for removal of foreign matter, including microorganisms, from the dilution air. The air could then flow directly to the dilution air manifold (Q), (See also Figure 5) or be

---

\*Sears Roebuck Co. and GMC Frigidaire.

\*\*Copeland Refrigeration Corp., Sidney, Ohio.

\*\*\*Super-Micro-Toxicol, American Optical Co., Safety Products Division.

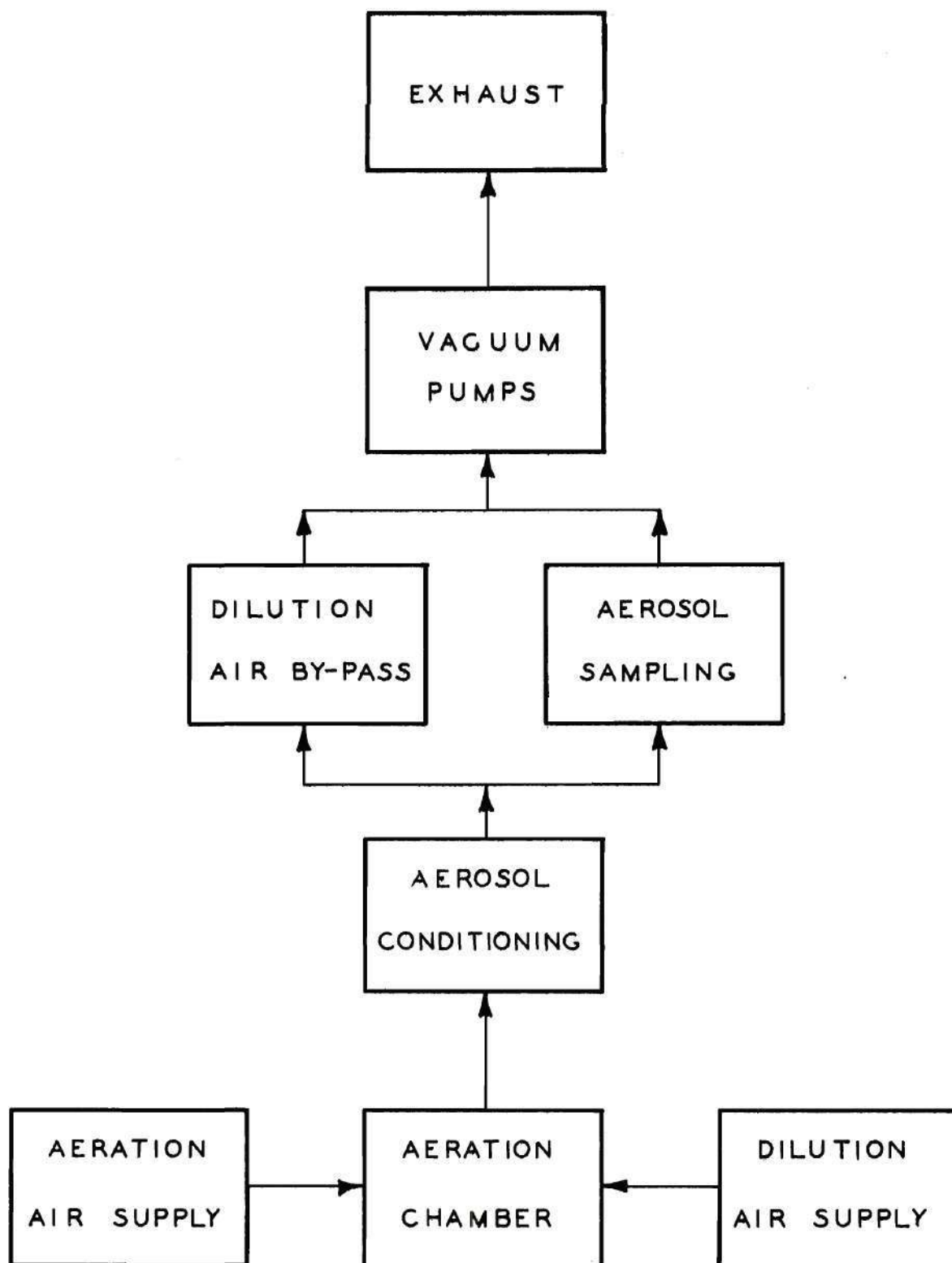


Figure 3. Flow Diagram-Experimental Bioaerosol System

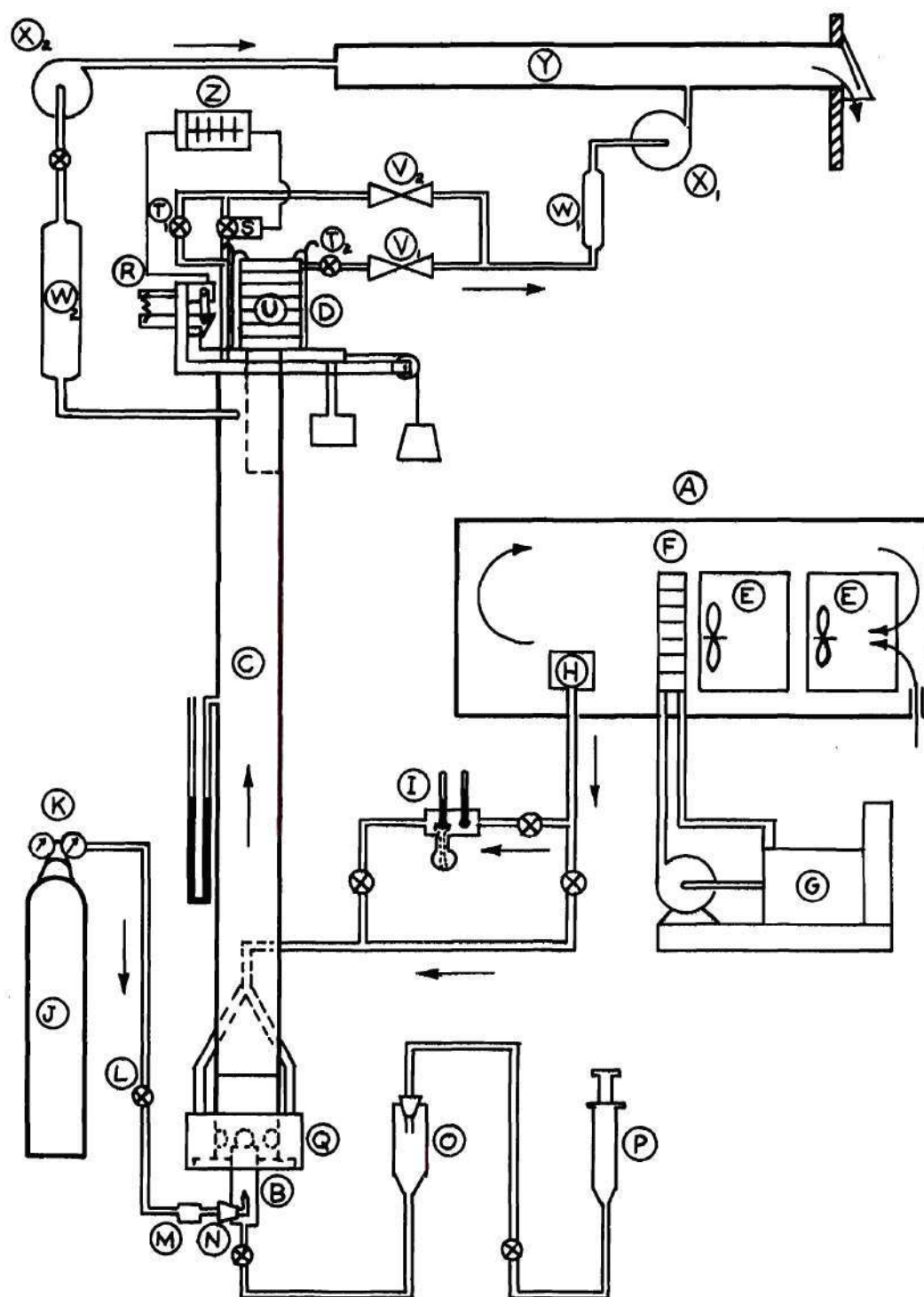


Figure 4. Schematic Diagram-Experimental Bioaerosol System



Figure 4. Schematic Diagram-Experimental Bioaerosol System

Legend

- (A) Dilution air conditioning chamber for temperature and humidity control.
- (B) Aeration chamber for containing test liquid with microorganisms.
- (C) Vertical bioaerosol dilution and conditioning column.
- (D) Semiautomatic sample charger.
- (E) Dehumidifiers for humidity control.
- (F) Water cooler radiator for temperature control.
- (G) Water cooler with thermostat.
- (H) High efficiency aerosol filters.
- (I) Wet bulb-dry bulb psychrometers for relative humidity determinations.
- (J) Compressed air supply for aerator.
- (K) Compressed air pressure regulator.
- (L) Micro-needle valve for control of air to aerator.
- (M) Micro-pore filter to remove foreign matter from aerator air.
- (N) Single orifice aerator.
- (O) Hypodermic syringe for liquid media handling.
- (P) Liquid media reservoir.
- (Q) Dilution air manifold.
- (R) Solenoid latch to release semiautomatic sample changer.
- (S) Solenoid by-pass air valve.
- (T) Manual by-pass air valve.
- (U) Bioaerosol sampler.
- (V) Air flow regulator.
- (W) Air flow meter.
- (X) Vacuum pump.
- (Y) Exhaust manifold.
- (Z) Timer for controlling sample changer solenoid latch and solenoid valve.

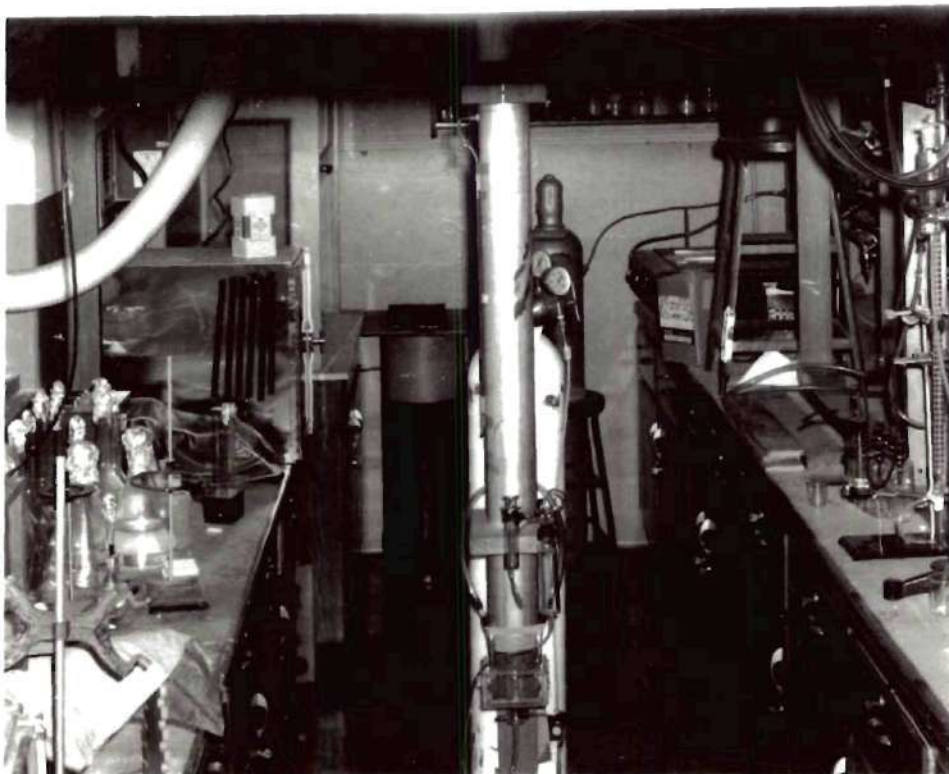
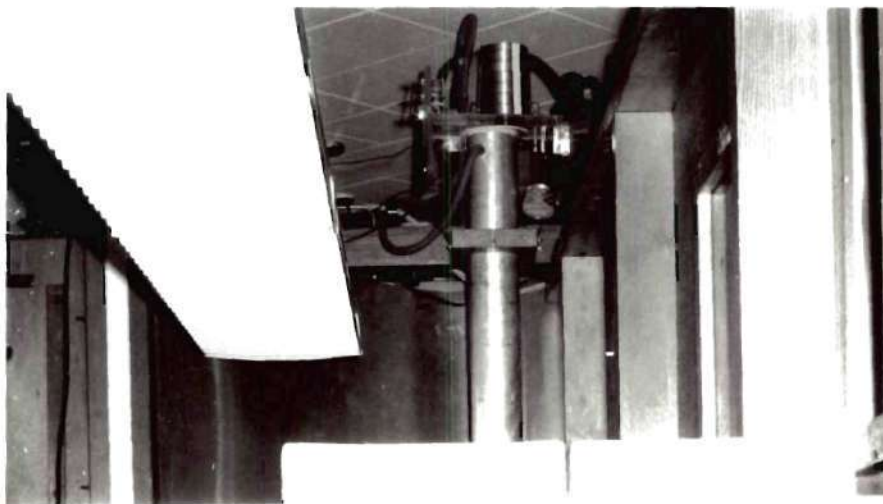


Figure 5. Photograph of Experimental  
Bioaerosol System

by-passed through a wet bulb - dry bulb psychrometer (I) for relative humidity measurement. From the dilution air manifold (Q), the air flowed through ten entrance ports into the vertical bioaerosol dilution and conditioning column (C). The entrance ports were covered with 100 mesh sieve wire to prevent short-circuiting and allow uniform, turbulent air flow into the column.

The conditioning column (C) was fabricated from 10.16-cm inside diameter polished aluminum electrical conduit with 6.4-mm thick walls. The column was 259 cm long (measured from the top edge of the aeration chamber (B) to the bottom surface of the sample changer (D) ). Both the sieve wire and the column were grounded to prevent the buildup of charges on them and thereby attract the aerosols being transported by the column.

Air for the bubbling system was supplied from a compressed air cylinder (J). Air pressure was regulated to and maintained at 1.5 Kg per square cm by a pressure regulator valve\* (K). Air flow was regulated by a micro-needle valve\*\* (L). The regulated air was then filtered through a micro-pore membrane filter\*\*\* (M) before it was delivered to the bubbler (N). Details on the fabrication and calibration of the bubbler is presented in a subsequent section. Bubbles were generated by the bubbler (N) submerged in liquid in the aeration tank (B). A detailed sketch of the aeration tank and appurtenances is presented in Figure 6.

The test liquid handling system consisted of a reservoir (O) for containing the liquid and a hypodermic syringe (P) for filling and emptying the aeration tank.

---

\*AIRCO, New York, New York.

\*\*NUPRO, Model B-4M, Cleveland, Ohio.

\*\*\*Millipore type HA, 0.45 micron.



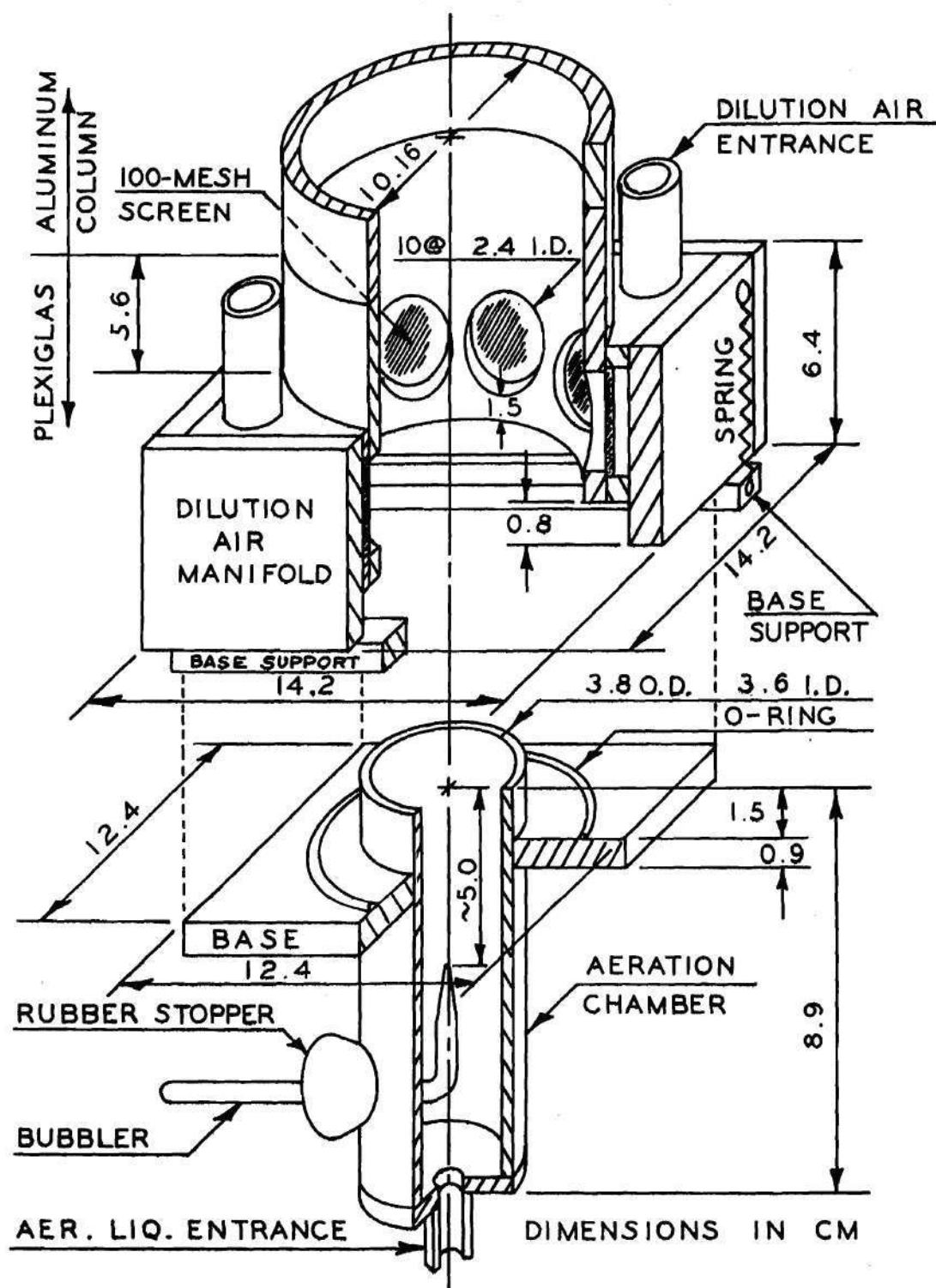


Figure 6. Isometric Sketch-Aeration Chamber Details

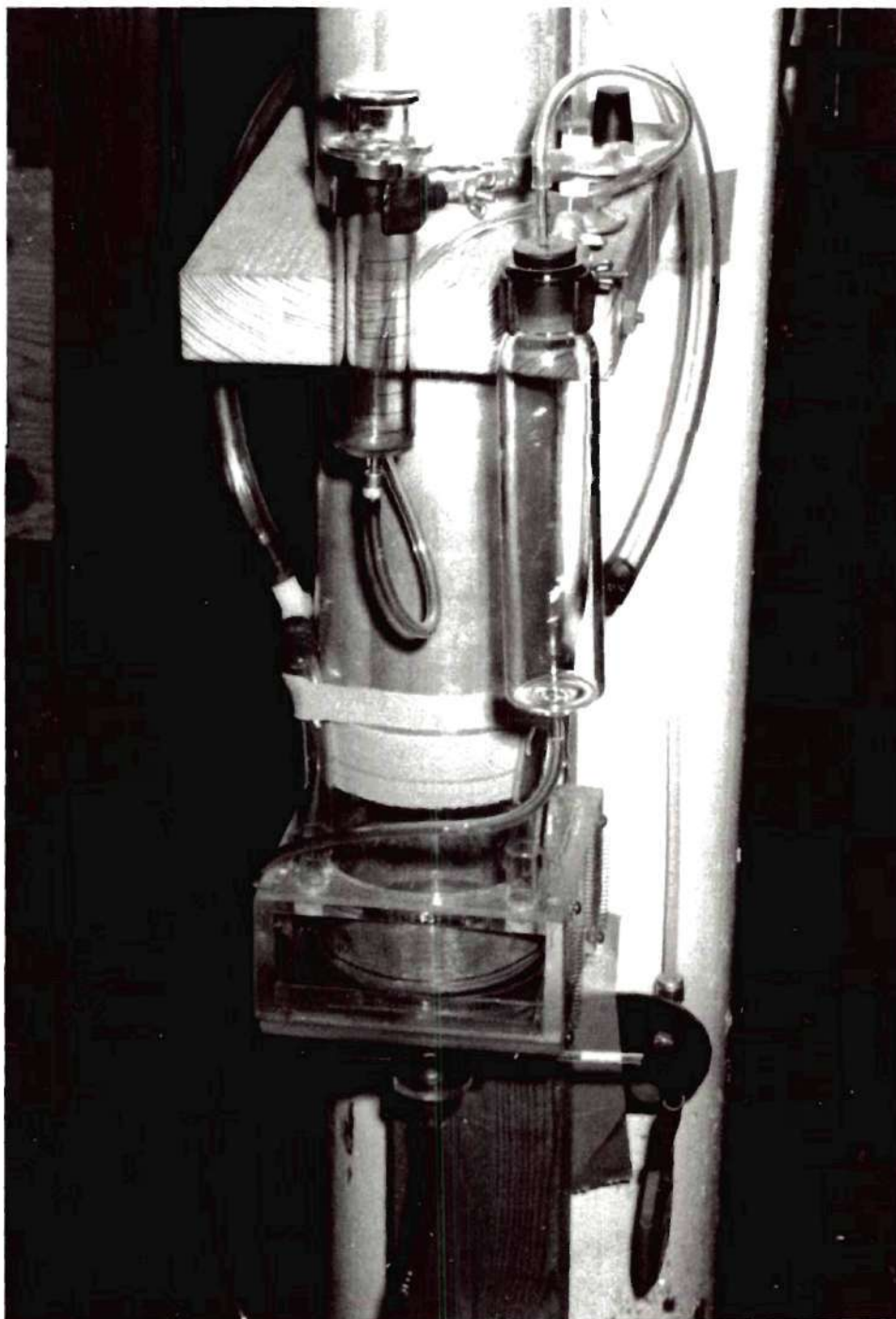


Figure 7. Photograph of Aeration Chamber



Undisturbed sampling was accomplished by means of a pie-shaped sampling port with a cross-sectional area equal to one-fifth of the total cross-sectional area of the dilution column. The semi-automatic sample changer mechanism (D) is presented in Figures 8 and 9. It consisted of a base plate upon which a slide was allowed to move back and forth. The slide was lubricated with petroleum jelly. The bioaerosol sampler was positioned over a circular hole in the slide. The hole in the slide could subsequently be positioned over the pie-shaped sampling port and the slide held in position by a solenoid\* operated trip-latch (R). A 3 Kg counterweight attached to the slide moved the sampler from its position over the sampling port when the trip-latch was released by the solenoid (R).

An air flow of 28.4 liters of air per minute as required by the sampler was pulled through the sampler by a vacuum pump\*\* (X-1). This flow rate was maintained by a critical orifice (V-1) and monitored by a calibrated rotameter\*\*\* (W-1). The rotameters used in this system were calibrated by means of a wet test meter\*\*\*\*. The remaining 113.6 liters of air per minute (four-fifths of the total air flow through the column) was provided by two vacuum pumps\*\*\*\*\* (X-2) and monitored by a rotameter\*\*\*\*\* (W-2).

When the sampler was removed by the counterweight from over the sampling port, it was automatically positioned over a by-pass which

---

\*Guardian Type 16-INT, Santurce, Puerto Rico.

\*\*Gast Model 0321, Gast Manufacturing Corp., Benton Harbor, Mass.

\*\*\*Fisher and Porter Model T7 1104/1-100, Hatboro, Pennsylvania.

\*\*\*\*Precision Scientific Model 63111, Chicago, Illinois.

\*\*\*\*\*GE Model 5KH32EG, Fort Wayne, Indiana.

Gast Model 0440V105, Gast Manufacturing Corp., Benton Harbor, Mass.

\*\*\*\*\*Fisher and Porter Model FP-3/4-21-G110/8-, Hatboro, Pennsylvania.

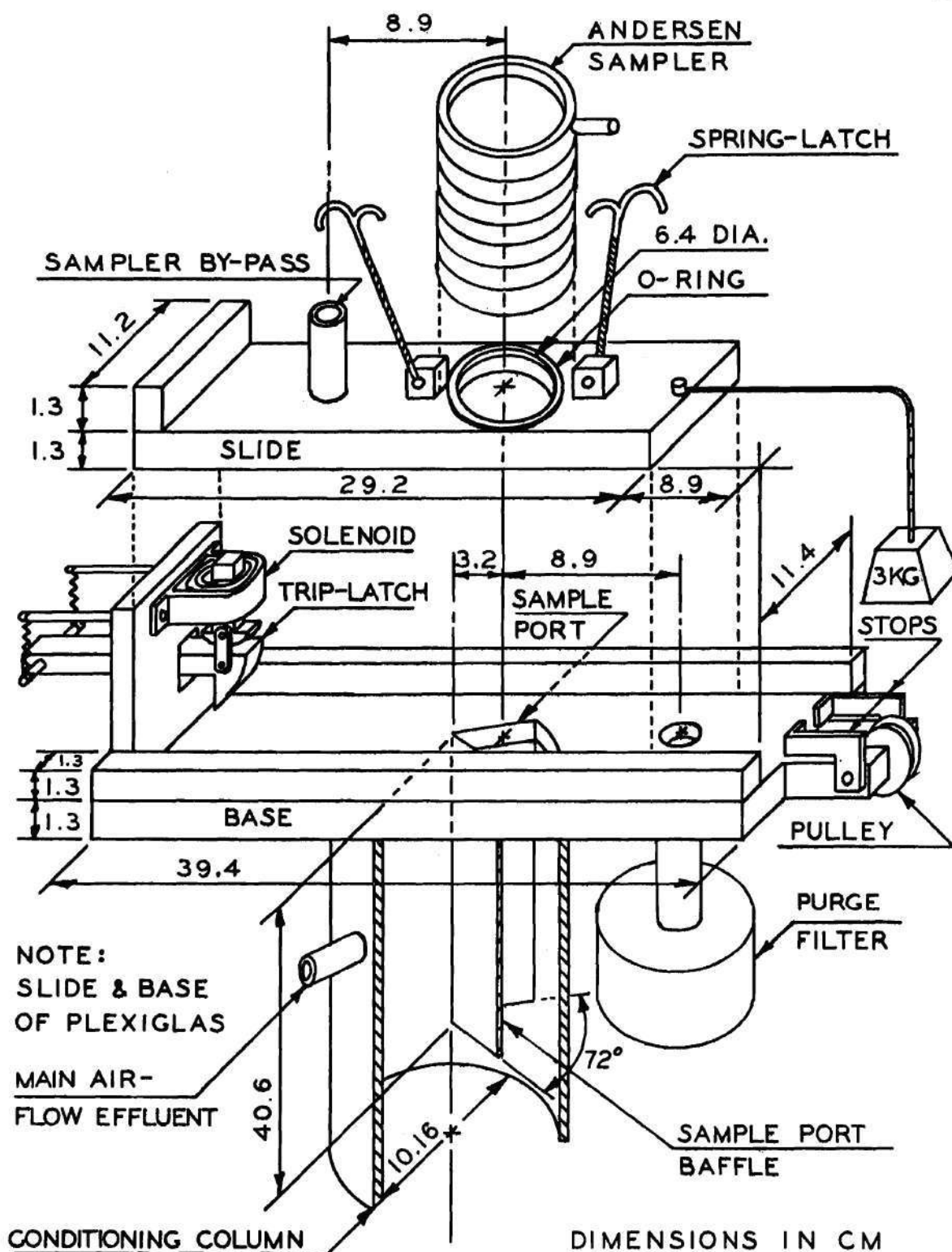


Figure 8. Isometric Sketch-Sampling Mechanism Details

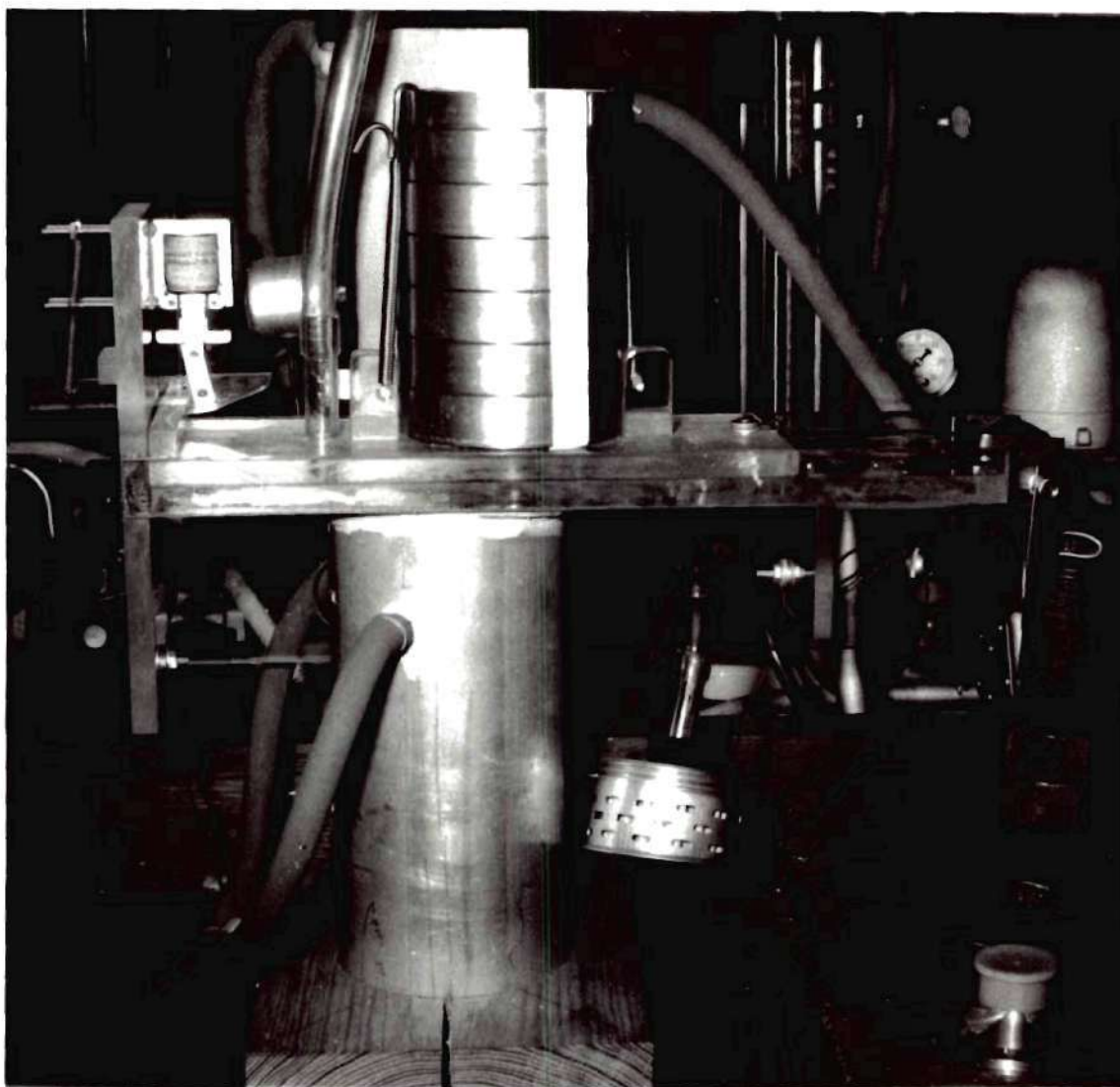


Figure 9. Photograph of Sampling Mechanism



allowed purging air to flow through a high efficiency aerosol filter\* and then through the sampler. Air continued to be drawn through the sampling port at the rate of 28.4 liters per minute to maintain a constant flow of air in the dilution column.

A cam-operated timer (Z) controlled the sampling operation. Sampling was initiated manually by positioning the sampler (U) over the sampling port and engaging the trip-latch (R). The manual by-pass cut-off solenoid valve\*\* (S) already in a closed position. At the instant the sampler was positioned over the sampling port, the sampler air line cut-off valve (T-2) would be opened and the timer activated. At the end of a pre-determined sampling time, the timer would in sequence (1) activate the solenoid operated trip-latch allowing the counterweight to shift the sampler from its position over the sampling port and thereby bring the sampler by-pass line over the port, (2) activate and thus open the by-pass solenoid valve (S), and (3) deactivate itself (the timer). The manual valve T-2 would then be closed, the manual valve T-1 opened and the timer reset to deactivate the solenoid valve (S) in order to prepare for another sampling period. The sampler would then be removed and prepared for further sampling. Exhaust air from the sampling and by-pass systems was discharged to the atmosphere through a 10.16-cm diameter laundry dryer hose and vent\*\*\*.

---

\*Super-Micro-Toxicol, American Optical Company, Safety Products Division.

\*\*General Controls, Inc., Model K27HA112B Magnetic valve, normally closed, International Telephone and Telegraph Co.

\*\*\*Sears Roebuck and Company.

### Conditioning Column Design

The principal part of the experimental system was the bioaerosol conditioning column. Higgins (24) encountered difficulties with his wind tunnel which was approximately 61 cm by 76 cm by 488 cm long. Among the difficulties encountered were: (1) maintaining constant wind velocities, (2) obtaining representative bioaerosol samples, (3) obtaining sufficient time for the bioparticles to evaporate to a constant size distribution before either settling out or reaching the sampling point, and (4) obtaining desired experimental conditions of humidity and temperature. De Ome (47) made use of a horizontal length of glass tubing but observed reductions in bioaerosol concentrations due to sedimentation and impingement on the tubing walls. Kethley, et al. (48-50) employed large settling chambers in which to condition and sample bioaerosols atomized into them.

A straight vertical conditioning column with air flow upward was chosen for this research for three major reasons: (1) to eliminate the settling out of aerosols of interest, (2) to reduce impingement to a minimum and (3) to allow selection of particle size range to be studied. Such a column can be designed to transport in an upward direction an aerosol with a selected maximum particle size by proper air flow selection.

Newitt, et al. (33) observed that water droplets produced when a bubble film disrupts are projected horizontally as far as five cm. Jet droplets, as previously stated, are ejected vertically. The conditioning column was designed to have a radius of 5.08 cm.

Irani and Callis (51) state that the normal diameter of airborne particles lies in a range of 100 microns and smaller. Thus the conditioning column was designed with a sufficient upward air velocity to



entrain a water droplet of approximately 100 microns diameter and with a height to allow (under selected conditions of temperature and humidity) complete evaporation of such a droplet ejected to its maximum height by the jet droplet mechanism. Smaller droplets would, of course, also completely evaporate under such conditions. Larger droplets would, in general, settle out before evaporating.

The terminal settling velocity of a 100-micron diameter sphere of water is approximately 30 cm/sec (52). An air flow of 142 l/min in a 10.16-cm inside diameter pipe (cross-sectional area 81 square cm) yields a mean air velocity ( $\bar{V}$ ) of 29 cm/sec. As a droplet of approximately 100 microns diameter will settle in the Stokian range, for it to be entrained in an upward flow of 29 cm/sec, its actual diameter may be found using the Stokes equation for a droplet falling through air as presented by Rouse (53).

$$D_d = (18\omega\mu_a/\rho_d - \rho_a)^{0.5} \quad (4)$$

where:  $D_d$  = droplet diameter  
 $\omega$  = fall velocity or terminal settling velocity  
 $\mu_a$  = dynamic viscosity of air  
 $\rho_d$  = density of droplet  
 $\rho_a$  = density of air.

The droplet size was calculated to be 99 microns.

The vertical distance traveled by a water droplet while it is evaporating depends upon the following: (1) velocity and direction of air flow, (2) distance and direction of droplet ejection from bursting

bubble, (3) air temperature and humidity conditions, (4) initial droplet size, (5) droplet evaporation, and (6) terminal velocity of the droplet.

The size bubble which, upon bursting in water, ejects a droplet of 99 microns diameter was found by Kientzler, et al. (35) to be approximately one mm in diameter. Stuhleman (32) observed that bubbles of this size eject droplets to a height of approximately 14 cm, the maximum observed for any droplet. Newitt, et al. (33) indicate that the maximum height to entrainment for a droplet ejected into upward flowing air is approximately equal to the sum of the height in still air plus the upward air velocity times the time required for entrainment. They also observed the time required to achieve this height to be of the order to approximately 0.2 second. Therefore, the distance, or height in this case, to achieve entrainment was approximately 18.3 cm.

The vertical distance in still air required for complete evaporation of a water droplet may be derived from the Stokes equation, equation (1):

$$-dH/dt = D_d^2(\rho_d - \rho_a)/18\mu_a = \omega \quad (5)$$

where:

H = vertical distance

t = time.

Therefore, the vertical distance traveled by a droplet during time t is:

$$H = \int_0^H dH = -\int_0^t D_d^2(\rho_d - \rho_a)dt/18\mu_a. \quad (6)$$

The total vertical distance traveled by the droplet during time t in an

up-flow of air is therefore:

$$H_T = V_a t + H = V_a t - \int_0^t D_d^2 (\rho_d - \rho_a) dt / 18 \mu_a \quad (7)$$

where:  $V_a$  = air velocity

The droplet diameter will, of course, be continually changing due to evaporation at relative humidities of less than 100 per cent.

Houghton (54) determined that the diameter of an evaporating droplet can be determined by the expression:

$$D_d = (D_{d_o}^2 - (8k/\rho_d)(\rho_s - \rho_e)t)^{0.5} \quad (8)$$

where:

- $D_{d_o}$  = initial droplet diameter
- $k$  = coefficient of diffusion of water vapor in air
- $\rho_s$  = vapor density of water at the surface of the droplet
- $\rho_e$  = vapor density of the environment.

If it is assumed that no lag exists between incremental changes in droplet diameter due to evaporation and the corresponding changes in fall velocity due to changes in droplet diameter, then equation (8) may be properly substituted into equation (7). If the time  $t$  equals the time required for complete evaporation of the droplet ( $t_e$ ), then  $H_T$  equals the total vertical distance required for evaporation ( $H_{T_e}$ ).

$$H_{T_e} = V_a t_e - \int_0^{t_e} (D_{d_o}^2 - (8k/\rho_d)(\rho_s - \rho_e)t(\rho_d - \rho_a)/18\mu_a) dt \quad (9)$$

When integrated, equation (9) reduces to:

$$H_{T_e} = V_a t_e - (\rho_d - \rho_a) D_{d_o}^2 t_e / 18 \mu_a + (\rho_d - \rho_a) 4k(\rho_s - \rho_e) t_e^2 / 18 \mu_a \rho_d \quad (10)$$

The first term equals the vertical distance traveled by the air during time  $t_e$ . The second term is the vertical distance traveled in still air by a droplet of diameter  $D_{d_o}$  during time  $t_e$ . The third term is equal to the net vertical distance traveled by the droplet in time  $t_e$  due to its changing diameter.

The air entrance to the conditioning column was designed to provide, as near as practicable, turbulent flow conductions to the air entering the conditioning column thus producing essentially a constant cross-sectional velocity profile with the maximum (centerline) velocity ( $V_c$ ) equal to the mean velocity  $\bar{V}$ . Since the design flow should be laminar at stable conditions, the centerline velocity should, therefore, gradually increase and the central turbulent region become smaller as the flow approaches laminar conditions.

The following equation for centerline velocity ( $V_c$ ) during the flow transition in the inlet of circular pipes was developed from data presented by Goldstein (55):

$$V_c = dH/dt = \bar{V} + (2v_a \bar{V} H / 0.0575)^{0.5} / D_p \quad (11)$$

where:  $V_c$  = centerline velocity  
 $\nu_a$  = kinematic viscosity of air  
 $D_p$  = pipe diameter.

The integral equation for time of droplet evaporation is:

$$\int_0^{t_e} dt = \int_0^{H_{T_e}} (\bar{V} + (2\nu_a \bar{V} H / 0.0575)^{0.5} / D_p)^{-1} dH \quad (12)$$

Integration of the first five terms of the binomial expansion (56) yields:

$$\begin{aligned} t_e = & (H_{T_e} / \bar{V}) - (3.93 \nu_a^{0.5} H_{T_e}^{1.5} / \bar{V}^{1.5} D_p) + (17.4 \nu_a (H_{T_e} / \bar{V} D_p)^2) + \dots \\ & \dots - (82.0 \nu_a^{1.5} H_{T_e}^{2.5} / \bar{V}^{2.5} D_p^3) + (403 \nu_a^2 H_{T_e}^3 / \bar{V}^3 D_p^4). \end{aligned} \quad (13)$$

All that remains unknown for the solutions of equations (10) and (13) for  $H_{T_e}$  is the time required for droplet evaporation ( $t_e$ ). Again, Houghton (54) presents an appropriate equation:

$$t_e = D_d^2 \rho_d / 8k(\rho_s - \rho_e). \quad (14)$$

Values for the term  $k(\rho_s - \rho_e)$  are given by List (57) and Kinzer (58) for water evaporating in air at various temperatures and humidities. Solution of equation (14) for an initial water droplet diameter of 99 microns yields, for an air temperature of 22°C and a relative humidity of 35 per cent, an evaporation time of 11 sec. Entering this result into equations



(10) and (13) yields a total evaporation height of 241 cm. Therefore, the total design height of the conditioning column is the sum of the maximum vertical distance from bubble burst to droplet entrainment as discussed previously (18.3 cm) and the total evaporation height (241 cm) or 259 cm.

Van Zoonen (59) studied small particle diffusion in vertical columns or risers and reported that the diffusion coefficient is so small that in a riser with a length to radius ratio of 100 (twice that of the column used in this research), the particles do not usually travel the entire distance from the center of the column to the wall during their passage through the riser. This statement is significant to the design of the conditioning column in that the bioaerosols were generated by design in the center of the column. Jet droplets would not, therefore, be expected to reach the column wall before leaving the system. The straight-through column design without obstruction or other restriction of air and particle flow from the bioaerosol generator to the sampling port assures maximum aerosol recovery with minimum losses due to impaction or segregation of particle sizes.

#### Bubbler Design

Bubbles were formed in the aeration tank liquid by means of single orifices or bubblers. These orifices were constructed of Pyrex glass tubing of five mm outside diameter and three mm inside diameter. The glass tubing was drawn into capillaries and bent at right angles approximately 2.5 cm from the capillary end in order that the capillaries might be oriented vertically as shown in Figure 6. Various size orifices were constructed and calibrated to provide bubbles of from 0.5 mm to 5.7 mm

diameter.

Assuming spherical bubbles, the volume velocity of air passing through a submerged orifice is equal to  $N\pi D_b^3/6$  where  $N$  is the number of bubbles produced per unit time and  $D_b$  is the diameter of the bubbles (60). Use was made of this relationship in estimating the diameter of bubbles produced by the prepared orifices. The number of bubbles produced in unit time by each orifice was determined by observing the bubbles in stroboscopic light\*. The volume velocity was determined by use of a gasometer consisting of a graduated glass column partially filled with water and an adjustable water reservoir for equalizing the air pressure within the system as shown in Figure 10.

Preliminary experiments were conducted in order to determine the most practical bubbling rate for the study, and a bubbling rate of 1000 bubbles per minute was established for use in the study.

#### Bioaerosol Sampler

Mandatory to the success of this research was an air sampler capable of providing reliable determinations of numbers and size distributions of bioparticles (aerosol particles containing microorganisms) produced in the experimental system. The Andersen sampler\*\* (30,31) was found to comply with these requirements.

A schematic diagram of the Andersen sampler is presented in Figure 11. As may be seen, the sampler consists of a series of six stages through which the sample of air or aerosol is consecutively drawn. Each

---

\*Strobotac, Type 631-13, General Radio Co., Cambridge, Mass.

\*\*Andersen Sampler, Model 101, Provo, Utah.

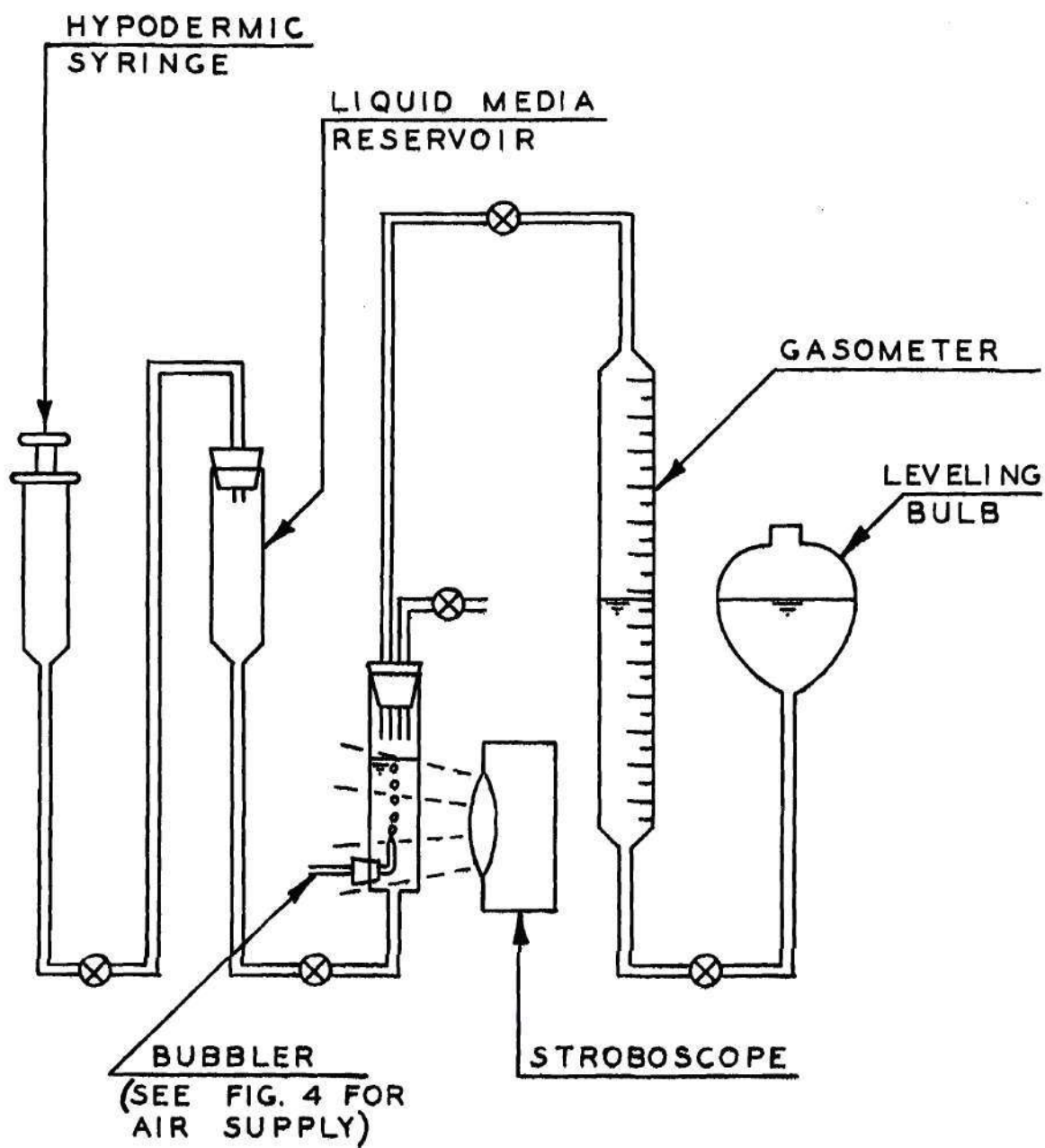


Figure 10. Bubbler Calibration System

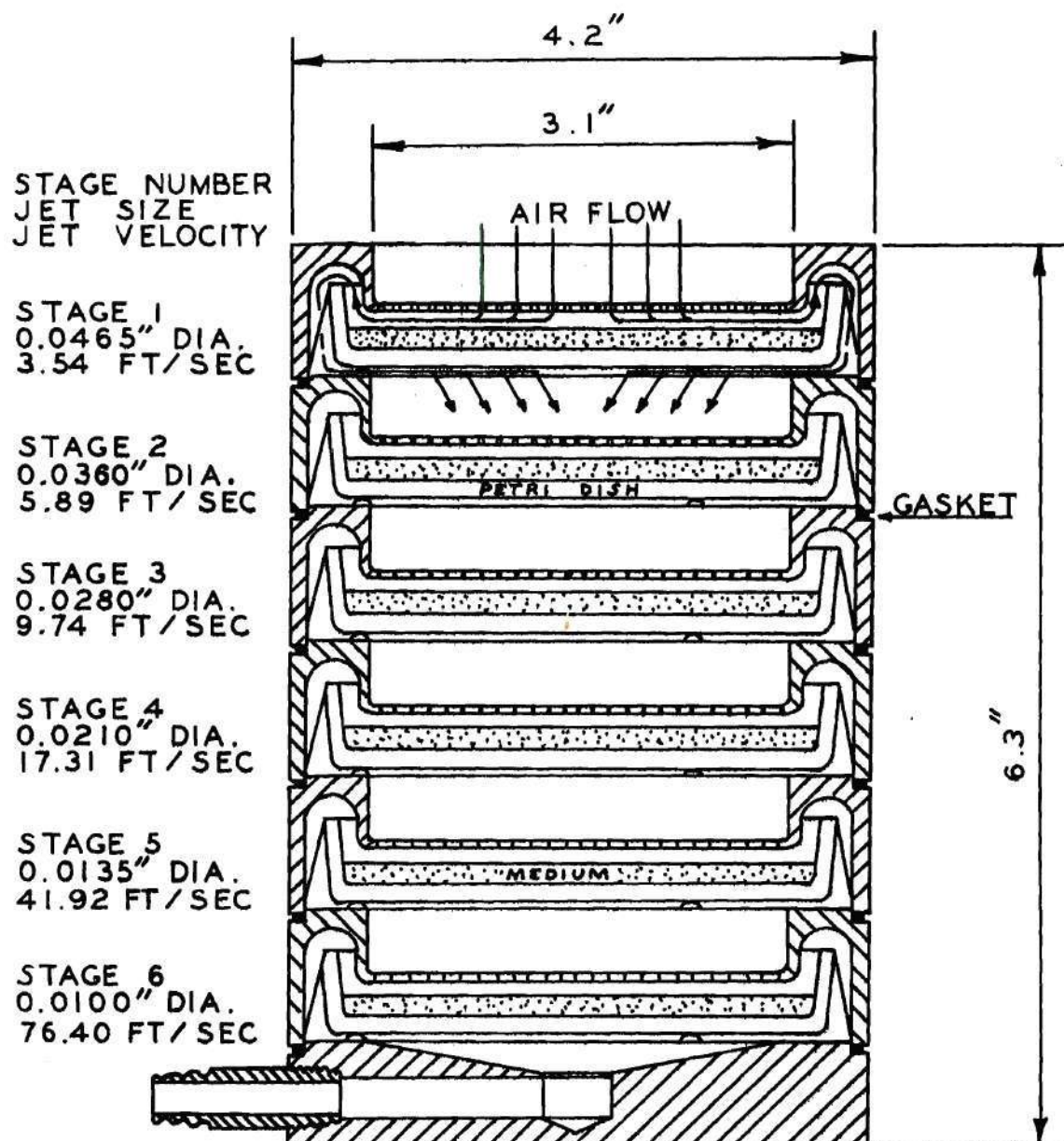


Figure 11. Schematic Diagram-Andersen Sampler (31)





Figure 12. Photograph of Andersen Sampler



stage contains a plate perforated with 400 holes with a petri dish of agar culture medium below. Air is drawn through the sampler at the rate of 28.4 l/min and impinges on the agar surface below each jet. The size of the holes is constant for each stage but is smaller in each succeeding stage as may be seen from Figure 11. The sampler is designed to operate at a flow rate of 28.4 l/min. Any airborne particle from about 0.5 to 100 microns diameter will be collected on one stage or another depending upon particle size. If the particle size spectrum being sampled is sufficiently broad, particles will be collected on all stages. Each succeeding stage will remove a top fraction (largest particles) of the remaining particles with the last stage completing the collection of bacteria size particles.

The collection and assessment of bioparticles is as follows. Six petri dishes each containing 27 ml of agar medium are placed in the sampler and a sample of air taken. The plates are then removed, inverted in their covers, incubated and counted. Colonies on petri stages one and two are scattered over the plates and are counted in the usual way. In stages three through six, the colonies conform to the pattern of the jets and are counted by the "positive hole" method. The "positive hole" method is essentially a count of jets which delivered viable particles to the petri plates and the conversion of this count to a particle count by the use of a "positive hole" conversion table supplied by the manufacturer. This table is based upon the principle that as the number of viable particles being impinged on a given plate increases, the probability of the next particle going into an "empty hole" decreases. By this method, as many as 1500 particles per stage may be reliably determined.

There are no dead air spaces in the sampler and the velocity of the air moving through the device is greatest in the jets. The velocity at other points is not sufficient to carry particles to any surface other than that of the sampling medium. Laboratory experiments (31) have shown that cleaning or sterilization of the sampler between runs is not required. This was verified by negative control plates following collection of positive samples.

The Andersen sampler is designed to simulate retention of airborne particles in the human respiratory system. Particles five microns and larger are retained in the upper respiratory tract (Brown, et al. 61). This same fraction is collected on the first three stages of the sampler. Penetration into the respiratory tract increases with decreasing particle size as it also does in the sampler. The one-micron particles retained in the respiratory system are all found in the alveoli (61), and in the sampler, they are found on the two lower stages. The Andersen sampler has been calibrated by Kethley at the Georgia Institute of Technology (62). He found effective mean diameters of particles trapped on each plate to be 9.8 microns on the second stage, 6.2 microns on the third, 3.8 microns on the fourth, 2.2 microns of the fifth, and 0.9 micron on the sixth stage.

## CHAPTER III

## EXPERIMENTAL TECHNIQUES

Microorganisms

To provide an effective means of studying the aerosolization of microorganisms by bursting bubbles, a microorganism with known ability to withstand the stresses of aerosolization as well as maintain a predictable viability under conditions imposed upon it in the aeration tank and in the airborne state in the conditioning column is desirable. Such an organism should also be positively detectable in representative numbers through the use of an aerosol sampler.

The spores of Bacillus subtilis var. niger meet these requirements. The spores have been found by Miller, et al. (63) to be excellent physical tracers for bacterial aerosols. Miller, et al. were not able to demonstrate in any of their tests that the spores germinated or became susceptible to environmental conditions during aerosolization or during their existence in the aerosol state. Samples of the aerosol at ages up to thirty minutes were assayed, heat treated for thirty minutes at 65°C, and again assayed with no discernible decrease in viable numbers. They also found, when comparing the spores as tracers with radio-chemical tracer techniques, a relative sensitivity difference of about 48 to one in favor of the spore method. The original presence of as few as a single Bacillus subtilis spore upon a properly incubated nutrient agar plate can be demonstrated (64).



Bacillus subtilis var. niger spores were described by Bradley and Franklin (65) to be cylindrical in shape with well-rounded ends and ribbed surfaces. Spore dimensions were reported to be approximately 1.0 to 1.5 microns in length and 0.8 micron in diameter. Spore volume was reported by Fitz-James and Young (66) to be  $0.165 \pm 0.025$  cubic microns with an average weight of  $0.53 \times 10^{-12}$  gm per spore. Harden and Harris (67) found the spore isoelectric point to be approximately pH 2.19 with a range of from pH 1.75 to 4.15. Bacillus subtilis is normally negatively charged.

As indicated above, the spores of Bacillus subtilis are extremely viable under even severe conditions. They may be frozen and desiccated (68) without significant loss of viability. Evans and Curran (69) found no reduction in viability of Bacillus subtilis spores for 31 months in buffered substrate at zero degrees C. Fleming and Ordal (70) observed the germination of Bacillus subtilis spores in ionic environments and found the per cent germination of spores stored for six days in one-tenth molar salt solutions at pH 7.0 and 24 degrees C of (1) two per cent for sodium chloride, (2) two per cent for calcium chloride, (3) four per cent for di-basic sodium phosphate, and (4) three per cent in deionized water.

The spores used in this research were procured from Professor T.W. Kethley of the Georgia Institute of Technology who had originally obtained them from the U.S. Army Chemical Corps Biological Laboratories, Fort Detrick, Frederick, Maryland. The spores were triple washed and centrifuged for removal of dissolved solids.

#### Bacteriological Assay

Stock suspensions of the Bacillus subtilis spores were prepared containing approximately  $10^{-3}$  gm of air-dried spores per ml of deionized



water\* of greater than  $10^6$  ohms resistance. The stock suspensions in 100 ml quantities were stored in standard glass dilution bottles at 5°C until they were used in experiments. The deionized water and dilution bottles were previously autoclaved for 15 minutes at 121°C to render them sterile.

Each stock suspension was assayed immediately after preparation to aid in the later preparation of experimental liquid. The following technique was employed. Each stock suspension was first heat treated for 45 minutes in a 65°C water bath to destroy vegetative cells. The suspension was allowed to cool to room temperature and shaken vigorously for five minutes to assure uniform dispersal of spores. One ml of stock suspension was pipetted into another dilution bottle containing 99 ml of deionized water. All glassware used in this research was sterilized before use as described above. This new suspension was then shaken vigorously for five minutes. From this bottle, one ml was pipetted into still another dilution bottle containing 99 ml of deionized water and the above process repeated. In all, four successive dilutions of each stock solution were performed based upon preliminary estimates of the number of spores per gm of dried spore stock.

From the last dilution, one ml of suspension was pipetted into each of ten petri plates. Immediately, the petri plates were filled with nutrient agar to about one-third capacity. The agar was poured at about 50°C and each dish was swirled as soon as poured. After about 15 minutes to allow the agar to set up or solidify, the plates were inverted, incubated at 37°C for from 24 to 48 hours, and counted. This process was

---

\*Mixed Resin Bantam Demineralizer, Barnsted Still and Sterilizer Co., Boston, Mass.

repeated for the second from last dilution, and data from the series of plates yielding from 50 to 300 colonies per plate utilized for the assay.

The nutrient agar\* used in this study was prepared according to manufacturer's directions, autoclaved for 15 minutes at 121°C, and stored in a water bath at about 50°C until used but not exceeding three days to assure sterile media.

Each liquid employed in the study was assayed for Bacillus subtilis spores in the above manner after preparation. The number of dilutions was, of course, altered to conform with the dilution factor employed in the preparation of the experimental liquids.

#### Test Liquid Composition

Several types of liquids were utilized in this study to demonstrate the effects of liquid composition on bioaerosol production and to demonstrate differences in production mechanisms. Seven different liquids in varying concentrations were used. They were of three types as follows: (1) inert liquids, demineralized water and hydrophilic sols of gelatin and peptone employed for their solids concentrations; (2) electrolyte solutions of sodium chloride and dibasic potassium phosphate to facilitate reduction of spore surface charges and thus enhance spore association with the air-liquid interface; and (3) organic "collector" solutions, octanoic acid and dipentylamine, used to render spore surfaces more hydrophobic and allow greater association of spores with the air-liquid interface. All solutions and sols were prepared with demineralized water.

---

\*Catalogue No. J-1087-C, Fisher Scientific Co., Fair Lawn, N.J.

Gaudin, et al. (71) found the presence of salt or amine or fatty acid collectors in the liquid being aerated to be among the factors which influence the flotational behavior of Bacillus subtilis var. niger spores. They found that the addition of salts, dioctyl amine, and propanoic, hexanoic, and octanoic acids to the liquid individually enhanced flotation of the spores by aeration. They also state that, although both cationic and anionic sites are available on the spore surface to effect adsorption, the spores have an excess of carboxyl groups. However, they point out that the outer coats of an organism differs from strain to strain and from species to species.

Salts affect hydrophilic sols by first lowering the zeta potential, requiring only a very small amount of electrolyte, and then rendering them more hydrophobic by withdrawing water from the hydration shell (72).

The effect, then, of addition of an electrolyte to an aerated suspension of Bacillus subtilis spores would be to lower or reverse the magnitude of the primarily negatively charged spore surface and thereby reduce or reverse the electrostatic repulsion of spores and the air-liquid interface and enhance the association of spores with the interface. The ionizable radicals of the amine and fatty acid organic collectors interact with or adsorb on the negatively and positively charged surface sites on the spores respectively to render the spore surfaces more hydrophobic due to the insolubility of the hydrocarbon chains of the collectors. This increase in hydrophobicity will also enhance the association of the spores with the air-liquid interface.

The primary purpose of the electrolyte and organic collector solutions used in this research was to bring about this spore-interface



association in order that the resulting bioaerosol production changes thus imposed might be used to study production mechanisms. The hydrophilic gelatin and peptone sols in the concentrations in which they were used were not expected to alter spore characteristics to an appreciable extent.

Harkins and McLaughlin (73) have calculated that in dilute electrolyte solutions such as were employed in this research there is a solute-free surface layer approximately one molecule thick. Surface tension data substantiates this finding. Thus the concentrations of the salts used in this research would not be expected to affect bubble production or aerosol production. Kientzler, et al. (35) observed that bubbles bursting in sea water produce essentially the same droplet characteristics as those bursting in fresh water with the exception that a much longer period of time is required for rupture of the bubble in sea water.

Surface tension and viscosity data for the liquids used in this research are presented in Table 21, Appendix F. Surface tension ranged from 66.0 to 72.3 dynes/cm while viscosity was observed to range from 0.93 to 1.01 centipoise. Newitt, et al. (33) observed no significant differences in mean droplet size from a surface tension of 68.74 dynes/cm to 71.97 dynes/cm or from a viscosity of from 0.59 centipoise to 0.89 centipoise.

#### Experimental Procedures

The following is a discussion of the procedures and equipment operation employed in conducting the various experiments of this study. The approach involved in the experimental design was to have only one variable per experiment. In general, the variable was the composition of the test liquid. The other variable used at times was bubble size.



Prior to each experiment, all necessary glassware and manipulative hardware were autoclaved at 121°C for 15 minutes. Nutrient agar for test liquid spore assays and deionized water for the preparation of the test liquids were also prepared and autoclaved as above. The special agar plates for use with the Andersen samplers were sterilized and each filled with the required 27 ml of nutrient agar at the Bioengineering Laboratory, Georgia Institute of Technology.

A stock spore suspension was removed from refrigeration and allowed to come to room temperature. A quantity, usually 10 or 20 ml, of this suspension was transferred to a previously sterilized milk dilution bottle, and the stock suspension returned to the refrigerator. This aliquot was heat treated in a water bath for 45 minutes at 65°C in order to destroy any vegetative cells present in the suspension. When cool, the aliquot was sampled and a spore assay performed as discussed in the previous section on bacteriological assay.

The liquids for use in the experiment at hand were then prepared. Into each glass dilution bottle was placed the amount of spore suspension required for the experiment. Next, sterilized deionized water or other special liquid for study was added in the proper amount to bring the total liquid volume to 100 m. All inorganic chemicals for use in the preparation of liquids were of reagent grade. All liquids employed were sterile except for the added spores. Each liquid was then analyzed for viscosity\*, surface tension\*\* (74), and pH\*\*\*.

---

\*Capillary

\*\*Ostwald

\*\*\*Beckman Model G

The bubbler for use in the experiment was prepared by a thorough cleaning with chromic acid cleaning solution followed by several rinses with deionized water while air was flowing through the orifice. According to Bikerman (60), the bubble size varies with the radius of the capillary opening for wetted orifices and with the outside diameter for non-wetted orifices. The cleaning was to assure a constant bubble sizes throughout the study. The bubbler was then inserted into the aeration chamber and the chamber sealed to the conditioning column (See Figures 4-7).

After all tubing had been connected to the aeration tank, the test liquid was poured into the holding reservoir. From the dilution air conditioning chamber, air which had been in the conditioning process for some minutes was then allowed to flow through the entire experimental system at the design flow. The sampler was not yet in place and the sampler by-pass was functioning. The air was monitored for wet bulb-dry bulb temperatures until stabilized at about 35 per cent relative humidity at 22°C. The entire laboratory was conditioned by steam heat and a room air conditioner to provide a constant temperature of  $22 \pm 1^\circ\text{C}$ . When stabilized, the relative humidity device was by-passed. Relative humidity measurements were made at various times during the experimental day.

Next, the hypodermic syringe was employed to introduce the liquid into the aeration chamber. The liquid was allowed to rise to the very top of the aeration chamber so that surface tension would cause the liquid surface to become and remain convex upward throughout the run. This was to insure that bubbles would tend to remain in the very center of the chamber and conditioning column, and provide adequately reproducible geometry.

Air flow was regulated through the bubbler to provide the proper bubbling rate, generally about 1000 bubbles per minute. Bubbling rate was established and monitored by means of a stroboscopic light. Bubbles were observed to be produced always at very stable rates and to have consistent size and shape. Bubbling rates once established varied at most by five per cent.

Andersen samplers were prepared by positioning in the samplers six special petri plates each containing 27 ml of nutrient agar. A sampler was placed inverted on the sample changer slide (See Figure 8). Then in sequence, the by-pass valve was closed, the slide immediately positioned to bring the sampler over the sample port, the sampler valve opened, the timer immediately engaged, and the flow gauges checked. The manometer was checked to assure no leaks in the system. All experiments were conducted at 2.5 cm mercury vacuum (2.5 cm below atmospheric pressure).

At the end of a pre-determined and pre-set time (never more than 20 minutes to prevent drying out of agar), the timer would activate the trip-latch and allow the sampler mechanism slide to remove the sampler from over the sample port, purge the sampler, and open the by-pass valve. The completed sample was then removed, a new sampler put in place on the slide, and the timer re-set. According to the experimental design, another sample would be taken as above, or the test liquid removed from the aeration chamber, a new liquid introduced, and another series of samples taken.

The liquid was removed from the aeration chamber by use of the hypodermic syringe while the system was in continuous operation. After removal of the liquid, the chamber was rinsed several times with deionized water before a new liquid was introduced.



As each sample was taken, the petri plates were removed from the sampler, inverted in their cover plates and incubated for 24 hours at 37°C.

At the beginning and end of each experimental series, background samples were obtained. Not more than four background colonies per ten-minute sample were observed during the study.

At the end of the experiment, the liquid was removed from its chamber, the dilution air conditioning system and vacuum pumps were shut down, and the entire aeration and sampling system thoroughly cleaned.

At the end of the incubation time, the plates were counted to determine the numbers of Bacillus subtilis colonies present. On the average of only about once per 100 plates were any colonies other than those of Bacillus subtilis found on a plate, and then usually only one or two at most. Bacillus subtilis colonies are easily recognized by their characteristic brown-orange color. The counts were made on a standard Quebec counter. "Positive hole" corrections were applied to counts made on plates three through six as discussed in Chapter II.

The distribution of bioparticle counts may be described by the Poisson distribution (75). From the experience of other workers (62), the collection and counting of bioparticles from bioaerosols can result in errors averaging 15 per cent of the numbers counted. As a result, experiments were designed to yield counts of 172 or greater in order to maintain a 95 per cent statistical level of confidence, accepting experimental errors of 15 per cent or less. Under these circumstances, the goodness-of-fit of observed counts to the Poisson expectancy could be determined by Chi Square testing (75) (See Appendix E, Table 13).



## CHAPTER IV

### RESULTS AND DISCUSSION

#### General

The results of this research are discussed in general in terms of their relationship to the primary research objectives, i.e. to demonstrate whether or not viable bioaerosols can be produced by the aeration of liquids containing microorganisms, and in particular in terms of the jet droplet and the film droplet mechanisms. The discussion of results is independent of the time sequence of experimentation.

Bacillus subtilis var. niger spores were used as tracer organisms because of their resistance to desiccation and other environmental conditions employed in the research and because of the ease by which they may be detected. They were sampled in the airborne state by use of an Andersen bioaerosol sampler. The sampler was used without its customary entrance cone. Without this restricting cone, the sampler is capable of collecting all airborne particles over an effective size range of from less than  $0.5\mu$  diameter to greater than  $100\mu$  diameter. The size range of bioparticles of interest in this study was from approximately one  $\mu$  diameter (the effective diameter of one spore) to approximately  $100\mu$  diameter (the maximum particle size which could be entrained in the experimental system). All results and conclusions discussed in this chapter assume these conditions.

The design of the experimental system was such as to preclude the formation of aerosols of the size range of interest in any manner except

the bursting of bubbles, e.g. no wind action, no wave action, no mechanical action, etc. The aeration chamber and the bubbler depth was designed to reduce to a minimum any flotation of spores which may have occurred. No significant evidence was found of flotation having occurred during the experimentation. The distribution of Bacillus subtilis colonies on the first or any other stage of the Andersen sampler was observed to be generally uniform indicating that there was no significant concentration of airborne spores in any region of the sampler intake. A check of spore contamination on the interior walls of the conditioning column revealed numbers small in comparison to the numbers passing through the column, approximately 12 per 100 cm<sup>2</sup> per experiment. Higher numbers, averaging about 60 spores per 100 cm<sup>2</sup> per experiment, were detected on the walls within 15 cm of the aeration chamber indicating that some liquid droplets containing spores were projected directly to the column walls.

Microscopic examinations revealed that no agglomeration of spores occurred in any of the liquids used in this study. The spore suspensions were essentially completely dispersed during experimentation.

The following conveniences were adopted for use in this chapter to facilitate the presentation of results. They are as follows: (1) spore means spore of Bacillus subtilis var. niger; (2) all aerosol production data and references to bioparticles and bioaerosols refer to viable production, viable bioparticles, and viable bioaerosols whether stated or not, where the term viable refers to ability to form colonies on the growth media employed; (3) bubble size refers to bubble diameter; and (4) particle, bioparticle, bioaerosol, and aerosol size refers to count median diameter (CMD) as the case may be, as determined by means of the Andersen

sampler (76). Also, the test liquids were coded for ease of reference. Definition of the symbols employed are found in Table 3. The number following the letter symbol refers to the concentration of the added chemical in milligrams per liter except for A and DA in which cases the numbers refer to concentration in microliters per liter. For example G-150 refers to DM plus 150 milligrams of gelatin per liter. A-100 refers to DM plus 100 microliters of octanoic acid per liter.

Table 3. Definition of Test Liquid Symbols

Symbol	Definition
DM	Demineralized water
A	DM plus octanoic acid
DA	DM plus dipentylamine
G	DM plus gelatin
P	DM plus peptone
PH	DM plus dibasic potassium phosphate
S	DM plus sodium chloride

The basic experimental data are presented in Appendix A. Appendix B contains the sampling data as determined by means of the Andersen sampler. Appendix C presents a basic summary of the sample data in a reduced form and contains information on bioparticle median size, size distribution and production rate.

The data obtained by means of the Andersen sampler when plotted on



log probability paper usually yielded straight lines. The bioparticle size distribution data in Appendix C were determined from log probability plots.

To aid interpretation of the sampling results obtained from the experiments, information was also obtained on the background spore concentration of the dilution air and aeration air before and during the experimental period. These data are presented as Appendix D.

#### Bioparticle Size Distribution

The possibility of air being a route for the spread of infection lends importance to the study of bioaerosol production. Airborne infection may be produced in two ways, (1) lung penetration by infectious bioparticles and (2) the deposition of infectious bioparticles in the upper respiratory tract with subsequent ingestion. The route followed by an inhaled bioparticle is determined by the particle's effective aerodynamic diameter. This is thought to be the same quantity which is determined by the Andersen sampler. In general, particles with diameters smaller than about five microns can penetrate and be retained by the lung to varying degrees. Particles larger than about five microns diameter are usually retained in the upper respiratory tract and subsequently ingested. A graphical representation of particle penetration into the human lung is presented in Figure 13.

Data collected in this research allowed the determination of the size distributions of viable bioparticles produced by aeration of various liquids with several different size bubbles. The bioparticle size distributions usually plotted as straight lines on log-probability paper. Count median diameters (CMD) ranged from a minimum of  $2.4\ \mu$  to  $22.5\ \mu$  with the



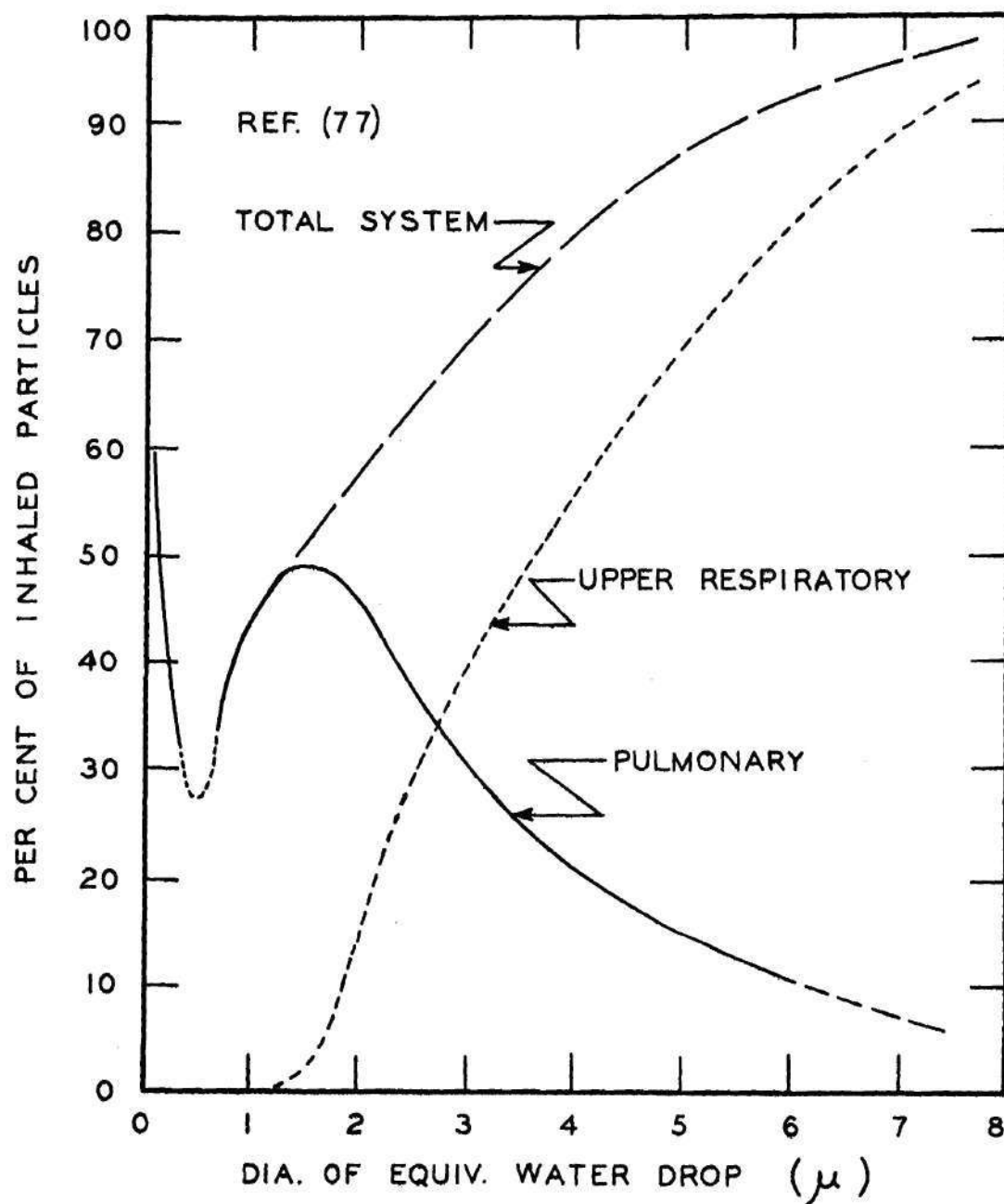


Figure 13. Total and Regional Deposition of Inhaled Particles in the Human Lung

majority being less than ten  $\mu$ . The geometric standard deviations of the bioparticle distributions ranged from 1.26 to 8.33 with a majority less than 3.00.

Solids concentration in the liquids studied was varied up to 1600 mg/l. Generally, increased solids concentrations were accompanied by increased median diameters. However, certain ionizable inorganic and simple organic solids actually resulted in reduced mean diameters as is discussed in the section on the effect of test liquid composition on bioaerosol production. Other factors which influenced bioparticle size distribution were spore concentration in the liquid and bubble diameter. Each of these are discussed in detail elsewhere in this report.

#### Effect of Spore Concentration on Bioparticle Production

If a bioaerosol is produced by bubbling air through a liquid containing spores, then an increase in the spore concentration in the liquid would presumably result in an increase in the bioparticle production rate. However, once each liquid droplet produced contains at least one spore, then any increase in spore concentration in the liquid should not result in an increase in bioparticle production, but should only increase the number of spores per particle.

Several experiments were conducted to determine the effect of spore concentration on bioaerosol production. Four bubble sizes and seven different liquids were utilized. Data for two bubble sizes, 0.5 mm and 2.2 mm diameter, are presented in Figures 14 and 15 respectively. Data collected from all six stages of the Andersen sampler were totaled and presented as the number of bioparticles produced per 1000 bubbles.

Data for each experimental condition were observed to fall into two

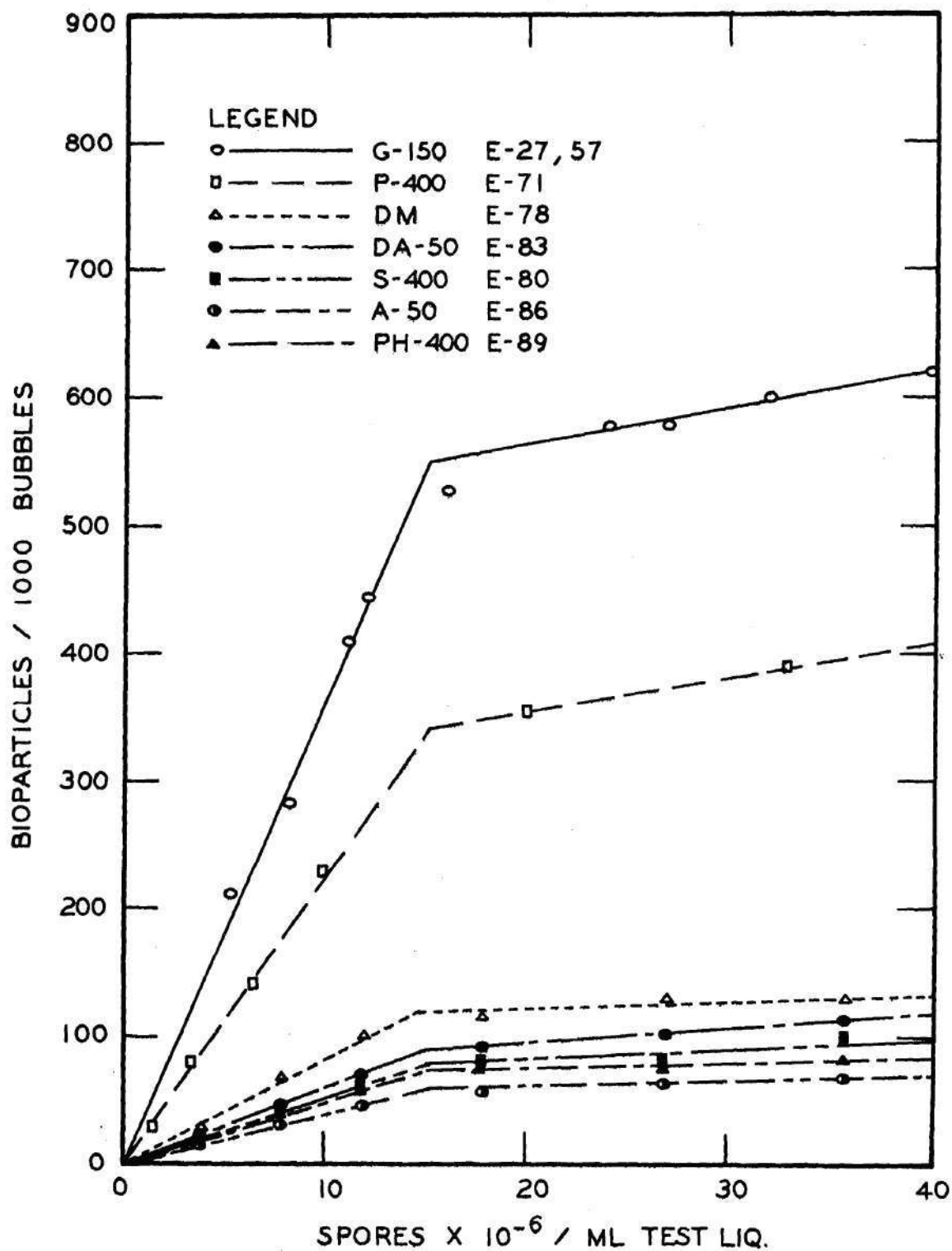


Figure 14. Bioparticle Production Rate in Relation to Test Liquid Spore Concentration for 0.5 mm Bubbles

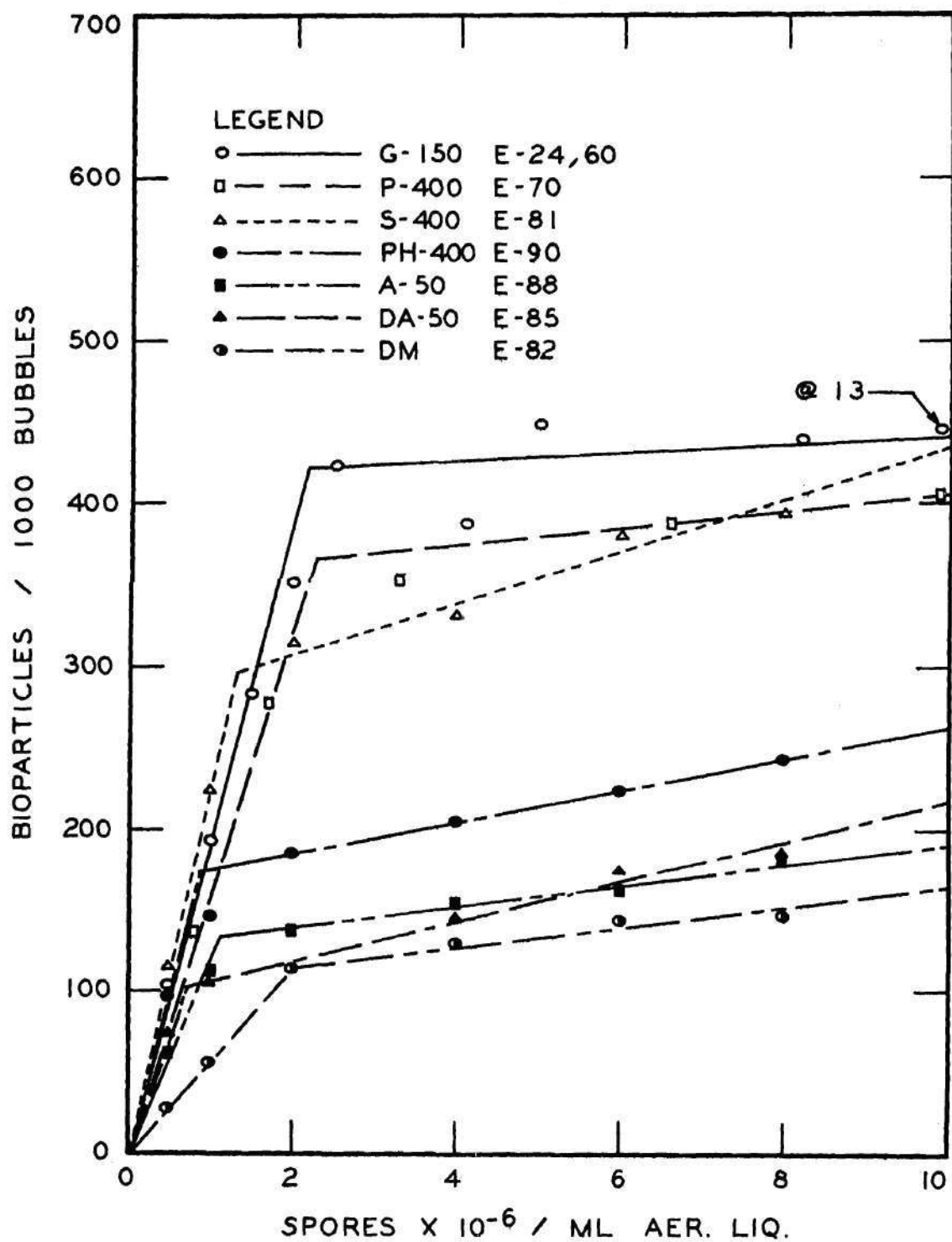


Figure 15. Bioparticle Production Rate in Relation to Test Liquid Spore Concentration for 2.2 mm Bubbles



distinct groups. One group plotted as a straight line on rectangular graph paper. The line has positive slope and passes through the origin, i.e. zero bioaerosol production at zero spore concentration, as may be seen in both Figures 14 and 15. Thus in this regime, an increase in spore concentration in the liquid by a factor of two results in an increase in bioparticle production rate by a factor of two. Bioparticle production is seen to be directly proportional to spore concentration.

The other group of data also plotted as essentially a straight line on rectangular graph paper for each experimental condition. However, the line does not pass through the origin and is, in general, almost parallel to the abscissa. This indicates that the liquid droplets being produced by aeration of the liquid became somewhat saturated with spores, i.e. most droplets contained at least one spore.

The point where extensions of the two lines intersect represents that concentration of spores in the liquid sufficient to contribute at least one spore to each droplet of the median size produced by aeration. The absence of a sharp breakpoint is most likely due to the fact that a range of droplet sizes are produced. The positive slope of the group of data beyond the breakpoint may also be due to the existence of a range of droplet sizes (the smaller sizes continuing to approach saturation) as well as to the statistical variation in the probability of each droplet containing at least one spore at concentrations equal to or greater than that which simple probability would dictate that saturation be achieved. The significance of the locations of the breakpoints for the various bubble sizes is discussed in the following section on initial droplet size distribution.

### Initial Droplet Size Distribution

Experiments were conducted to determine the effect of liquid composition on mean initial droplet sizes. If initial droplet size is independent of the liquid used, then observed variations in bioparticle distribution and median size may be said to be due to factors other than changes in initial droplet size.

For bubble sizes of 0.5, 0.9, 1.1, and 2.2 mm diameter, representative liquids were utilized in experiments in which spore concentration was varied. Since Andersen plates are designed to indicate only viable bioparticles, liquid droplets which do not contain spores will not be demonstrated. Thus, when the spore concentration in the liquid is increased, an increase in colonies on the Andersen plates for the droplet size of interest should be observed until the spore concentration becomes such that the probability is that each droplet will contain one spore. There should then be no further increase in Andersen colony counts since a droplet containing more than one spore is observed as a single colony. Experiments 24-27, 35-38, 57-60, 69-72, and 77-90 were designed primarily to indicate initial droplet size.

Figure 14 is a plot of data for a bubble size of 0.5 mm while Figure 15 is for a bubble size of 2.2 mm. As may be observed, all data indicate a breakpoint at about  $1.5 \times 10^7$  spores per ml for a bubble size of 0.5 mm, while for a bubble size of 2.2 mm, only data for G-150, P-400, and DM average about the same at  $2.1 \times 10^6$  spores per ml. A summary of results for bubble sizes of 0.5, 0.9, 1.1, and 2.2 mm is presented in Table 4. Initial droplet CMD was computed as follows:

$$D_{d_o} \cong (6/\pi C_{sp})^{1/3} \quad (15)$$

Where:  $D_{d_o}$  = initial droplet CMD

$C_{sp}$  = aeration liquid spore concentration.

Table 4. Initial Count Median Diameters of Droplets Containing Spores

Bubble dia. (mm)	Exp. no.	Liquid test media	Spore conc. at breakpoint $\times 10^{-7}/\text{ml}$	Initial droplet CMD ( $\mu$ )
0.5	78	DM	1.5	50
	27 & 57	G-150	1.5	50
	71	P-400	1.5	50
	80	S-400	1.5	50
	89	PH-400	1.5	50
	83	DA-50	1.5	50
	86	A-50	1.5	50
0.9	77	DM	0.67	66
	26 & 58	G-150	0.67	66
	72	P-400	0.67	66
	79	S-400	0.67	66
	84	DA-50	0.67	66
	87	A-50	0.67	66
1.1	25 & 59	G-150	0.35	82
	69	P-400	0.35	82
2.2	82	DM	0.20	97
	24-60	G-150	0.21	97
	70	P-400	0.22	97
	81	S-400	0.13	
	90	PH-400	0.08	
	88	A-50	0.11	
	85	DA-50	0.07	

Data for all Sampler plates in each experiment were summed to give the data used in determining the initial observable droplet sizes. Therefore, the initial droplet sizes determined were the initial observable



median sizes. The breakpoint was observed not to be a sharp point but rather a point of inflection, and the data beyond the breakpoint was found to have a positive slope due to the droplets smaller than the median size which continued to approach their respective saturation concentrations. This is further indicated by a decrease in median diameter and in general an increase in  $\sigma_g$  with increase spore concentration in the liquid as may be seen in Table 11, Appendix C.

As may be observed in Figure 15 for a bubble size of 2.2 mm, the breakpoint spore concentration for liquids S-400, PH-400, A-50, and DA-50 is smaller than that for DM, G-150, and P-400. Since DM, G-150, and P-400 contain either pure water or water with biological material similar to the spores themselves, these liquids were selected to calculate the initial droplet size. The smaller spore concentration necessary to reach mean droplet saturation with the electrolyte and simple organic liquids indicates basically two possibilities, (1) an alteration of the droplet formation mechanism and/or (2) a concentration of spores in the droplet forming liquid. Possibility number (2) is the more realistic assumption for several reasons. First, experimental evidence was gathered which shows little if any variation of the basic liquid properties which affect droplet formation namely viscosity and surface tension (See Table 21, Appendix F). Second, initial mean droplet sizes for 0.5 and 0.9 mm diameter bubbles were constant irrespective of the liquid. These bubble sizes produce droplets primarily by the jet droplet mechanism (35). Third, the smaller breakpoint concentrations indicate either larger initial droplets or a concentration of spores in the droplet forming liquid. However, the liquids producing the smaller breakpoint spore concentrations were chosen



for the purpose of spore concentration at the air-liquid interface as discussed in a later section.

It is interesting to note that the experimentally observed median droplet size produced by the 0.5 mm diameter bubbles is identical to the theoretical of 50 $\mu$  diameter (35) as produced by the jet-droplet mechanism. Table 5 presents this data for the 0.9, 1.1, and 2.2 mm bubbles also. It should be pointed out that the maximum droplet size capable of being transported by the air flow in the conditioning column is approximately 100 $\mu$  diameter.

Table 5. Experimental vs. Theoretical Droplet Sizes

Bubble dia. (mm)	Observed droplet CMD ( $\mu$ )	Theoretical jet droplet CMD ( $\mu$ )	Ratio of Observed to Theoretical
0.5	50	50	1.00
0.9	66	90	0.73
1.1	82	110	0.75
2.2	97	220	0.44

In Table 6 is presented a comparison among observed and calculated droplet and bioparticle sizes. Calculated bioparticle CMD was determined using the following equation:

$$D_a \cong \left( (V_{sp} + \pi D_o^3 C_s / 6) / \pi \right)^{1/3} \quad (16)$$

where:  $D_a$  = bioparticle CMD

$V_{sp}$  = volume of one spore

$D_{d_o}$  = initial droplet CMD

$C_s$  = test liquid solids concentration (vol./vol.)

Table 6. Comparison Among Observed and Calculated Droplet and Particle Sizes

Liq. media	Exp. no.	Bubble dia.	Observed initial droplet CMD	Observed bio-particle CMD	Calculated bioparticle CMD	Ratio (4)/(5)	Ratio (5)/(6)
		(mm)	( $\mu$ )	( $\mu$ )	( $\mu$ )		
(1)	(2)	(3)	(4)	(5)	(6)	(7)	(8)
G-150	57	0.5	50	7.2	2.7	6.95	2.66
	26	0.9	66	9.5	3.5	6.95	2.71
	59	1.1	82	10.7	4.4	7.66	2.44
	60	2.2	97	10.1	5.2	9.60	1.95
P-400	71	0.5	50	5.5	3.7	9.10	1.49
	72	0.9	66	6.5	4.8	10.2	1.35
	69	1.1	82	8.5	6.0	9.65	1.42
	70	2.2	97	7.2	7.2	13.5	1.00
S-400	80	0.5	50	7.5	3.7	6.66	2.03
	79	0.9	66	8.0	4.8	8.25	1.67
DA-50	83	0.5	50	5.4	2.0	9.25	2.70
	84	0.9	66	12.0	2.5	4.50	4.80
A-50	86	0.5	50	5.2	2.0	9.61	2.60
	87	0.9	66	5.8	2.5	11.4	2.32
PH-400	89	0.5	50	4.6	3.7	10.9	1.24

The discrepancy between observed and calculated bioparticle CMD (Table 6, Columns 5 and 6) is represented by the ratio of observed to calculated (column 8) and is thought to be the result of water associated

with the observed bioparticles. The sample closest to the breakpoint was used to obtain the observed mean bioparticle CMD used in these calculations. The ratio between observed and calculated bioparticle CMD indicates, therefore, that G-150, DA-50, and A-50 produced bioparticles which contained a higher percentage of water at the sampling point, while P-400, S-400, and PH-400 tended to evaporate to a greater extent. Since the Andersen sampler is an impactor sampler, the calculated bioparticle CMD's were derived using the assumptions that all water is evaporated and that all solids have an effective specific gravity of one compared with water. Further, the volume of a spore, approximately  $0.6\mu^3$ , was applied as a correction factor since each bioparticle must contain at least one such spore to be observed. It is noted, however, that droplets may contain two or more spores.

Figure 16 presents for bubble diameters 0.5, 0.9, 1.1, and 2.2 mm theoretical initial droplet distributions. The distributions are for all droplets produced and not merely those containing one or more spores. The distributions were derived by employing the probability that the various droplet sizes will contain at least one spore (See Table 22, Appendix F). Note that for 0.5 mm bubbles, the calculated mean initial droplet size of  $45.5\mu$  is approximately equal to the theoretical jet droplet size of  $50\mu$ .

#### Effect of Bubble Size on Bioparticle Production

A study to demonstrate the effect of aeration bubble size on the production of bioparticles was conducted to provide insight into the mechanisms involved. Andersen sampler data allowed determination not only of numerical bioparticle production rates but also of particle size distributions.

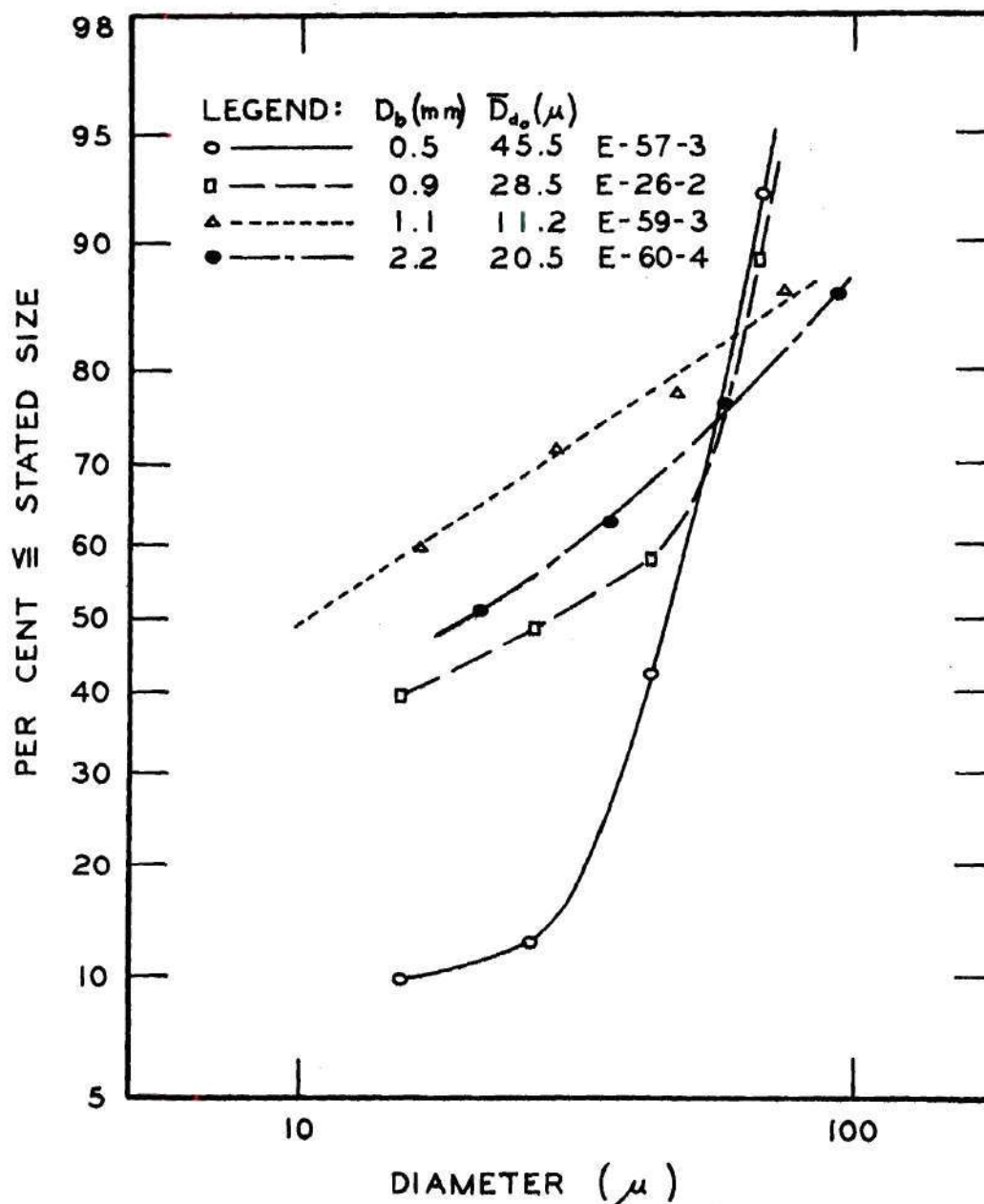


Figure 16. Log Probability Plot of Calculated Initial Droplet Size Distribution for 0.5, 0.9, 1.1, and 2.2 mm Bubbles



Presented in Figure 17 are frequency distribution curves for the bubble sizes used most frequently in this research. The liquid used to obtain these data was DM. As may be observed, the distributions shift from generally smaller size particles for 0.5 mm bubbles to relatively larger particles for 0.9 and 1.1 mm. For the larger bubbles of 2.2, 3.7, and 5.7 mm, the shift in particle size is back to the smaller sizes. Note that the largest bubbles produced the smallest particles. Figure 18 is a log normal presentation of this same particle size data. Log normal plots of the data yielded straight lines. The median particle size ranged from  $3.6\mu$  for 0.5 mm bubbles to a maximum of  $5.1\mu$  for 1.1 mm bubbles and to a minimum of  $3.3\mu$  for 5.7 mm bubbles. This trend of median diameter in relation to bubble size is evident throughout the experimental data.

Data from all appropriate experimental series were combined in a manner which would best show the variation of particle size versus bubble size. The data was reduced to mean ratios of bioparticle CMD for the various bubble sizes to the bioparticle CMD for 0.5 mm bubbles. In such a representation, all variables except those plotted are eliminated. The observed differences in bioparticle CMD in relation to bubble size were determined to be significant at the 99 per cent level of confidence (See Appendix E). The trend was toward a maximum bioparticle CMD for the 0.9 mm bubble and to a minimum for the 5.7 mm size (see Figure 19). The indication is that there was a change in droplet production mechanism. In general, investigators have observed only jet droplets to be formed by bubbles up to about two mm in diameter (35) and primarily film droplets from bubbles 3 mm in diameter and larger (33). Jet droplets would be expected to become continuously larger with larger bubble sizes (35).

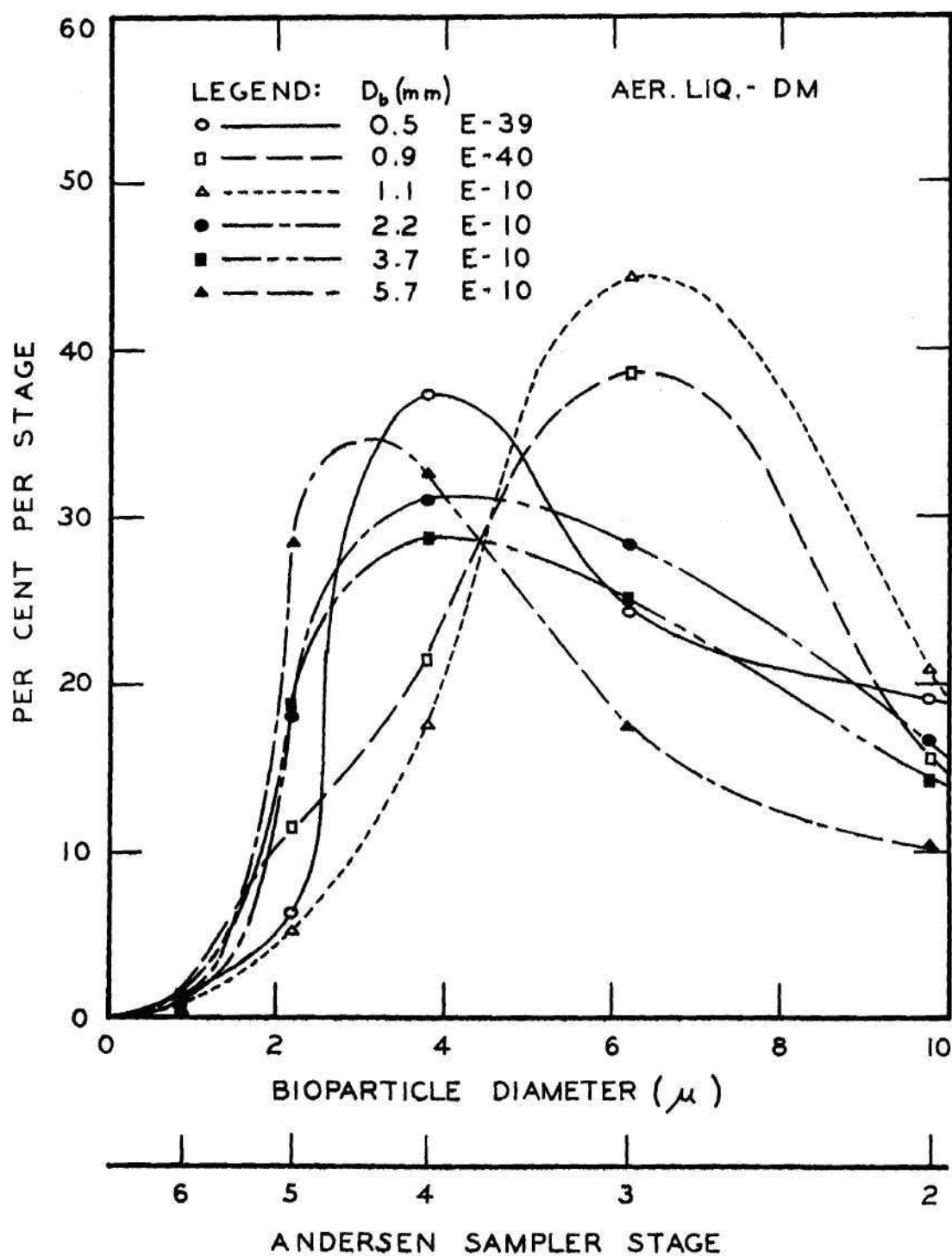


Figure 17. Bioparticle Size Frequency Curves for 0.5, 0.9, 1.1, 2.2, 3.7, and 5.7 mm Bubbles

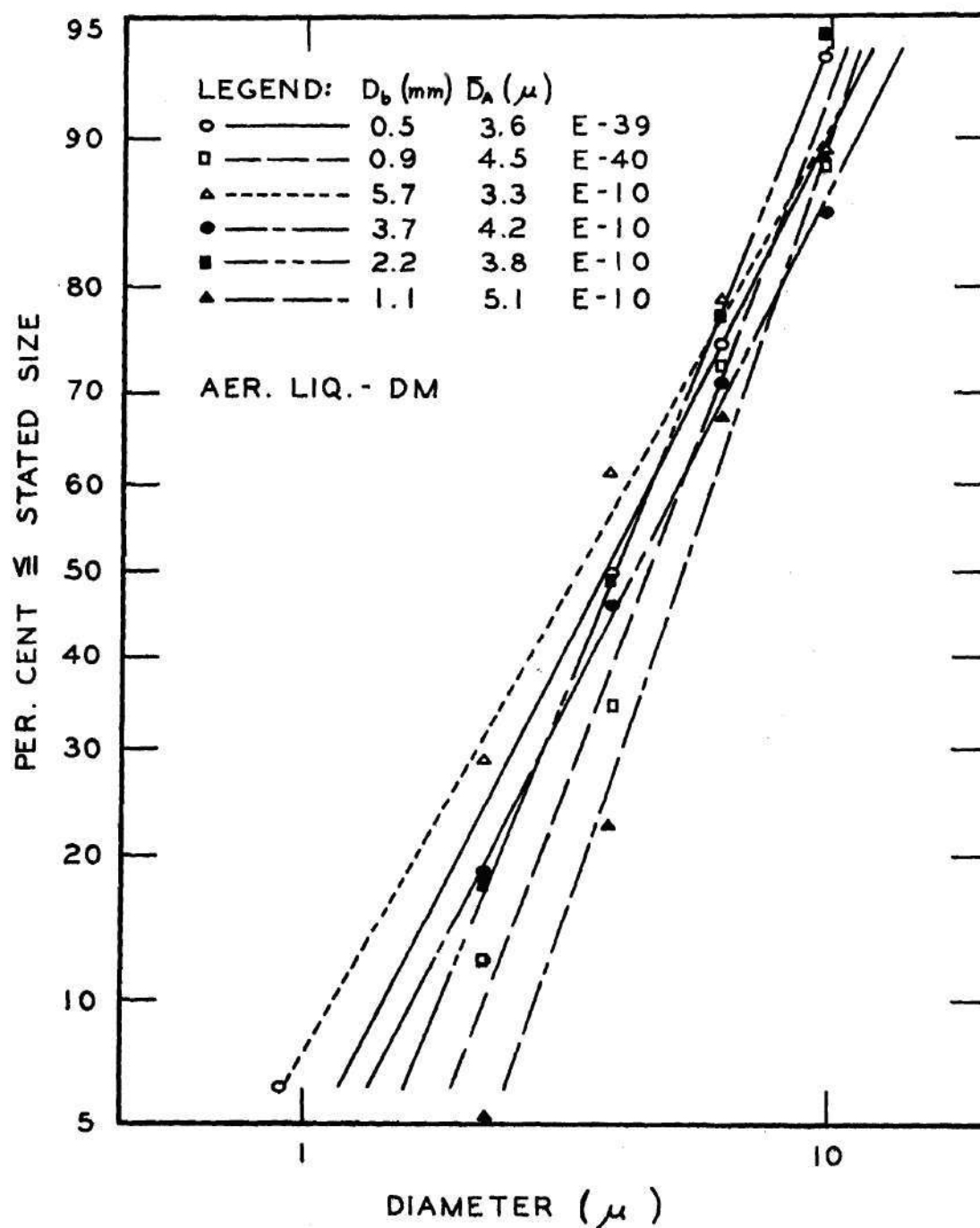


Figure 18. Log Probability Plot of Bioparticle Size Distributions for 0.5, 0.9, 1.1, 2.2, 3.7, and 5.7 mm Bubbles

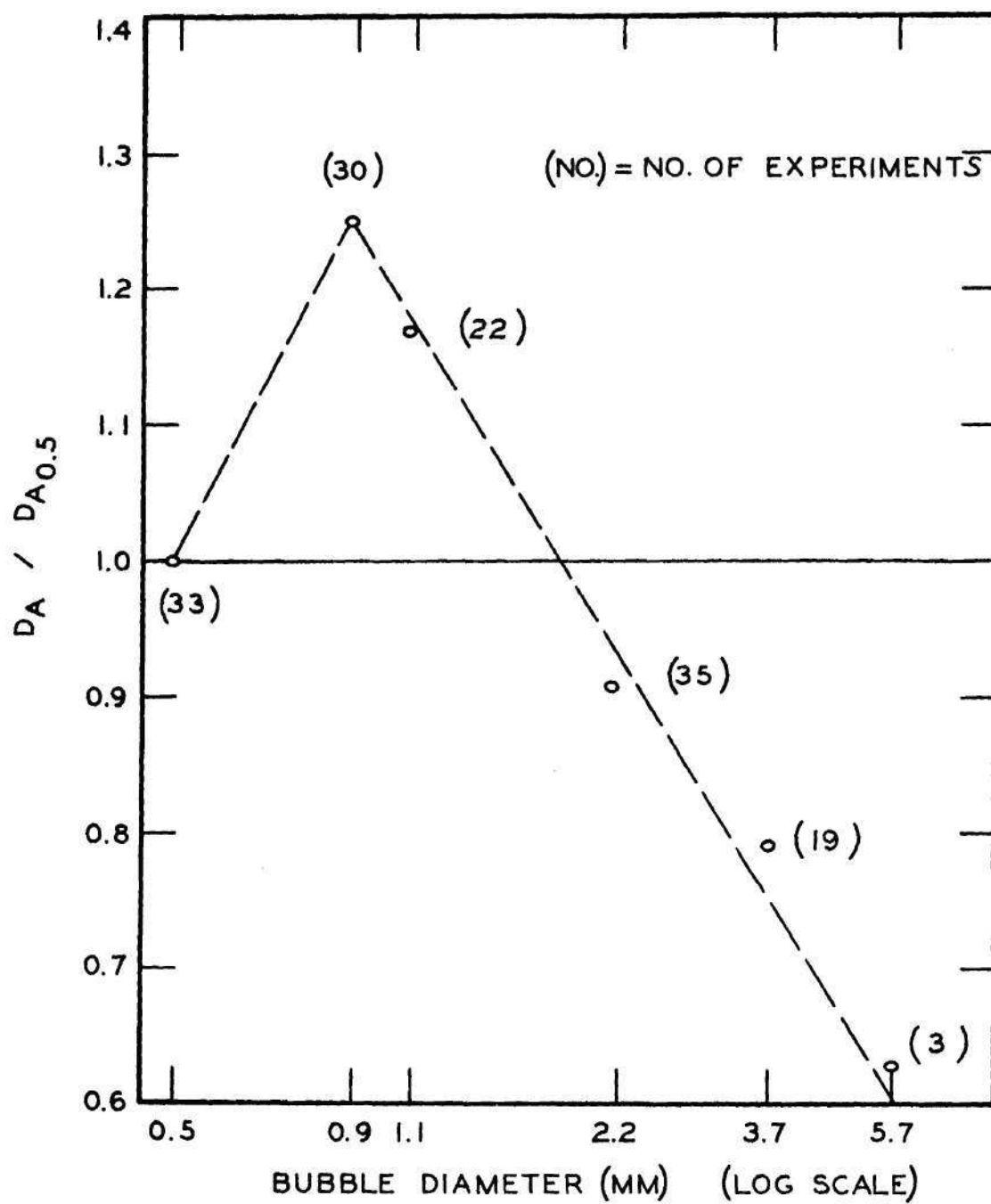


Figure 19. Ratio of Mean Bioparticle Size to Mean Size for 0.5 mm Bubbles versus Bubble Diameter



However, droplets larger than the median size expected from the jet droplets produced by 1.0 mm bubbles could not be entrained in the conditioning column and were therefore not observed in sampling data. Some decrease in mean bioparticle size may be justified in such a manner, but the decrease is larger than would be expected due to the maximum entrained droplet size alone. In fact, increased bubble size would be expected to produce smaller film droplets because of progressively thinner films.

The number of jet droplets per bubble burst has been shown to decrease as the bubble size becomes larger than 1.2 mm diameter (32). Figure 20 confirms that the number of observable droplets per bubble burst not only increased from a bubble size of 0.5 mm to one of 1.1 mm diameter as would be expected (32), but also increased with increasing bubble size to 5.7 mm. This finding further indicates that not only the jet droplet mechanism is in operation, but also that an additional mechanism (film droplet) is in evidence, especially for bubbles of 2.2 mm diameter and larger. The observed differences in droplet production in relation to bubble size were found to be significant at the 99 per cent level of confidence (See Appendix E).

Closer examination of the size distribution data reveals a trend in the dispersion of bioparticle sizes. The mean geometric standard deviations of the distributions for the different bubble sizes, reduced to a common base, are plotted in Figure 21 (See also Appendix E). The mean geometric standard deviation is shown to increase with bubble size to a maximum at a bubble size of about 1.1 mm and then to decrease to a bubble size of 5.7 mm. Again, these data indicate two mechanisms of droplet production. The dispersion of droplet sizes for either of the two mechanisms

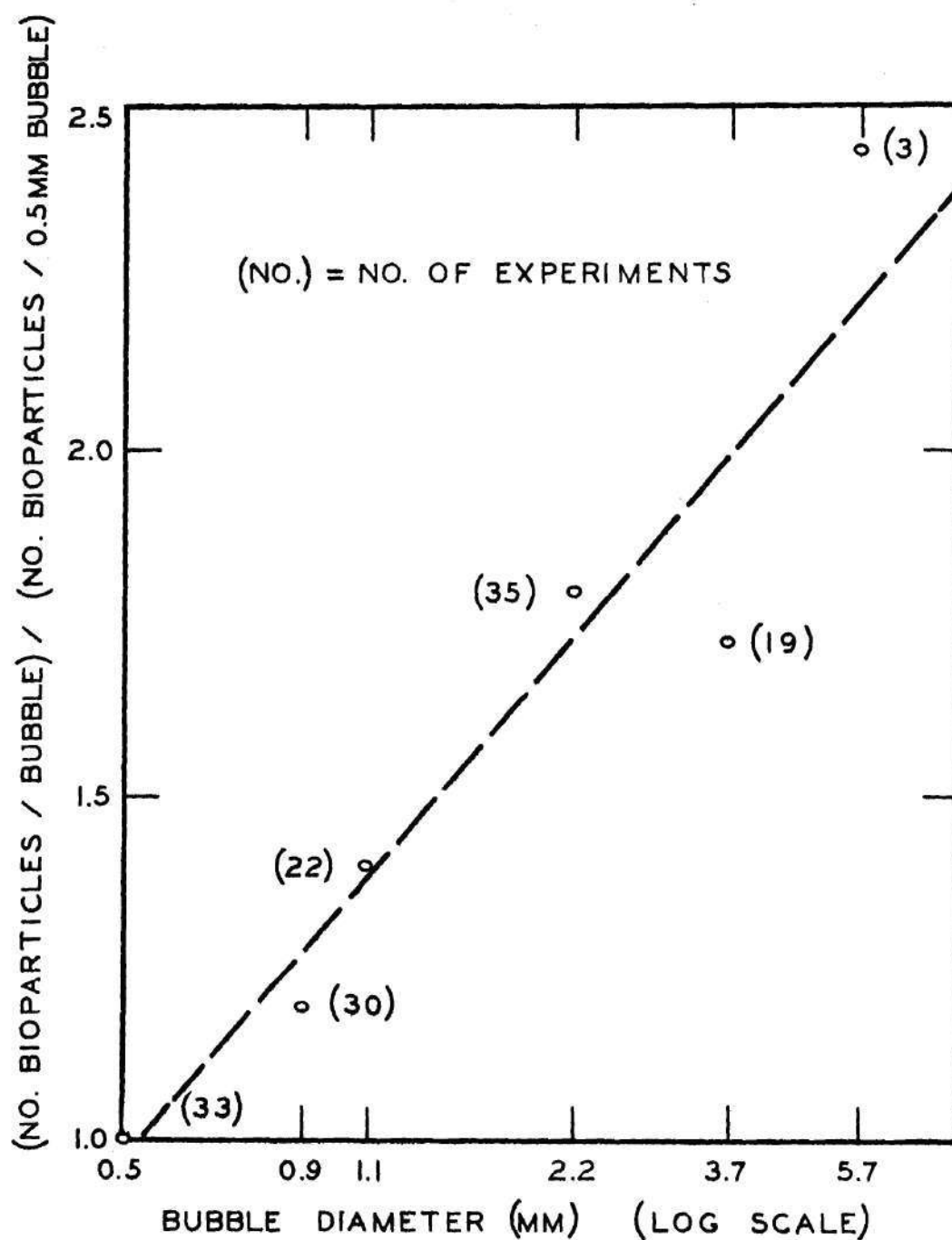


Figure 20. Ratio of Bioparticle Production Rate to Production Rate for 0.5 mm Bubbles versus Bubble Diameter

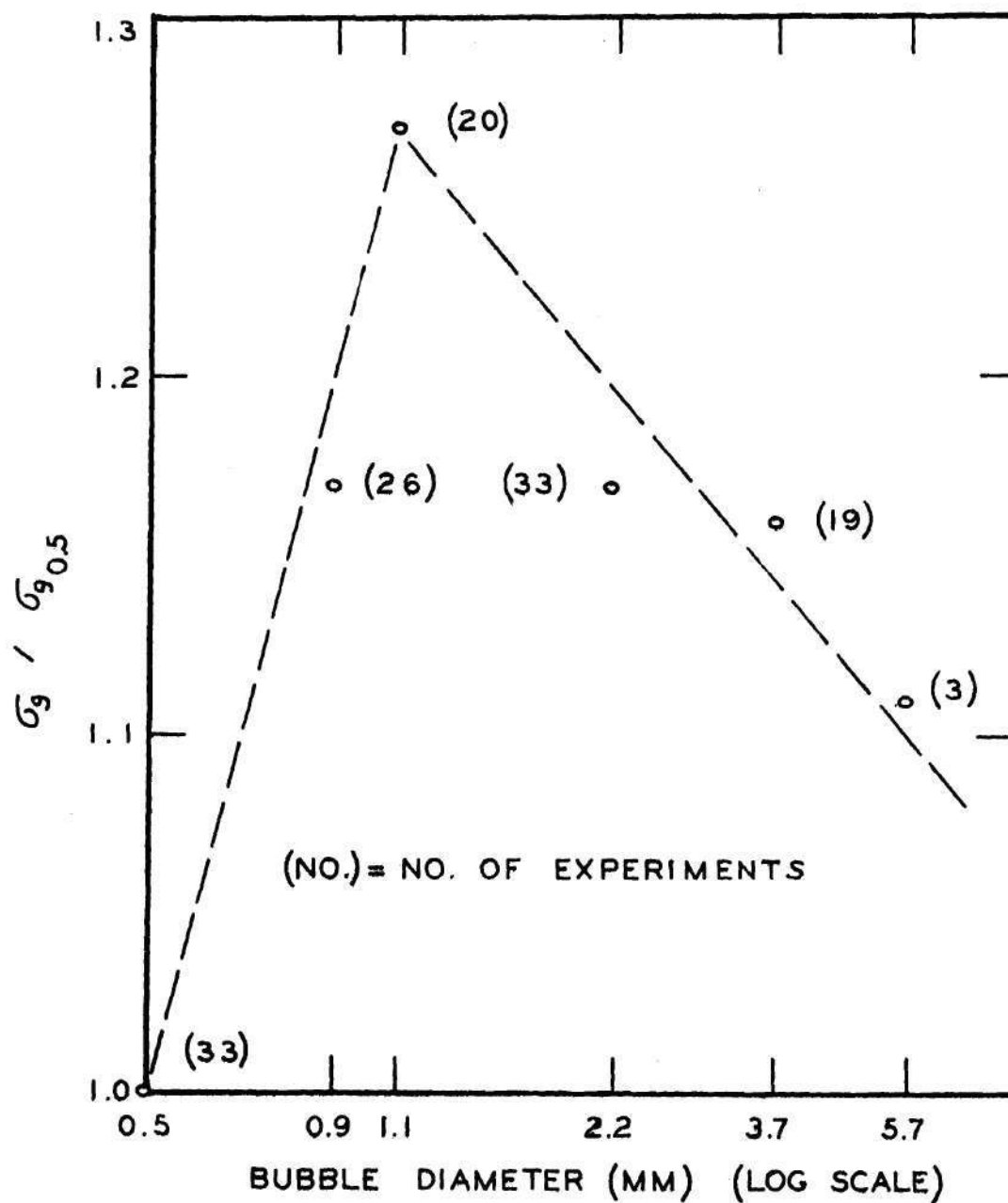


Figure 21. Ratio of Geometric Standard Deviation of Bioparticle Size Distribution to Geometric Standard Deviation for 0.5 mm Bubbles versus Bubble Diameter

(jet droplet and film droplet) would be expected to be relatively small. But the mean sizes would be expected to differ (33). Therefore, the dispersion of the distribution of droplets produced by both mechanisms taken together would be expected to be greater. Since jet droplets are expected for the 0.5 mm bubble size (35) and film droplets at the 5.7 mm size (33), the existence of the two together at the 1.1 mm size is indicated by the larger mean geometric standard deviation. The trend toward more film droplets and fewer jet droplets as bubble size increases is indicated by a decrease in mean geometric standard deviation.

The data for mean bioparticle production when reported as production per liter of aeration air, under the conditions of this research, become even more significant. Production of bioparticles per liter of aeration air as related to bubble size is shown in Figure 22. An average of over three million viable bioparticles were produced per liter of aeration air with 0.5 mm bubbles. Production is reduced to less than six thousand bioparticles per liter with 5.7 mm bubbles. These data are highly significant when considered from the standpoint that approximately half of the bioparticles produced were of a size range permitting lung penetration. The solids concentrations employed in the liquids were not significantly different from those observed for many domestic sewages as they undergo treatment (78). The mean spore concentration of the liquids employed to obtain these data ranged from  $1.2 \times 10^7$  to  $7.8 \times 10^7$  per ml and is comparable with microorganism concentrations reported for domestic sewage (79).

Plotted for comparison along with production data in Figure 22 is a curve representing the expected variation of bioparticle production rate



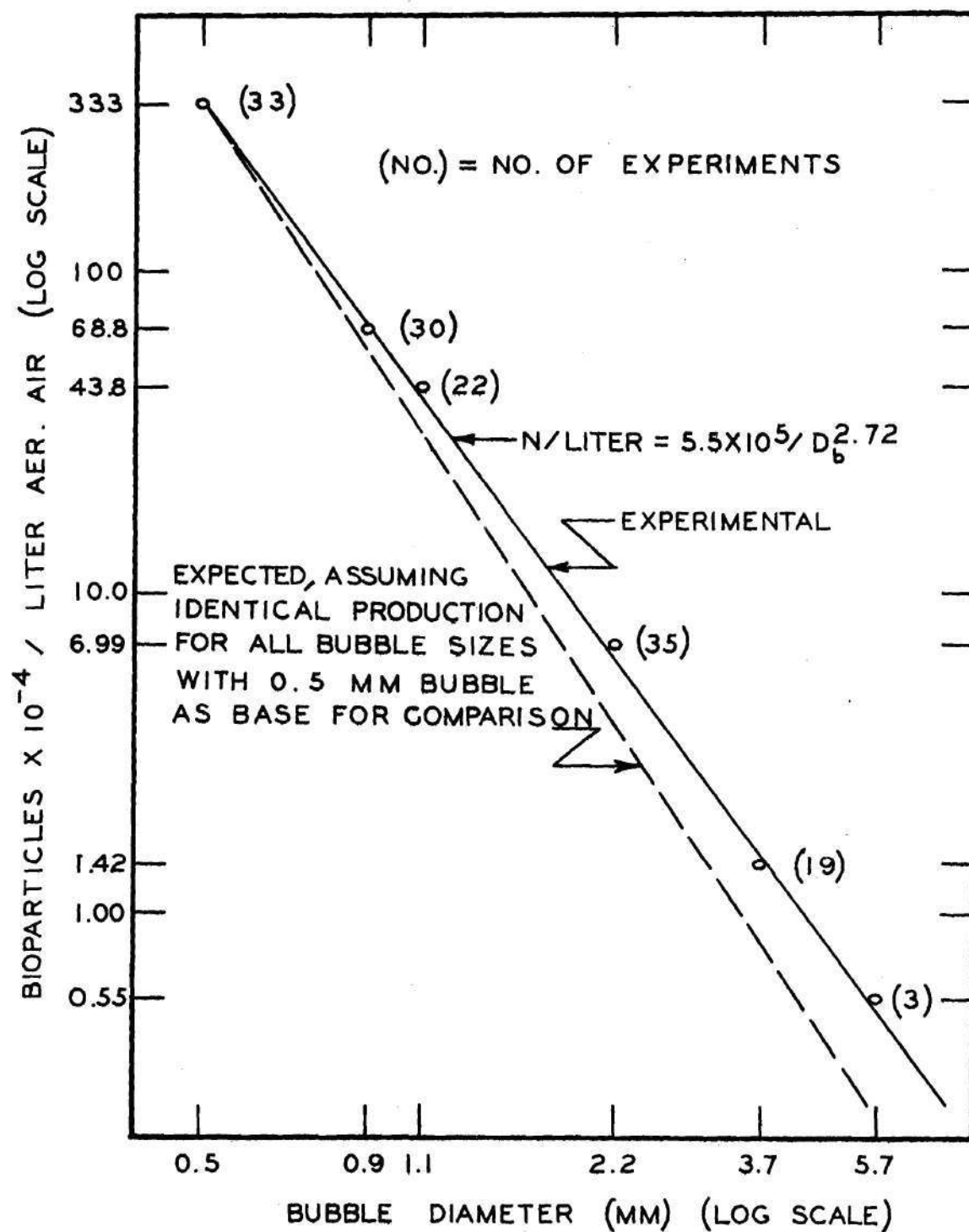


Figure 22. Bioparticle Production per Liter of Aeration Air in Relation to Bubble Diameter

per liter of aeration air assuming identical production per bubble irrespective of bubble size with the production for 0.5 mm bubbles taken as a base for comparison. The variation in bioparticle production per liter of aeration air is thus seen to depend to a greater extent upon volume of air per bubble than upon the variation of bioparticle production per bubble.

It should be pointed out that in sewage treatment practices involving aeration, smaller bubble sizes are desirable to obtain maximum oxygen transfer from air to liquid.

#### Effect of Test Liquid Composition on Bioparticle Production

The liquids used in this study were chosen not only to demonstrate the effects of liquid composition but to allow observation of the bioaerosol production mechanisms. Typical results obtained by use of the various liquids are presented in Figures 23, 24, 25, and 26.

With the jet droplet mechanism, an amount of liquid from the bulk of the liquid is projected into the air upon collapse of a bubble crater. Whether or not there is any association of spores with liquid films and the air-liquid interface can have little or no effect upon the probability that a droplet of liquid containing a given spore concentration will actually contain a spore. Therefore, the primary effect of the use of any one of the three types of liquids should only shift the median particle diameter to a larger size based upon the equilibrium water content of the particle as dictated by the experimental conditions. Shown in Figure 23 are typical bioparticle size distribution plots for DM and G-150 liquids produced by 0.9 mm bubbles. The distribution for the G-150 liquid is essentially identical to the distribution for the DM liquid with only a

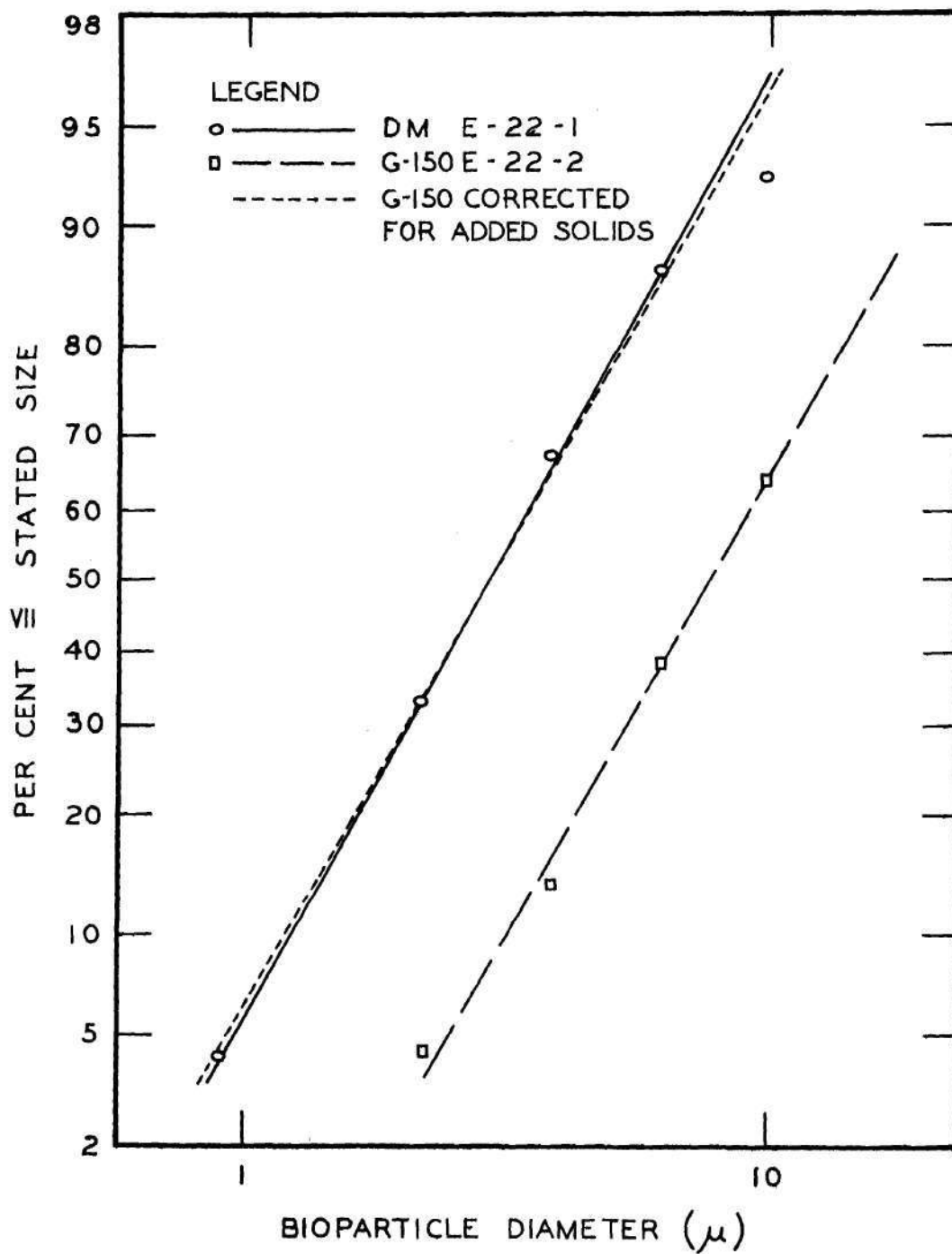


Figure 23. Log Probability Plot of Bioparticle Size Distributions for DM and G-150 Test Liquids and 0.9 mm Bubbles

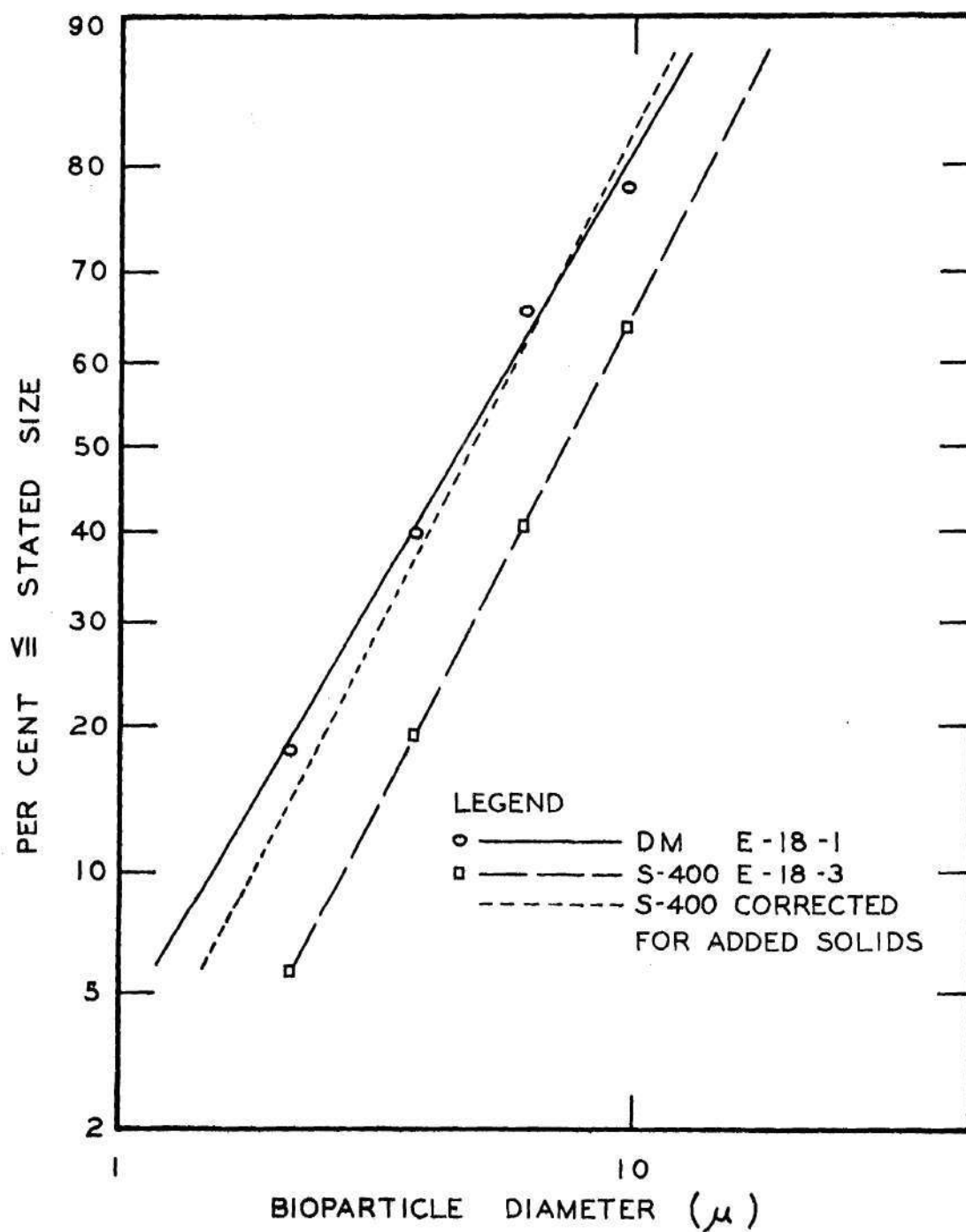


Figure 24. Log Probability Plot of Bioparticle Size Distributions for DM and S-400 Test Liquids and 0.8 mm Bubbles



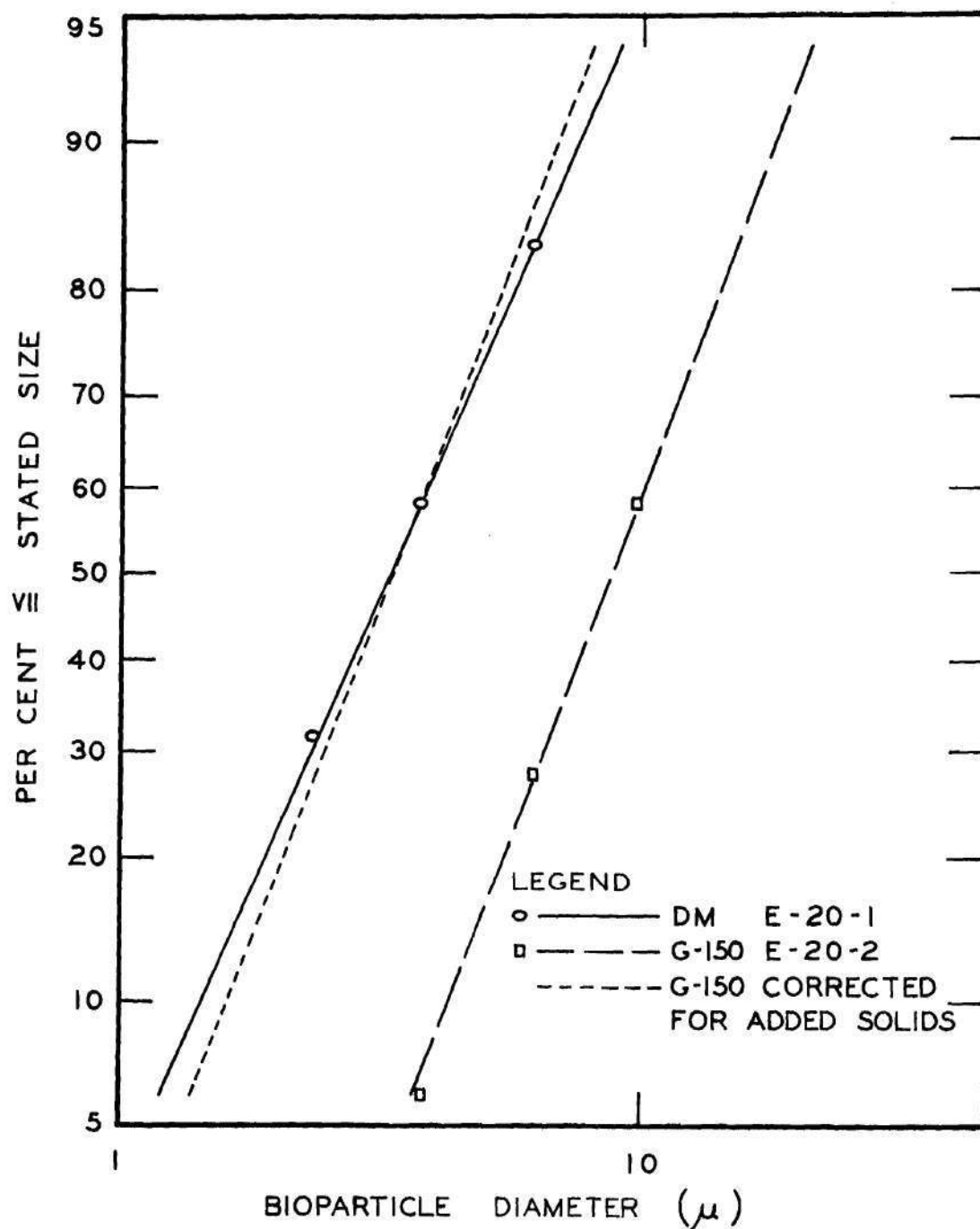


Figure 25. Log Probability Plot of Bioparticle Size Distributions for DM and G-150 Test Liquids and 3.7 mm Bubbles

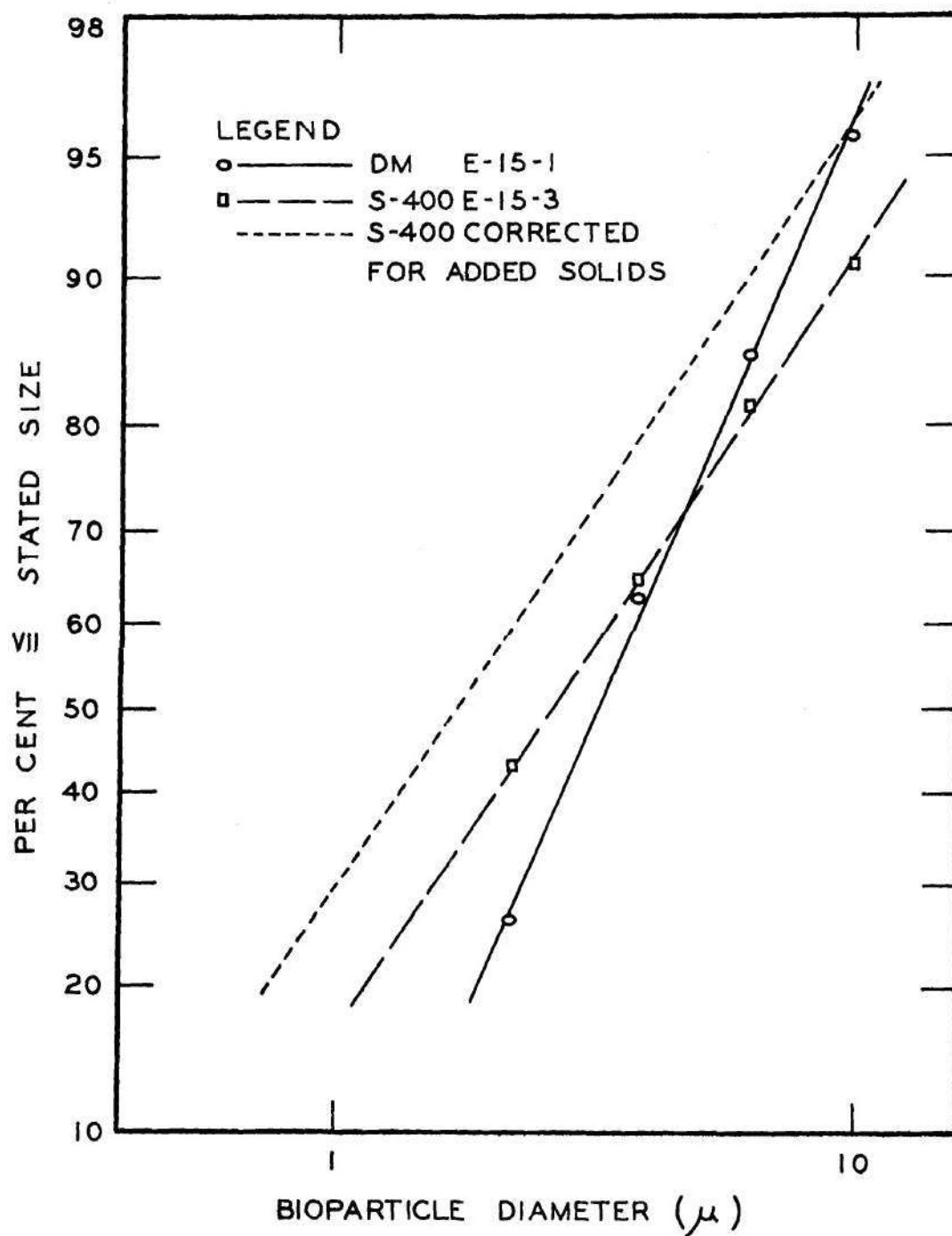


Figure 26. Log Probability Plot of Bioparticle Size Distributions for DM and S-400 Test Liquids and 3.7 mm Bubbles

shift in median particle size. When the G-150 distribution is shifted to nullify the effect of the increased solids concentration, the two distributions become essentially one and the same. Figure 24 shows the same type data for DM and S-400 liquids for a bubble size of 0.8 mm. Again, the essential difference is the shift in median particle size to account for the increased solids content of the liquid. The fact that S-400 liquid is an electrolytic solution and interacts with the spore surface is not evident in the plot. These same types of relationships were observed to hold for all liquids used with bubble sizes of 0.9 mm and smaller. A summary of the data upon which this statement is based is presented in Table 7. The indication again is that the jet droplet mechanism is the mechanism primarily responsible for droplet production with bubble sizes of 0.9 mm and smaller. The evidence is that the jet droplet mechanism can produce viable bioaerosols.

Table 7. Effect of Test Liquid on Bioparticle Distribution Characteristics

Exp. no.	Bubble dia. (mm)	Test liq.	Per Cent $\leq 2.2\mu$ dia.	Mean dia. ( $\mu$ )
(1)	(2)	(3)	(4)	(5)
15	3.7	DM	28	3.2
		S-100	40	2.8
		S-400	62	1.7
16	2.2	DM	41	2.6
		S-100	39	2.8
		S-400	66	1.5
17	1.2	DM	18	6.1
		S-100	35	3.2
		S-400	57	1.9

Table 7. Effect of Test Liquid on Bioparticle  
Distribution Characteristics (Continued)

Exp. no.	Bubble dia. (mm)	Test liq.	Per Cent ≤ 2.2 $\mu$ dia.	Mean dia. ( $\mu$ )
(1)	(2)	(3)	(4)	(5)
18	0.8	DM	20	4.7
		S-100	20	4.6
		S-400	16	4.7
19	0.5	DM	12	4.8
		S-400	22	4.6
20	3.7	DM	27	3.3
		G-150	24	3.3
21	2.2	DM	25	3.3
		G-150	16	3.9
22	0.5	DM	33	2.9
		G-150	33	2.9
23	1.2	DM	22	3.4
		G-150	37	3.3
39	0.5	DM	25	3.6
		DA-50	30	3.6
		A-50	25	4.5
40	0.9	DM	15	4.5
		DA-50	11	13.8
		A-50	13	4.5
41	1.7	DM	24	3.1
		DA-50	23	4.5
		A-50	33	2.9
42	3.7	DM	19	3.6
		DA-50	25	3.4
		A-50	34	2.8
53	3.7	DM	28	3.1
		DA-100	64	1.3
		A-100	65	1.8



Table 7. Effect of Test Liquid on Bioparticle  
Distribution Characteristics (Continued)

Exp. no.	Bubble dia. (mm)	Test liq.	Per Cent $\leq 2.2 \mu$ dia.	Mean dia. ( $\mu$ )
(1)	(2)	(3)	(4)	(5)
54	2.2	DM	17	3.1
		DA-100	44	2.5
		A-100	65	1.8
55	0.9	DM	28	2.9
		DA-100	4	8.3
		A-100	28	2.9
56	0.5	DM	34	2.9
		DA-100	34	2.9
		A-100	22	3.5
61	0.8	DM	44	2.5
		P-400	32	2.8
		P-200	27	3.0
62	2.2	DM	32	3.2
		P-200	19	3.8
		P-400	18	3.6
63	1.1	DM	10	4.7
		P-200	5	4.4
		P-400	8	4.3
64	0.5	DM	30	3.2
		P-200	21	3.2
		P-400	16	3.2
65	0.6	DM	33	3.0
		PH-400	32	3.2
66	1.1	DM	19	3.9
		PH-400	38	2.6
67	2.2	DM	17	4.0
		PH-400	33	2.8
68	0.9	DM	35	2.8
		PH-400	30	2.8

Table 7. Effect of Test Liquid on Bioparticle Distribution Characteristics (Continued)

Exp. no.	Bubble dia. (mm)	Test liq.	Per Cent $\leq 2.2 \mu$ dia.	Mean dia. ( $\mu$ )
(1)	(2)	(3)	(4)	(5)
74	0.9	DM	20	3.2
		A-25	25	3.2
75	1.7	DM	18	4.4
		A-25	35	2.7
76	3.7	DM	8	4.9
		A-25	23	3.4

Note: Data in columns (4) and (5) have been adjusted for solids concentration to compare with DM.

For bubbles of a size to permit the formation of droplets by the film droplet mechanism, some of the different types of liquids should produce distribution changes. Again, since they should have essentially no effect upon the spore surface characteristics, the inert liquids should have no effect on distribution except to shift the mean diameter to a larger size as indicated by the typical results shown in Figure 25 for G-150 and a bubble size of 3.7 mm. The G-150 distribution when shifted to account for the increased solids concentration becomes almost identical to the distribution for DM as was observed for all experimental data involving inert liquids (See Table 7).

The electrolytic and collector type liquids were observed to cause changes in bioparticle size distributions for the larger bubbles when compared to those for DM. Figure 26 is for DM and S-400 liquids and 3.7 mm

bubbles. As may be seen the mean particle size did not become larger as was the case for G-150 and as would be expected merely from an increase in solids concentration, but instead became smaller. Moreover, when the distribution was shifted to account for the increased solids concentration, the median particle size became even smaller. As may be seen from Figure 26, the corrected median particle size for S-400 is  $1.7\mu$  as compared with  $3.2\mu$  for DM. Approximately 65 per cent of the particles produced by the S-400 liquid were equal to or less than  $2.2\mu$  while only about 25 per cent of the particles produced by DM were equal to or less than  $2.2\mu$ . The indication is that a significant change in droplet production and resulting distribution has occurred. This same type alteration of particle size distribution occurred also with liquids containing organic collectors and other electrolytes for bubble sizes of from 3.7 mm to 1.7 mm and to a lesser degree to 1.1 mm. A summary of these data are presented in Table 7.

As shown in Figure 27 and as presented by other investigators, salt concentrations of the magnitude used in these experiments have very little effect upon the production of droplets by the jet droplet mechanism. Thus the modification of the particle size distribution noted in Figure 26 is regarded due to the presence of film droplets.

The alteration of particle size distribution as discussed above leads to an explanation as follows: The addition of electrolytes or organic collectors to the liquid allows the apores in the liquid to be less repulsive to the air-liquid interface, in other words, to be less hydrophylic and more hydrophobic. As the bubble film drains prior to rupture, the less hydrophylic a spore becomes, the greater the change it has of becoming entrapped between the two air-liquid interfaces of the film.

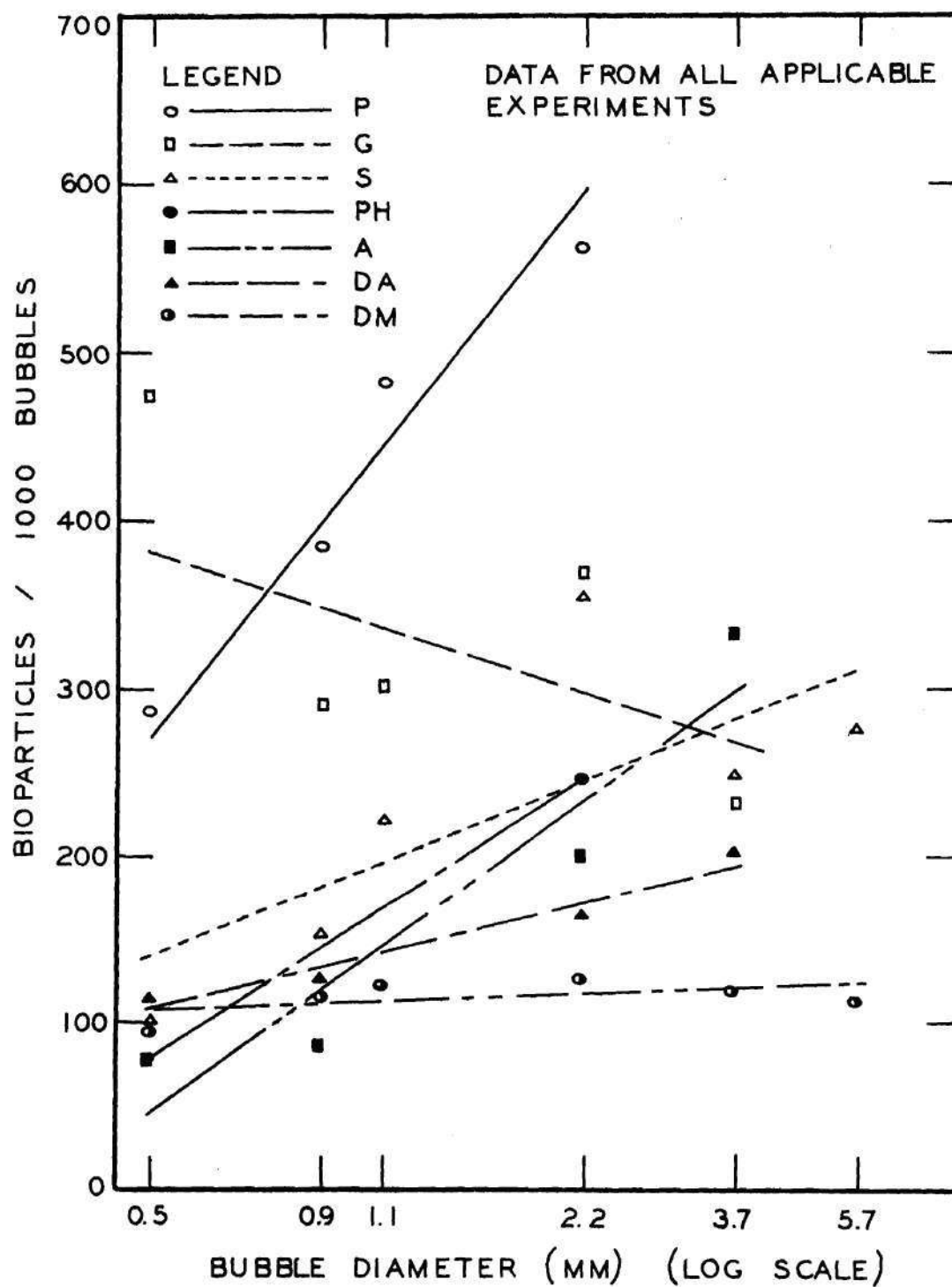


Figure 27. Bioparticle Production Rate for Various Test Liquids in Relation to Bubble Diameter



The greater the chance of being trapped, the higher the spore concentration is in the drained film, and therefore, the greater the chance that a film droplet will contain a spore. This process would have no effect upon the bioaerosol produced by the jet droplet mechanism. Even if the observed distribution changes are in part the result of minor changes in surface tension and viscosity, the fact that the changes occur with large bubbles shown by investigation (33) to produce film droplets and does not occur with small bubbles shown by others (35) not to produce film droplets is indication that the changes are a result of the presence of film droplets. Thus the indication is that the film droplet mechanism is capable of producing viable bioaerosols.

Figure 28 was constructed to allow observation of the effectiveness of the various test liquids in producing bioaerosols. Mean production rates were compared with the mean production rates of DM for the various bubble sizes employed. The production rates for DM, DA, A, PH, and S were approximately the same for bubble sizes of 0.5 mm and 0.9 mm. In each case, the bubbles burst quickly upon reaching the liquid surface with some bubble mergers for the 0.9 mm bubble size. The production rates for both G and P were substantially greater. The bubbles remained at the liquid surface for periods of time up to six seconds before bursting with no bubble mergers. The indication is that bioaerosol production by the jet droplet mechanism may be somewhat dependent upon bubble stability at the liquid surface.

For bubble sizes of 1.1 mm and greater, every liquid showed substantially greater production of bioparticles per 1000 bubbles than did DM. For DM, DA, A, PH, and S, the bubbles burst quickly upon reaching the

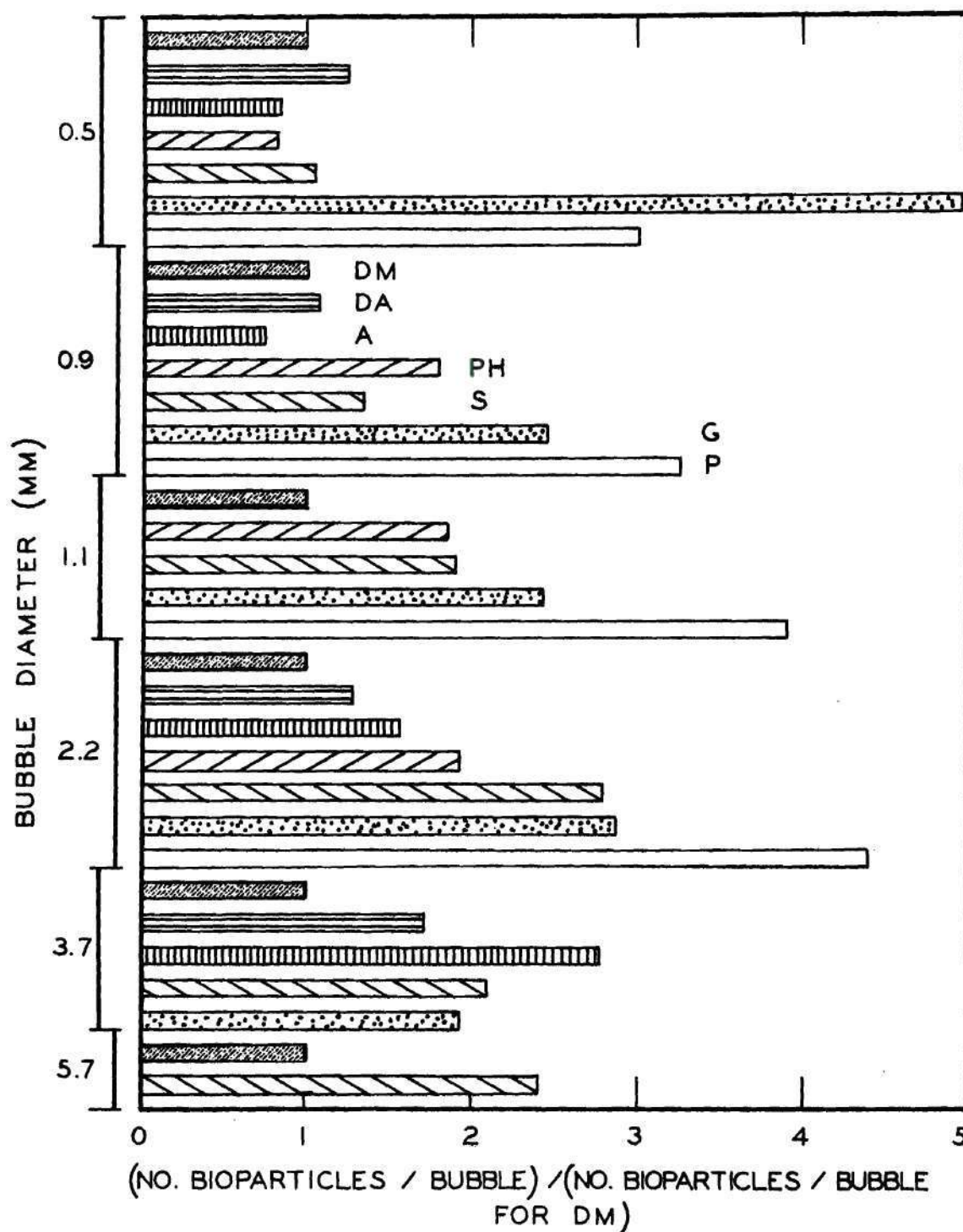


Figure 28. Comparison of Bioparticle Production Rates for Various Test Liquids and Bubble Sizes in Relation to Production Rates for DM Test Liquid

surface but less quickly than for the smaller bubble sizes. There were some bubble mergers. Again, G and P produced bubble stability at the surface up to six seconds.

The continued increase in bioparticle production rates with increase in bubble size in a bubble size range where the production of jet droplets has been shown to decrease with increasing bubble size provides further indication of the action of the film droplet mechanism in bioaerosol production. Table 8 provides a comparison of bioparticle production rates for the various bubble sizes for each test liquid based upon production rates for the 0.5 mm bubble size. The only liquid other than DM which does not show marked increase in production rate for the larger bubble sizes is G which actually shows a decrease. The surface viscosity of gelatin is high compared with water. The greater surface viscosity may account for the reduced relative production in the range of bubble sizes in which film droplets presumably account for the major production of bioparticles.

Table 8. Comparison of Bioparticle Production Rates

Test liquid	Per cent mean bioparticle production rate for various bubble sizes based upon production rate for bubble size 0.5 mm.					
	0.5	0.9	1.1	2.2	3.7	5.7
DM	100	123	129	133	125	120
DA	100	108		140	176	
A	100	107		251	417	
PH	100	268	290	310		
S	100	156	220	354	249	276
G	100	61	63	77	49	
P	100	133	168	195		



## CHAPTER V

## SUMMARY AND CONCLUSION

The major goals of this study were achieved. Bioaerosols were found to be produced by the bursting of 0.5 mm to 5.7 mm diameter bubbles (the range of bubble sizes studied) at the surface of liquids containing tracer spores of Bacillus subtilis var. niger. Jet droplets formed by the collapse of bubble craters were observed to provide a mode of bioaerosol generation from bubbles of 0.5 mm to approximately 1.0 mm diameter. Film droplets created by the rupture of bubble films were found to supply a means of bioaerosol generation from bubbles of approximately 1.0 mm to 5.7 mm diameter.

Other findings of importance were also made. Bioparticle production rate varied in direct proportion to the spore concentration of the test liquid to a concentration at which each droplet contained at least one spore. With further increases in spore concentration, production rate remained essentially constant. For a mean spore concentration comparable with microorganism concentrations found in domestic wastes, mean bioparticle production was observed to range from a maximum of approximately three million bioparticles per liter of aeration air for 0.5 mm diameter bubbles to a minimum of approximately five thousand per liter for 5.7 mm diameter bubbles. Bioparticle size distribution in air varied with the spore concentration of the liquid. Increases in spore concentration resulted in decreased mean bioparticle size and increased dispersion of size distribution as the chance for smaller and smaller droplets to

contain at least one spore increased.

Bioparticle size distribution characteristics were found to vary with bubble size. Median bioparticle size increased with bubble size to a maximum for bubbles of approximately 0.9 mm diameter and then decreased to a minimum for 5.7 mm bubbles. Dispersion of size distribution increased with bubble size from a minimum for bubbles of 0.5 mm diameter to a maximum for 1.1 mm bubbles and then decreased to an intermediate value for 5.7 mm bubbles. Bioparticle production per bubble burst increased with bubble size.

Bioparticle production varied with the composition of the liquid being aerated. Bioparticle production was from two to five times greater for gelatin and peptone sols than for demineralized water. Although essentially the same for bubbles of from 0.5 to 1.0 mm diameter, production for larger bubbles ranged up to three times greater for sodium chloride, dibasic potassium phosphate, octanoic acid, and dipentylamine solutions than for demineralized water. Water sols of gelatin and peptone affected the size distribution of bioparticles over the entire range of bubble sizes studied by increasing the median bioparticle size without significantly affecting dispersion. Water solutions of sodium chloride and dibasic potassium phosphate and collector solutions of octanoic acid and dipentylamine affected bioparticle size distribution by increasing the median sizes without significantly affecting dispersion for bubbles up to approximately one mm diameter. However, the electrolyte and collector solutions were observed to decrease median bioparticle size and increase dispersion for bubbles larger than approximately one mm diameter.

The median bioparticle sizes produced under the conditions of this

study were generally small enough to remain airborne and to permit lung penetration with the larger sizes capable of being retained in the upper regions of the human respiratory system.

#### Conclusion

It was concluded within the limits of this research that: (1) bio-aerosols are produced by bubbles bursting at the surface of liquids containing microorganisms; (2) that both the rupture of bubble films as well as the subsequent collapse of bubble craters provide mechanisms for the production of bioaerosols; (3) that bubble size and the composition and microorganism concentration of the liquid being aerated significantly affect bioparticle size distribution and production rate; and (4) that aeration of contaminated wastes and other liquids could be responsible for the production of hazardous aerosols.



## CHAPTER VI

### RECOMMENDATIONS

Based upon the findings of this study, the following recommendations are presented.

Domestic waste treatment devices and processes employing aeration should be considered as potentially hazardous from the standpoint of airborne infection. A comprehensive epidemiological study of the incidence of respiratory and other diseases in sewage treatment plant personnel should be initiated. Such studies should also be conducted in residential and other areas surrounding aeration facilities which are used to treat domestic wastes from Tuberculosis hospitals in an effort to search out a possible factor in the rising incidence of Tuberculosis in this country.

Thought should be given to possible ways of controlling bioaerosol production from the activated sludge process. Potential corrective measures might include (1) addition of chemicals to the waste being aerated to reduce the association of pathogenic microorganisms with the air-water interface, (2) addition of chemicals to alter the characteristics of the wastes which allow the production of bioaerosols, (3) supplying of oxygen to the process by means other than bubble aeration such as the use of oxygen transfer membranes, (4) covering the aeration tanks and providing for recirculation and/or filtration of process air or passage of the air through incinerators and (5) possibly replacing the process with one which does not present a potential airborne infection hazard.

Laboratory experiments involving aeration of contaminated liquids



should be conducted in vented hoods or possibly in well vented rooms provided with means for high efficiency filtration of recirculated and wasted air.

Studies should be conducted to determine if there is any selectivity in the aerosolization of pathogenic and potentially pathogenic microorganisms by aeration. Studies should also be directed toward alteration of the aeration process and/or microorganisms involved in an effort to determine ways of reducing and possibly eliminating the production of hazardous bioaerosols by aeration. The vertical column experimental design used in this study proved to be a useful device for studies of this nature. It can be very easily converted into a completely closed system design for the study of pathogenic microorganisms.

An index or index organism should be formulated or discovered which will allow evaluation of the airborne infection potential from sewage treatment devices.

## APPENDIX A

## BASIC EXPERIMENTAL DATA

Table 9. Basic Experimental Data

Exp. no.	Run no.	Date	Test liq.	Spore conc.  $\times 10^{-7}/\text{ml}$	Bubble		Temp.  (°C)	Rel. hum.  (%)
					Dia. (mm)	Rate /min		
(1)	(2)	(3)	(4)	(5)	(6)	(7)	(8)	(9)
10	1	9-21-65	DM	7.1	5.7	1000	23	40
10	2	9-21-65	DM	7.1	3.7	1000	23	40
10	3	9-21-65	DM	7.1	2.2	1000	23	40
10	4	9-21-65	DM	7.1	1.1	1000	23	40
11	1	9-22-65	S-100	7.1	5.7	1000	23	37
11	2	9-22-65	S-100	7.1	3.7	1000	23	37
11	3	9-22-65	S-100	7.1	2.2	1000	23	37
11	4	9-22-65	S-100	7.1	1.1	1000	23	37
12	1	9-23-65	S-1600	7.1	5.7	1000	24	35
12	2	9-23-65	S-1600	7.1	3.7	1000	24	35
12	3	9-23-65	S-1600	7.1	2.2	1000	24	35
12	4	9-23-65	S-1600	7.1	1.1	1000	24	35
13	1	9-24-65	S-400	7.1	5.7	1000	24	38
13	2	9-24-65	S-400	7.1	3.7	1000	24	38
13	3	9-24-65	S-400	7.1	2.2	1000	24	38
13	4	9-24-65	S-400	7.1	1.1	1000	24	38
15	1	10-7-65	DM	5.2	3.7	1000	24	35
15	2	10-7-65	S-100	5.2	3.7	1000	24	35
15	3	10-7-65	S-400	5.4	3.7	1000	24	35
15	4	10-7-65	S-1600	5.4	3.7	1000	24	35
16	1	10-8-65	DM	7.8	2.2	1000	24	35
16	2	10-8-65	S-100	7.8	2.2	1000	24	35
16	3	10-8-65	S-400	7.8	2.2	1000	24	35
17	1	10-8-65	DM	7.8	1.2	1000	24	35
17	2	10-8-65	S-100	7.8	1.2	1000	24	35
17	3	10-8-65	S-400	7.8	1.2	1000	24	35
18	1	10-9-65	DM	4.6	0.8	1000	24	35
18	2	10-9-65	S-100	4.6	0.8	1000	24	35
18	3	10-9-65	S-400	4.6	0.8	1000	24	35
19	1	10-9-65	DM	4.6	0.5	800	24	35
19	2	10-9-65	S-100	4.6	0.5	800	24	35
19	3	10-9-65	S-400	4.6	0.5	800	24	35

Table 9. Basic Experimental Data (Continued)

Exp. no.	Run no.	Date	Test liq.	Spore conc.  X10 <sup>-7</sup> /ml	Bubble		Temp.  (°C)	Rel. hum.  (%)
					Dia. (mm)	Rate /min		
(1)	(2)	(3)	(4)	(5)	(6)	(7)	(8)	(9)
20	1	10-14-65	DM	3.5	3.7	1000	24	35
20	2	10-14-65	G-150	3.5	3.7	1000	24	35
20	3	10-14-65	G-300	3.5	3.7	1000	24	35
21	1	10-14-65	DM	3.5	2.2	1000	24	35
21	2	10-14-65	G-150	3.5	2.2	1000	24	35
21	3	10-14-65	G-300	3.5	2.2	1000	24	35
22	1	10-15-65	DM	1.2	0.5	800	24	35
22	2	10-15-65	G-150	1.2	0.5	800	24	35
22	3	10-15-65	G-300	1.2	0.5	800	24	35
23	1	10-15-65	DM	1.2	1.2	1000	24	35
23	2	10-15-65	G-150	1.2	1.2	1000	24	35
23	3	10-15-65	G-300	1.2	1.2	1000	24	35
24	1	10-19-65	G-150	0.25	2.2	1000	24	35
24	2	10-19-65	G-150	0.50	2.2	1000	24	35
24	3	10-19-65	G-150	1.3	2.2	1000	24	35
24	4	10-19-65	G-150	2.5	2.2	1000	24	35
25	1	10-20-65	G-150	0.12	1.1	1000	23	37
25	2	10-20-65	G-150	0.24	1.1	1000	23	37
25	3	10-20-65	G-150	0.60	1.1	1000	23	37
25	4	10-20-65	G-150	1.2	1.1	1000	23	37
26	1	10-21-65	G-150	0.15	0.9	1000	24	35
26	2	10-21-65	G-150	0.30	0.9	1000	24	35
26	3	10-21-65	G-150	0.75	0.9	1000	24	35
26	4	10-21-65	G-150	1.5	0.9	1000	24	35
27	1	10-21-65	G-150	0.53	0.5	800	24	35
27	2	10-21-65	G-150	1.1	0.5	800	24	35
27	3	10-21-65	G-150	2.7	0.5	800	24	35
27	4	10-21-65	G-150	5.3	0.5	800	24	35
28	1	11-16-65	G-50	5.4	0.9	1000	23	34
28	2	11-16-65	G-75	5.4	0.9	1000	23	34
28	3	11-16-65	G-100	5.4	0.9	1000	23	34



Table 9. Basic Experimental Data (Continued)

Exp. no.	Run no.	Date	Test liq.	Spore conc.  $\times 10^{-7}/\text{ml}$	Bubble		Temp.  (°C)	Rel. hum.  (%)
					Dia. (mm)	Rate /min		
(1)	(2)	(3)	(4)	(5)	(6)	(7)	(8)	(9)
29	1	11-16-65	G-50	3.7	1.1	1000	23	34
29	2	11-16-65	G-100	3.7	1.1	1000	23	34
29	3	11-16-65	G-150	3.7	1.1	1000	23	34
29	4	11-16-65	G-200	3.7	1.1	1000	23	34
29	5	11-16-65	G-250	3.7	1.1	1000	23	34
30	1	11-16-65	G-100	2.6	1.7	1000	23	34
30	2	11-16-65	G-150	2.6	1.7	1000	23	34
30	3	11-16-65	G-200	2.6	1.7	1000	23	34
31	1	11-16-65	G-100	2.6	3.7	1000	23	34
31	2	11-16-65	G-150	2.6	3.7	1000	23	34
31	3	11-16-65	G-200	2.6	3.7	1000	23	34
32	1	11-16-65	G-100	2.6	0.5	800	23	34
32	2	11-16-65	G-150	2.6	0.5	800	23	34
32	3	11-16-65	G-200	2.6	0.5	800	23	34
33	1	11-16-65	G-100	2.6	0.9	1000	23	30
33	2	11-16-65	G-150	2.6	0.9	1000	23	30
33	3	11-16-65	G-200	2.6	0.9	1000	23	30
34	1	11-16-65	G-100	2.6	1.1	1000	23	30
34	2	11-16-65	G-150	2.6	1.1	1150	23	30
34	3	11-16-65	G-200	2.6	1.1	1300	23	30
35	1	11-23-65	G-100	0.15	0.5	800	23	30
35	2	11-23-65	G-100	0.45	0.5	800	23	30
35	3	11-23-65	G-100	0.6	0.5	800	23	30
35	4	11-23-65	G-100	0.9	0.5	800	23	30
35	5	11-23-65	G-100	1.1	0.5	800	23	30
35	6	11-23-65	G-100	1.5	0.5	800	23	30
36	1	11-23-65	G-100	0.08	0.9	900	23	34
36	2	11-23-65	G-100	0.15	0.9	900	23	34
36	3	11-23-65	G-100	0.3	0.9	900	23	34
36	4	11-23-65	G-100	0.45	0.9	900	23	34
36	5	11-23-65	G-100	0.6	0.9	900	23	34
36	6	11-23-65	G-100	1.1	0.9	900	23	34

Table 9. Basic Experimental Data (Continued)

Exp. no.	Run no.	Date	Test liq.	Spore conc.  X10 <sup>-7</sup> /ml	Bubble		Temp.  (°C)	Rel. hum.  (%)
					Dia. (mm)	Rate /min		
(1)	(2)	(3)	(4)	(5)	(6)	(7)	(8)	(9)
37	1	11-24-65	G-100	0.08	1.1	940	23	30
37	2	11-24-65	G-100	0.16	1.1	940	23	30
37	3	11-24-65	G-100	0.32	1.1	940	23	30
37	4	11-24-65	G-100	0.64	1.1	940	23	30
37	5	11-24-65	G-100	0.96	1.1	940	23	30
37	6	11-24-65	G-100	1.9	1.1	940	23	30
38	1	11-24-65	G-100	0.08	2.2	1000	23	30
38	2	11-24-65	G-100	0.16	2.2	1000	23	30
38	3	11-24-65	G-100	0.32	2.2	1000	23	30
38	4	11-24-65	G-100	0.64	2.2	1000	23	30
38	5	11-24-65	G-100	0.96	2.2	1000	23	30
38	6	11-24-65	G-100	1.9	2.2	1000	23	30
39	1	11-25-65	DM	3.5	0.5	780	22	26
39	2	11-25-65	DA-50	3.5	0.5	640	22	26
39	3	11-25-65	A-50	3.5	0.5	980	22	26
40	1	11-25-65	DM	3.5	0.9	950	22	26
40	2	11-25-65	DA-50	3.5	0.9	1100	22	26
40	3	11-25-65	A-50	3.5	0.9	1450	22	26
41	1	11-25-65	DM	3.5	1.7	1000	22	26
41	2	11-25-65	DA-50	3.5	1.7	1000	22	26
41	3	11-25-65	A-50	3.5	1.7	1000	22	26
42	1	11-25-65	DM	3.5	3.7	1000	22	26
42	2	11-25-65	DA-50	3.5	3.7	1000	22	26
42	3	11-25-65	A-50	3.5	3.7	1000	22	26
47	1	12-4-65	G-50	3.0	0.9	900	23	27
47	2	12-4-65	G-100	3.0	0.9	900	23	27
47	3	12-4-65	G-150	3.0	0.9	900	23	27
48	1	12-5-65	G-50	3.0	1.7	1000	23	27
48	2	12-5-65	G-100	3.0	1.7	1000	23	27
49	1	12-4-65	G-50	3.0	0.5	800	23	27
49	2	12-4-65	G-100	3.0	0.5	800	23	27
49	3	12-4-65	G-150	3.0	0.5	800	23	27

Table 9. Basic Experimental Data (Continued)

Exp. no.	Run no.	Date	Test liq.	Spore conc. $\times 10^{-7}/\text{ml}$	Bubble		Temp. (°C)	Rel. hum. (%)
					Dia. (mm)	Rate /min		
(1)	(2)	(3)	(4)	(5)	(6)	(7)	(8)	(9)
50	1	12-4-65	G-50	2.8	1.1	1000	23	27
50	2	12-4-65	G-100	2.8	1.1	1000	23	27
50	3	12-4-65	G-150	2.8	1.1	1000	23	27
51	1	12-5-65	G-50	2.8	2.2	1000	23	27
51	2	12-5-65	G-100	2.8	2.2	1000	23	27
51	3	12-5-65	G-150	2.8	2.2	1000	23	27
52	1	12-5-65	G-50	2.8	3.7	1000	23	27
52	2	12-5-65	G-100	2.8	3.7	1000	23	27
53	1	12-6-65	DM	3.2	3.7	1000	23	28
53	2	12-6-65	DA-100	3.2	3.7	1000	23	28
53	3	12-6-65	A-100	3.2	3.7	1000	23	28
54	1	12-6-65	DM	3.2	2.2	1000	23	28
54	2	12-6-65	DA-100	3.2	2.2	1000	23	28
54	3	12-6-65	A-100	3.2	2.2	1000	23	28
55	1	12-6-65	DM	3.2	0.9	1000	23	28
55	2	12-6-65	DA-100	3.2	0.9	1000	23	28
55	3	12-6-65	A-100	3.2	0.9	1000	23	28
56	1	12-6-65	DM	3.2	0.5	800	23	28
56	2	12-6-65	DA-100	3.2	0.5	800	23	28
56	3	12-6-65	A-100	3.2	0.5	800	23	28
57	1	12-7-65	G-150	0.82	0.5	800	23	30
57	2	12-7-65	G-150	1.2	0.5	800	23	30
57	3	12-7-65	G-150	1.6	0.5	800	23	30
57	4	12-7-65	G-150	2.4	0.5	800	23	30
57	5	12-7-65	G-150	3.2	0.5	800	23	30
57	6	12-7-65	G-150	4.0	0.5	800	23	30
58	1	12-7-65	G-150	0.41	0.9	1000	23	30
58	2	12-7-65	G-150	0.61	0.9	1000	23	30
58	3	12-7-65	G-150	0.82	0.9	1000	23	30
58	4	12-7-65	G-150	1.2	0.9	1000	23	30
58	5	12-7-65	G-150	1.6	0.9	1000	23	30
58	6	12-7-65	G-150	2.0	0.9	1000	23	20



Table 9. Basic Experimental Data (Continued)

Exp. no.	Run no.	Date	Test liq.	Spore conc.  $\times 10^{-7}/\text{ml}$	Bubble		Temp.  (°C)	Rel. hum.  (%)
					Dia. (mm)	Rate /min		
(1)	(2)	(3)	(4)	(5)	(6)	(7)	(8)	(9)
59	1	12-7-65	G-150	0.2	1.1	1000	23	20
59	2	12-7-65	G-150	0.3	1.1	1000	23	30
59	3	12-7-65	G-150	0.41	1.1	1000	23	30
59	4	12-7-65	G-150	0.61	1.1	1000	23	30
59	5	12-7-65	G-150	0.82	1.1	1000	23	30
59	6	12-7-65	G-150	1.2	1.1	1000	23	30
60	1	12-7-65	G-150	0.05	2.2	1000	23	30
60	2	12-7-65	G-150	0.1	2.2	1000	23	30
60	3	12-7-65	G-150	0.15	2.2	1000	23	30
60	4	12-7-65	G-150	0.2	2.2	1000	23	30
60	5	12-7-65	G-150	0.41	2.2	1000	23	30
60	6	12-7-65	G-150	0.82	2.2	1000	23	30
61	2	1-26-66	DM	3.7	0.8	1000	23	30
61	3	1-26-66	P-400	3.7	0.8	1000	23	30
61	4	1-26-66	P-200	3.7	0.8	1000	23	30
62	1	1-26-66	DM	3.7	2.2	1000	23	30
62	3	1-26-66	P-200	3.7	2.2	1000	23	30
62	4	1-26-66	P-400	3.7	2.2	1000	23	30
63	1	1-26-66	DM	3.7	1.1	1000	23	30
63	3	1-26-66	P-200	3.7	1.1	1000	23	30
63	4	1-26-66	P-400	3.7	1.1	1000	23	30
64	1	1-26-66	DM	3.7	0.5	800	23	30
64	3	1-26-66	P-200	3.7	0.5	1000	23	30
64	4	1-26-66	P-400	3.7	0.5	900	23	30
65	1	1-30-66	DM	3.7	0.6	1000	23	30
65	2	1-30-66	PH-400	3.7	0.6	1000	23	30
66	1	1-30-66	DM	3.7	1.1	1000	23	24
66	2	1-30-66	PH-400	3.7	1.1	1000	23	24
67	1	1-30-66	DM	3.7	2.2	1000	23	24
67	2	1-30-66	PH-400	3.7	2.2	1000	23	24



Table 9. Basic Experimental Data (Continued)

Exp. no.	Run no.	Date	Test liq.	Spore conc.  X10 <sup>-7</sup> /ml	Bubble		Temp.  (°C)	Rel. hum.  (%)
					Dia. (mm)	Rate /min		
(1)	(2)	(3)	(4)	(5)	(6)	(7)	(8)	(9)
68	1	2-3-66	PH-400	3.3	0.9	1000	23	28
68	2	2-3-66	DM	3.3	0.9	1000	23	28
69	1	1-31-66	P-400	0.08	1.1	1000	23	30
69	2	1-31-66	P-400	0.17	1.1	1000	23	30
69	3	1-31-66	P-400	0.33	1.1	1000	23	30
69	4	1-31-66	P-400	0.66	1.1	1000	23	30
69	5	1-31-66	P-400	0.99	1.1	1000	23	30
69	6	1-31-66	P-400	2.0	1.1	1000	23	30
70	1	1-31-66	P-400	0.08	2.2	1000	23	30
70	2	1-31-66	P-400	0.17	2.2	1000	23	30
70	3	1-31-66	P-400	0.33	2.2	1000	23	30
70	4	1-31-66	P-400	1.66	2.2	1000	23	30
70	5	1-31-66	P-400	0.99	2.2	1000	23	30
70	6	1-31-66	P-400	2.0	2.2	1000	23	30
71	1	2-3-66	P-400	0.17	0.5	800	23	28
71	2	2-3-66	P-400	0.33	0.5	800	23	28
71	3	2-3-66	P-400	0.66	0.5	800	23	28
71	4	2-3-66	P-400	0.99	0.5	800	23	28
71	5	2-3-66	P-400	2.0	0.5	800	23	28
71	6	2-3-66	P-400	3.3	0.5	800	23	28
72	1	2-3-66	P-400	0.17	0.9	1000	23	28
72	2	2-3-66	P-400	0.33	0.9	1000	23	28
72	3	2-3-66	P-400	0.66	0.9	1000	23	28
72	4	2-3-66	P-400	0.99	0.9	1000	23	28
72	5	2-3-66	P-400	2.0	0.9	1000	23	28
72	6	2-3-66	P-400	3.3	0.9	1000	23	28
74	1	2-4-66	A-25	3.3	0.9	1000	23	28
74	2	2-4-66	DA-25	3.3	0.9	1000	23	28
74	3	2-4-66	DM	3.3	0.9	1000	23	28
75	1	2-4-66	DM	3.3	1.7	1000	23	28
75	2	2-4-66	DA-25	3.3	1.7	1000	23	28
75	3	2-4-66	A-25	3.3	1.7	1000	23	28

Table 9. Basic Experimental Data (Continued)

Exp. no.	Run no.	Date	Test liq.	Spore conc.  X10 <sup>-7</sup> /ml	Bubble		Temp.  (°C)	Rel. hum.  (%)
					Dia. (mm)	Rate /min		
(1)	(2)	(3)	(4)	(5)	(6)	(7)	(8)	(9)
76	1	2-4-66	DM	3.3	3.7	1000	23	28
76	2	2-4-66	DA-25	3.3	3.7	1000	23	28
76	3	2-4-66	A-25	3.3	3.7	1000	23	28
77	1	2-5-66	DM	0.2	0.9	1000	23	34
77	2	2-5-66	DM	0.4	0.9	1000	23	34
77	3	2-5-66	DM	0.6	0.9	1000	23	34
77	4	2-5-66	DM	0.8	0.9	1000	23	34
77	5	2-5-66	DM	1.2	0.9	1000	23	34
77	6	2-5-66	DM	1.8	0.9	1000	23	34
78	1	2-5-66	DM	0.4	0.5	800	23	34
78	2	2-5-66	DM	0.8	0.5	800	23	34
78	3	2-5-66	DM	1.2	0.5	800	23	34
78	4	2-5-66	DM	1.8	0.5	800	23	34
78	5	2-5-66	DM	2.7	0.5	800	23	34
78	6	2-5-66	DM	3.6	0.5	800	23	34
79	1	2-5-66	S-400	0.2	0.9	1000	23	34
79	2	2-5-66	S-400	0.4	0.9	1000	23	34
79	3	2-5-66	S-400	0.6	0.9	1000	23	34
79	4	2-5-66	S-400	0.8	0.9	1000	23	34
79	5	2-5-66	S-400	1.2	0.9	1000	23	34
79	6	2-5-66	S-400	1.8	0.9	1000	23	34
80	1	2-5-66	S-400	0.4	0.5	800	23	34
80	2	2-5-66	S-400	0.8	0.5	800	23	34
80	3	2-5-66	S-400	1.2	0.5	800	23	34
80	4	2-5-66	S-400	1.8	0.5	800	23	34
80	5	2-5-66	S-400	2.7	0.5	800	23	34
80	6	2-5-66	S-400	3.6	0.5	800	23	34
81	1	2-6-66	S-400	0.05	2.2	1000	23	30
81	2	2-6-66	S-400	0.1	2.2	1000	23	30
81	3	2-6-66	S-400	0.2	2.2	1000	23	30
81	4	2-6-66	S-400	0.4	2.2	1000	23	30
81	5	2-6-66	S-400	0.6	2.2	1000	23	30
81	6	2-6-66	S-400	0.8	2.2	1000	23	30

Table 9. Basic Experimental Data (Continued)

Exp. no.	Run no.	Date	Test liq.	Spore conc. $\times 10^{-7}/\text{ml}$	Bubble		Temp. ( $^{\circ}\text{C}$ )	Rel. hum. (%)
					Dia. (mm)	Rate /min		
(1)	(2)	(3)	(4)	(5)	(6)	(7)	(8)	(9)
82	1	2-6-66	DM	0.05	2.2	1000	23	30
82	2	2-6-66	DM	0.1	2.2	1000	23	30
82	3	2-6-66	DM	0.2	2.2	1000	23	30
82	4	2-6-66	DM	0.4	2.2	1000	23	30
82	5	2-6-66	DM	0.6	2.2	1000	23	30
82	6	2-6-66	DM	0.8	2.2	1000	23	30
83	1	2-6-66	DA-50	0.4	0.5	800	23	30
83	2	2-6-66	DA-50	0.8	0.5	800	23	30
83	3	2-6-66	DA-50	1.2	0.5	800	23	30
83	4	2-6-66	DA-50	1.8	0.5	800	23	30
83	5	2-6-66	DA-50	2.7	0.5	800	23	30
83	6	2-6-66	DA-50	3.6	0.5	800	23	30
84	1	2-6-66	DA-50	0.2	0.9	1000	23	30
84	2	2-6-66	DA-50	0.4	0.9	1000	23	30
84	3	2-6-66	DA-50	0.6	0.9	1000	23	30
84	4	2-6-66	DA-50	0.8	0.9	1000	23	30
84	5	2-6-66	DA-50	1.2	0.9	1000	23	30
84	6	2-6-66	DA-50	1.8	0.9	1000	23	30
85	1	2-7-66	DA-50	0.05	2.2	1000	23	30
85	2	2-7-66	DA-50	0.1	2.2	1000	23	30
85	3	2-7-66	DA-50	0.2	2.2	1000	23	30
85	4	2-7-66	DA-50	0.4	2.2	1000	23	30
85	5	2-7-66	DA-50	0.6	2.2	1000	23	30
85	6	2-7-66	DA-50	0.8	2.2	1000	23	30
86	1	2-7-66	A-50	0.4	0.5	800	23	30
86	2	2-7-66	A-50	0.8	0.5	800	23	30
86	3	2-7-66	A-50	1.2	0.5	800	23	30
86	4	2-7-66	A-50	1.8	0.5	800	23	30
86	5	2-7-66	A-50	2.7	0.5	800	23	30
86	7	2-7-66	A-50	3.6	0.5	800	23	30
87	1	2-7-66	A-50	0.2	0.9	1000	23	30
87	2	2-7-66	A-50	0.4	0.9	1000	23	30
87	3	2-7-66	A-50	0.6	0.9	1000	23	30
87	4	2-7-66	A-50	0.8	0.9	1000	23	30



Table 9. Basic Experimental Data (Continued)

Exp. no.	Run no.	Date	Test liq.	Spore conc.  x10 <sup>-7</sup> /ml	Bubble		Temp.  (°C)	Rel. hum.  (%)
					Dia. (mm)	Rate /min		
(1)	(2)	(3)	(4)	(5)	(6)	(7)	(8)	(9)
87	5	2-7-66	A-50	1.2	0.9	1000	23	30
87	6	2-7-66	A-50	1.8	0.9	1000	23	30
88	1	2-7-66	A-50	0.05	2.2	1000	23	30
88	2	2-7-66	A-50	0.1	2.2	1000	23	30
88	3	2-7-66	A-50	0.2	2.2	1000	23	30
88	4	2-7-66	A-50	0.4	2.2	1000	23	30
88	5	2-7-66	A-50	0.6	2.2	1000	23	30
88	6	2-7-66	A-50	0.8	2.2	1000	23	30
89	1	2-8-66	PH-400	0.4	0.5	800	23	30
89	2	2-8-66	PH-400	0.8	0.5	800	23	30
89	3	2-8-66	PH-400	1.2	0.5	800	23	30
89	4	2-8-66	PH-400	1.8	0.5	800	23	30
89	5	2-8-66	PH-400	2.7	0.5	800	23	30
89	6	2-8-66	PH-400	3.6	0.5	800	23	30
90	1	2-8-66	PH-400	0.05	2.2	1000	23	30
90	2	2-8-66	PH-400	0.1	2.2	1000	23	30
90	3	2-8-66	PH-400	0.2	2.2	1000	23	30
90	4	2-8-66	PH-400	0.4	2.2	1000	23	30
90	5	2-8-66	PH-400	0.6	2.2	1000	23	30
90	6	2-8-66	PH-400	0.8	2.2	1000	23	30



## APPENDIX B

## EXPERIMENTAL SAMPLE DATA

Table 10. Experimental Sample Data

Exp. no.	Run no.	Sample time (min)	Corrected no. of colonies per Andersen Stage						
			6	5	4	3	2	1	1-6
(1)	(2)	(3)	(4)	(5)	(6)	(7)	(8)	(9)	(10)
10	1	50	4	329	378	202	118	123	1154
10	2	25	6	90	133	120	68	67	484
10	3	50	2	217	375	338	201	66	1199
10	4	50	4	50	165	426	200	104	949
11	1	15	22	250	231	195	85	64	847
11	2	10	10	191	160	82	70	71	584
11	3	25	15	444	424	363	232	122	1600
11	4	10	6	118	102	80	92	64	462
12	1	10	8	156	108	73	47	65	457
12	2	10	11	111	125	74	46	46	413
12	3	25	4	523	633	633	296	195	2284
12	4	25	3	167	294	487	373	324	1648
13	1	10	22	165	107	120	72	64	550
13	2	10	13	153	129	86	49	60	490
13	3	25	4	424	495	619	257	174	1973
13	4	25	10	150	145	210	195	305	1015
15	1	25	15	153	215	133	59	26	601
15	2	20	43	341	270	144	80	75	953
15	3	15	38	313	162	120	67	67	767
15	4	10	13	171	101	90	38	47	460
16	1	15	54	156	120	102	24	42	498
16	2	15	72	270	225	84	96	78	825
16	3	15	144	468	288	156	24	120	1200
17	1	15	9	54	59	59	66	115	362
17	2	15	60	216	150	66	84	114	690
17	3	15	66	108	225	183	48	42	672
18	1	25	14	83	99	119	55	99	469
18	2	25	8	178	137	206	160	143	832
18	3	25	14	42	101	158	171	264	750
19	1	25	2	48	103	125	83	60	421
19	2	25	13	48	156	93	84	83	477
19	3	25	6	31	43	64	56	124	324

Table 10. Experimental Sample Data (Continued)

Exp. no.	Run no.	Sample time (min)	Corrected no. of colonies per Andersen Stage						
			6	5	4	3	2	1	1-6
(1)	(2)	(3)	(4)	(5)	(6)	(7)	(8)	(9)	(10)
20	1	25	10	167	152	136	61	31	557
20	2	10	0	6	37	154	216	295	708
20	3	25	5	55	60	20	35	165	340
21	1	50	4	338	314	362	153	52	1223
21	2	100	0	25	137	774	2273	3041	6250
21	3	50	6	180	246	67	131	623	1253
22	1	20	12	83	99	57	16	21	288
22	2	20	1	72	161	415	437	605	1691
22	3	20	13	4	13	13	0	8	51
23	1	25	10	170	310	245	55	35	825
23	2	25	9	131	70	80	270	355	915
23	3	25	0	10	15	0	20	5	50
24	1	50	2	182	403	1039	1093	1512	4231
24	2	50	7	286	661	876	1543	1928	5301
24	3	25	5	127	172	246	587	1101	2238
24	4	10	2	50	46	54	136	353	641
25	1	50	3	36	49	46	303	828	1265
25	2	50	5	143	115	275	1182	1281	3001
25	3	25	2	109	104	127	730	1114	2186
25	4	25	1	72	90	89	295	360	1407
26	1	25	2	4	1	14	125	143	289
26	2	25	1	5	6	26	306	249	593
26	3	25	2	34	13	73	586	610	1318
26	4	25	5	121	40	60	475	783	1484
27	1	25	2	7	7	90	582	163	851
27	2	20	0	4	6	354	779	165	1308
27	3	25	0	12	21	582	1467	231	2313
27	4	15	4	28	18	225	888	295	1458
28	1	10	7	94	43	48	81	306	579
28	2	10	6	54	54	34	68	322	538
28	3	10	12	52	80	32	64	356	596

Table 10. Experimental Sample Data (Continued)

Exp. no.	Run no.	Sample time (min)	Corrected no. of colonies per Andersen Stage						
			6	5	4	3	2	1	1-6
(1)	(2)	(3)	(4)	(5)	(6)	(7)	(8)	(9)	(10)
29	1	25	36	89	72	80	163	552	992
29	2	50	12	153	268	304	836	2245	3818
29	3	25	16	120	36	24	152	772	1120
29	4	50	4	92	112	135	732	1424	2499
29	5	25	12	8	24	12	196	800	1052
30	1	10	5	82	62	51	80	246	526
30	2	10	12	144	75	50	121	312	714
30	3	10	18	110	48	14	10	140	340
31	1	10	10	26	55	84	100	135	410
31	2	10	32	20	80	104	104	256	596
31	3	10	16	32	33	47	40	100	268
32	1	20	3	28	15	154	588	255	1043
32	2	20	9	7	6	165	624	596	1407
32	3	20	8	5	5	278	695	943	1934
33	1	15	8	76	34	88	132	340	678
33	2	10	8	64	20	34	168	288	582
33	3	10	12	44	8	28	72	191	355
34	1	10	2	87	85	70	62	310	616
34	2	10	8	72	58	42	172	296	648
34	3	10	5	36	20	13	93	242	409
35	1	40	0	0	0	90	274	104	468
35	2	40	8	6	2	10	16	26	68
35	3	40	6	12	0	4	16	18	56
35	4	40	8	4	6	2	54	46	120
35	5	40	10	24	17	44	92	51	238
35	6	40	6	18	4	33	118	112	291
36	1	40	2	4	14	82	170	86	358
36	2	40	16	24	50	142	262	166	660
36	3	40	12	18	34	266	544	146	1020
36	4	40	6	58	86	270	548	166	1134
36	5	40	8	66	90	296	544	220	1224
36	6	40	4	98	106	350	530	278	1366



Table 10. Experimental Sample Data (Continued)

Exp. no.	Run no.	Sample time (min)	Corrected no. of colonies per Andersen Stage							
			(4)	(5)	(6)	(7)	(8)	(9)	(10)	
(1)	(2)	(3)	(4)	(5)	(6)	(7)	(8)	(9)	(10)	
37	1	40	0	4	12	111	112	69	308	
37	2	40	4	8	12	116	92	48	280	
37	3	40	0	4	20	112	68	49	253	
37	4	40	0	0	36	92	68	33	229	
37	5	40	4	4	8	64	24	52	156	
37	6	40	4	12	12	80	156	104	368	
38	1	40	4	4	68	600	453	156	1285	
38	2	40	0	12	112	521	348	416	1409	
38	3	40	0	8	68	472	344	244	1146	
38	4	40	12	52	88	289	268	224	933	
38	5	40	0	28	60	276	276	284	924	
38	6	40	8	40	76	193	204	336	857	
39	1	15	12	12	72	47	37	12	192	
39	2	15	11	61	24	60	99	0	255	
39	3	15	11	13	0	96	12	24	156	
40	1	15	3	30	57	102	42	30	264	
40	2	15	9	36	0	39	90	249	423	
40	3	15	0	36	45	108	72	33	294	
41	1	40	4	196	420	248	36	13	917	
41	2	20	8	100	160	136	100	221	725	
41	3	10	15	72	97	140	24	16	364	
42	1	10	3	39	90	99	27	12	270	
42	2	10	3	72	114	168	45	54	456	
42	3	10	16	168	256	176	64	8	688	
47	1	10	16	56	48	192	224	74	610	
47	2	10	0	36	12	140	336	135	659	
47	3	10	0	16	16	144	273	163	612	
48	1	15	16	82	32	296	356	183	965	
48	2	10	4	61	48	188	244	224	769	
49	1	20	22	109	43	394	475	243	1286	
49	2	20	7	122	97	375	488	446	1535	
49	3	20	0	70	159	412	429	599	1669	

Table 10. Experimental Sample Data (Continued)

Exp. no.	Run no.	Sample time (min)	Corrected no. of colonies per Andersen Stage						
			6	5	4	3	2	1	1-6
(1)	(2)	(3)	(4)	(5)	(6)	(7)	(8)	(9)	(10)
50	1	15	12	52	81	180	268	209	802
50	2	15	0	32	44	252	431	272	1031
50	3	15	12	40	4	108	412	228	804
51	1	5	11	44	40	148	57	104	404
51	2	20	8	104	192	496	236	880	1926
51	3	5	4	36	28	73	171	160	472
52	1	20	3	37	198	291	117	90	736
52	2	20	8	32	66	344	194	201	845
53	1	20	16	112	221	153	47	16	565
53	2	20	112	244	124	212	76	52	820
53	3	20	12	348	416	416	84	13	1289
54	1	20	4	85	213	188	29	3	522
54	2	20	16	76	108	149	123	112	584
54	3	20	12	315	329	228	60	9	953
55	1	20	1	122	229	112	24	5	493
55	2	20	5	3	10	5	79	320	422
55	3	20	2	20	65	170	81	22	360
56	1	20	11	65	102	58	15	20	291
56	2	20	1	33	59	97	74	65	329
56	3	20	3	21	49	130	100	70	373
57	1	20	1	0	4	221	669	110	1005
57	2	20	0	0	5	373	900	151	1429
57	3	20	1	7	9	415	1083	167	1682
57	4	20	1	7	14	501	1144	185	1852
57	5	20	0	10	19	477	1243	181	1930
57	6	20	4	11	28	563	1190	205	2001
58	1	20	1	4	8	34	287	310	644
58	2	20	1	7	13	35	417	410	883
58	3	20	0	9	15	71	443	510	1048
58	4	20	3	21	16	92	450	491	1073
58	5	20	4	59	21	110	433	533	1160
58	6	20	6	65	31	107	460	497	1166

Table 10. Experimental Sample Data (Continued)

Exp. no.	Run no.	Sample time (min)	Corrected no. of colonies per Andersen Stage						
			6	5	4	3	2	1	1-6
(1)	(2)	(3)	(4)	(5)	(6)	(7)	(8)	(9)	(10)
59	1	20	1	21	19	61	215	585	902
59	2	20	0	27	31	72	465	743	1338
59	3	20	1	39	40	83	511	859	1533
59	4	20	3	51	51	90	525	909	1629
59	5	20	5	79	81	110	570	900	1745
59	6	20	5	92	89	122	537	981	1826
60	1	20	1	5	8	52	120	228	414
60	2	20	2	12	18	110	211	420	773
60	3	20	0	20	23	133	321	642	1139
60	4	20	5	27	32	165	433	742	1404
60	5	20	7	51	72	186	425	815	1556
60	6	20	9	111	121	197	456	867	1761
61	2	15							
61	3	15	0	187	587	491	209	61	1535
61	4	15	7	104	416	509	256	99	1391
62	1	15	18	78	114	90	12	36	348
62	3	15	5	128	471	521	212	276	1613
62	4	15	0	59	478	690	339	373	1939
63	1	10	0	26	80	104	39	36	285
63	3	10	0	12	97	444	194	107	854
63	4	10	0	11	100	447	375	265	1198
64	1	10	4	28	44	26	10	8	120
64	3	10	10	50	140	220	100	20	540
64	4	10	2	8	62	232	114	16	434
65	1	20	12	81	103	56	16	20	288
65	2	20	6	67	55	62	34	52	276
66	1	20	2	64	160	119	23	16	384
66	2	20	9	200	241	257	138	70	915
67	1	20	4	47	114	142	45	29	381
67	2	20	5	181	317	289	118	60	970
68	1	20	0	64	464	224	48	47	847
68	2	20	0	156	224	70	44	16	510

Table 10. Experimental Sample Data (Continued)

Exp. no.	Run no.	Sample time (min)	Corrected no. of colonies per Andersen Stage							
			(4)	(5)	(6)	(7)	(8)	(9)	(10)	
(1)	(2)	(3)	(4)	(5)	(6)	(7)	(8)	(9)	(10)	
69	1	40	8	8	32	116	323	184	671	
69	2	40	12	24	60	275	608	344	1323	
69	3	40	5	24	80	452	676	709	1946	
69	4	40	4	8	108	835	1168	452	1575	
69	5	40	4	24	244	1131	938	740	3075	
69	6	70	0	40	580	2284	2175	936	6015	
70	1	40	4	6	21	232	580	254	1097	
70	2	40	0	12	71	711	888	547	2228	
70	3	40	0	10	193	1012	824	782	2821	
70	4	40	0	14	274	1068	832	931	3119	
70	5	40	6	22	378	1222	1026	604	3258	
70	6	40	2	58	764	1566	872	756	4018	
71	1	20	0	2	11	46	23	4	86	
71	2	20	0	4	33	138	77	11	263	
71	3	20	2	7	69	247	128	14	467	
71	4	20	1	15	84	338	271	21	730	
71	5	20	3	28	152	586	322	50	1141	
71	6	20	3	29	172	634	356	58	1252	
72	1	20	12	4	4	32	36	15	103	
72	2	20	3	1	12	160	80	25	281	
72	3	20	4	0	12	160	120	77	373	
72	4	20	4	0	36	308	80	100	528	
72	5	20	8	15	53	400	212	45	733	
72	6	20	16	12	64	536	241	61	930	
74	1	20	3	35	100	256	51	25	470	
74	2	20	32	44	36	35	29	352	528	
74	3	20	1	101	229	132	14	6	483	
75	1	20	24	40	178	256	62	96	656	
75	2	20	2	98	165	393	283	398	1339	
75	3	20	7	219	382	409	56	38	1111	
76	1	20	2	36	193	280	113	88	712	
76	2	20	10	136	165	203	106	96	716	
76	3	20	6	164	412	508	162	178	1430	



Table 10. Experimental Sample Data (Continued)

Exp. no.	Run no.	Sample time (min)	Corrected no. of colonies per Andersen Stage						
			6	5	4	3	2	1	1-6
(1)	(2)	(3)	(4)	(5)	(6)	(7)	(8)	(9)	(10)
77	1	20	1	20	34	47	37	38	177
77	2	20	3	42	67	105	70	69	356
77	3	20	5	65	101	157	107	85	520
77	4	20	7	80	117	195	95	73	567
77	5	20	9	101	115	242	123	92	682
77	6	20	14	149	184	250	127	81	805
78	1	20	0	8	24	32	23	19	106
78	2	20	0	17	49	66	55	38	225
78	3	20	2	28	78	100	64	47	319
78	4	20	1	27	95	121	74	45	363
78	5	20	3	29	110	130	79	60	411
78	6	20	4	40	120	127	76	51	418
79	1	20	1	7	18	28	31	44	129
79	2	20	3	15	40	44	59	87	248
79	3	20	5	18	51	72	90	134	370
79	4	20	6	21	50	85	100	141	383
79	5	20	8	28	69	84	115	201	505
79	6	20	12	32	80	128	136	216	604
80	1	20	1	3	9	12	12	24	61
80	2	20	0	7	17	27	25	52	128
80	3	20	3	13	19	48	34	81	198
80	4	20	5	21	27	61	40	101	255
80	5	20	4	24	33	52	45	103	261
80	6	20	5	31	58	75	49	123	341
81	1	20	0	36	84	135	99	111	465
81	2	20	0	78	165	334	181	140	898
81	3	20	1	156	288	478	190	138	1251
81	4	20	3	201	311	477	195	141	1328
81	5	20	3	303	375	487	199	152	1519
81	6	20	5	345	396	494	207	140	1587
82	1	20	0	23	25	38	19	39	144
82	2	20	2	47	51	59	23	38	220
82	3	20	7	121	159	95	30	51	463
82	4	20	13	153	171	100	29	55	521
82	5	20	23	202	160	99	32	61	577
82	6	20	35	208	161	103	32	56	595

Table 10. Experimental Sample Data (Continued)

Exp. no.	Run no.	Sample time (min)	Corrected no. of colonies per Andersen Stage							
			6	5	4	3	2	1	1-6	
(1)	(2)	(3)	(4)	(5)	(6)	(7)	(8)	(9)	(10)	
83	1	20	1	3	13	18	30	9	74	
83	2	20	3	7	28	37	78	8	161	
83	3	20	5	10	30	78	99	10	232	
83	4	20	7	15	65	89	115	10	301	
83	5	20	12	21	64	97	127	12	333	
83	6	20	16	31	79	101	132	11	370	
84	1	20	1	5	2	10	29	101	148	
84	2	20	3	10	6	21	61	200	301	
84	3	20	4	15	9	33	98	281	440	
84	4	20	6	21	10	40	115	308	500	
84	5	20	9	32	15	47	118	336	557	
84	6	20	12	48	21	52	123	332	588	
85	1	20	0	7	14	59	93	109	282	
85	2	20	1	15	25	110	145	120	416	
85	3	20	1	29	49	121	151	111	462	
85	4	20	3	61	90	151	162	129	596	
85	5	20	5	87	158	163	157	132	702	
85	6	20	7	113	169	167	159	122	737	
86	1	20	1	2	3	27	11	21	65	
86	2	20	2	4	7	63	13	24	113	
86	3	20	3	5	7	99	13	27	154	
86	4	20	5	8	15	111	15	33	187	
86	5	20	10	11	18	125	17	29	210	
86	6	20	15	16	20	128	16	32	227	
87	1	20	0	6	7	37	28	35	113	
87	2	20	1	14	15	73	63	37	203	
87	3	20	1	20	22	90	90	41	264	
87	4	20	0	27	30	115	95	38	305	
87	5	20	2	32	36	140	96	39	345	
87	6	20	0	49	60	145	96	44	394	
88	1	20	2	9	50	123	31	30	245	
88	2	20	4	16	95	259	40	29	443	
88	3	20	7	37	155	271	45	32	547	
88	4	20	16	75	174	265	52	33	615	
88	5	20	20	88	180	280	49	32	649	
88	6	20	30	144	195	279	48	32	728	

Table 10. Experimental Sample Data (Continued)

Exp. no.	Run no.	Sample time (min)	Corrected no. of colonies per Andersen Stage						
			6	5	4	3	2	1	1-6
(1)	(2)	(3)	(4)	(5)	(6)	(7)	(8)	(9)	(10)
89	1	20	1	13	13	14	14	21	76
89	2	20	1	20	25	35	28	43	153
89	3	20	2	13	49	60	27	50	201
89	4	20	1	48	53	58	31	52	243
89	5	20	4	48	53	59	30	49	243
89	6	20	6	68	55	63	34	52	278
90	1	20	1	49	75	154	75	52	406
90	2	20	1	94	157	191	85	59	587
90	3	20	3	121	124	235	88	61	632
90	4	20	5	178	217	269	98	60	827
90	5	20	7	189	262	275	110	62	905
90	6	20	6	185	318	290	117	66	982

## APPENDIX C

## SUMMARY OF DATA COMPUTATIONS



Table 11. Summary of Data Computations

Exp. no.	Run no.	Test liq.	Bubble dia.	Spore conc.  $\times 10^{-7}/\text{ml}$	Mean particle dia. ( $\mu$ )	Geom. std. dev.	Particles per 1000 bubbles
(1)	(2)	(3)	(4)	(5)	(6)	(7)	(8)
10	1	DM	5.7	7.1	3.3	2.27	115
10	2	DM	3.7	7.1	4.2	2.10	97
10	3	DM	2.2	7.1	3.8	1.85	120
10	4	DM	1.1	7.1	5.1	1.66	95
11	1	S-100	5.7	7.1	3.2	2.16	282
11	2	S-100	3.7	7.1	3.2	2.56	292
11	3	S-100	2.2	7.1	3.5	2.08	320
11	4	S-100	1.1	7.1	4.0	2.42	231
12	1	S-1600	5.7	7.1	3.1	2.84	229
12	2	S-1600	3.7	7.1	3.4	2.32	207
12	3	S-1600	2.2	7.1	3.7	2.00	457
12	4	S-1600	1.1	7.1	5.5	2.00	329
13	1	S-400	5.7	7.1	3.5	2.40	275
13	2	S-400	3.7	7.1	3.3	2.48	245
13	3	S-400	2.2	7.1	3.9	1.92	395
13	4	S-400	1.1	7.1	6.2	2.58	203
15	1	DM	3.7	5.2	3.2	1.88	120
15	2	S-100	3.7	5.2	2.8	2.36	238
15	3	S-400	3.7	5.4	2.6	2.65	256
15	4	S-1600	3.7	5.4	2.9	2.55	230
16	1	DM	2.2	7.8	2.6	2.42	166
16	2	S-100	2.2	7.8	2.8	2.47	275
16	3	S-400	2.2	7.8	2.4	2.46	400
17	1	DM	1.2	7.8	6.1	2.56	121
17	2	S-100	1.2	7.8	3.2	2.87	230
17	3	S-400	1.2	7.8	3.0	2.17	224
18	1	DM	0.8	4.6	4.7	2.34	93
18	2	S-100	0.8	4.6	4.6	2.28	166
18	3	S-400	0.8	4.6	7.4	2.11	150
19	1	DM	0.5	4.6	4.8	1.90	105
19	2	S-100	0.5	4.6	4.6	2.24	119
19	3	S-400	0.5	4.6	7.2	2.75	81

Table 11. Summary of Data Computations (Continued)

Exp. no.	Run no.	Test liq.	Bubble dia.	Spore conc. $\times 10^{-7}/\text{ml}$	Mean particle dia. ( $\mu$ )	Geom. std. dev.	Particles per 1000 bubbles
(1)	(2)	(3)	(4)	(5)	(6)	(7)	(8)
20	1	DM	3.7	3.5	3.3	1.91	111
20	2	G-150	3.7	3.5	8.7	1.77	354
20	3	G-300	3.7	3.5	7.5	2.94	68
21	1	DM	2.2	3.5	3.3	1.91	122
21	2	G-150	2.2	3.5	10.4	1.73	313
21	3	G-300	2.2	3.5	8.9	4.33	125
22	1	DM	0.5	1.2	2.9	1.96	90
22	2	G-150	0.5	1.2	7.7	2.00	529
22	3	G-300	0.5	1.2	3.1		16
23	1	DM	1.2	1.2	3.4	1.76	165
23	2	G-150	1.2	1.2	8.2	1.81	183
23	3	G-300	1.2	1.2	4.4	12.16	10
24	1	G-150	2.2	0.2	7.7	2.01	423
24	2	G-150	2.2	0.50	8.0	2.14	530
24	3	G-150	2.2	1.3	10.7	2.60	447
24	4	G-150	2.2	2.5	13.0	3.27	321
25	1	G-150	1.1	0.1	12.0		127
25	2	G-150	1.1	0.24	9.1		300
25	3	G-150	1.1	0.60	9.9		437
25	4	G-150	1.1	1.2	12.0		281
26	1	G-150	0.9	0.1	59.8		57
26	2	G-150	0.9	0.30	9.3		119
26	3	G-150	0.9	0.75	9.5		263
26	4	G-150	0.9	1.5	10.1		297
27	1	G-150	0.5	0.53	8.0	1.34	212
27	2	G-150	0.5	1.1	7.3	1.27	410
27	3	G-150	0.5	2.7	7.1	1.31	580
27	4	G-150	0.5	5.3	7.8	1.37	608
28	1	G-50	0.9	5.4	12.2	5.55	290
28	2	G-75	0.9	5.4	15.1	4.53	269
28	3	G-100	0.9	5.4	14.0	4.29	298

Table 11. Summary of Data Computations (Continued)

Exp. no.	Run no.	Test liq.	Bubble dia.	Spore conc. $\times 10^{-7}/\text{ml}$	Mean particle dia. ( $\mu$ )	Geom. std. dev.	Particles per 1000 bubbles
(1)	(2)	(3)	(4)	(5)	(6)	(7)	(8)
29	1	G-50	1.1	3.7	2.9	4.55	198
29	2	G-100	1.1	3.7	10.8	5.45	382
29	3	G-150	1.1	3.7	12.9	2.63	224
29	4	G-200	1.1	3.7	13.5	2.54	250
29	5	G-250	1.1	3.7	20.5	4.55	210
30	1	G-100	1.7	2.6	7.8	2.75	263
30	2	G-150	1.7	2.6	7.4	3.00	357
30	3	G-200	1.7	2.6	5.1	3.68	170
31	1	G-100	3.7	2.6	7.3	2.67	205
31	2	G-150	3.7	2.6	9.2	3.59	298
31	3	G-200	3.7	2.6	6.8	3.50	134
32	1	G-100	0.5	2.6	8.1	1.38	326
32	2	G-150	0.5	2.6	9.2	1.39	410
32	3	G-200	0.5	2.6	9.7	1.53	605
33	1	G-100	0.9	2.6	11.2	3.45	226
33	2	G-150	0.9	2.6	13.2	3.63	291
33	3	G-200	0.9	2.6	15.4	4.61	178
34	1	G-100	1.1	2.6	9.3	4.09	308
34	2	G-150	1.1	2.6	12.5	4.15	324
34	3	G-200	1.1	2.6	18.0	4.38	205
35	1	G-100	0.5	0.15			74
35	2	G-100	0.5	0.45			11
35	3	G-100	0.5	0.6			9
35	4	G-100	0.5	0.9			19
35	5	G-100	0.5	1.1			37
35	6	G-100	0.5	1.5			45
36	1	G-100	0.9	0.08	7.6	1.65	50
36	2	G-100	0.9	0.15	7.0	1.62	92
36	3	G-100	0.9	0.3	7.3	1.85	142
36	4	G-100	0.9	0.45	6.3	1.76	158
36	5	G-100	0.9	0.6	6.6	1.80	170
36	6	G-100	0.9	1.1	6.5	1.92	190

Table 11. Summary of Data Computations (Continued)

Exp. no.	Run no.	Test liq.	Bubble dia.	Spore conc. $\times 10^{-7}/\text{ml}$	Mean particle dia. ( $\mu$ )	Geom. std. dev.	Particles per 1000 bubbles
(1)	(2)	(3)	(4)	(5)	(6)	(7)	(8)
37	1	G-100	1.1	0.08	7.2	1.45	42
37	2	G-100	1.1	0.16	6.8	1.43	37
37	3	G-100	1.1	0.32	6.5	1.52	34
37	4	G-100	1.1	0.64	5.9	1.58	31
37	5	G-100	1.1	0.96	9.5	1.59	21
37	6	G-100	1.1	1.9	7.9	1.50	49
38	1	G-100	2.2	0.08	6.4	1.41	161
38	2	G-100	2.2	0.16	7.2	1.42	176
38	3	G-100	2.2	0.32	6.9	1.70	143
38	4	G-100	2.2	0.64	6.5	1.92	116
38	5	G-100	2.2	0.96	7.4	1.85	115
38	6	G-100	2.2	1.9	8.1	2.16	107
39	1	DM	0.5	3.5	3.6	12.17	82
39	2	DA-50	0.5	3.5	4.6	2.50	133
39	3	A-50	0.5	3.5	4.9	3.06	53
40	1	DM	0.9	3.5	4.5	1.91	93
40	2	DA-50	0.9	3.5	17.5	4.23	128
40	3	A-50	0.9	3.5	4.9	1.82	68
41	1	DM	1.7	3.5	3.1	1.64	115
41	2	DA-50	1.7	3.5	5.8	2.55	181
41	3	A-50	1.7	3.5	3.2	1.94	182
42	1	DM	3.7	3.5	3.6	1.80	135
42	2	DA-50	3.7	3.5	4.3	1.86	228
42	3	A-50	3.7	3.5	3.0	1.73	344
47	1	G-50	0.9	3.0	5.8	1.59	339
47	2	G-100	0.9	3.0	7.3	1.51	367
47	3	G-150	0.9	3.0	7.8	1.54	341
48	1	G-50	1.7	3.0	6.3	2.22	322
48	2	G-100	1.7	3.0	7.2	2.25	385
49	1	G-50	0.5	3.0	6.1	1.92	403
49	2	G-100	0.5	3.0	7.0	2.13	480
49	3	G-150	0.5	3.0	7.7	1.98	421



Table 11. Summary of Data Computations (Continued)

Exp. no.	Run no.	Test liq.	Bubble dia.	Spore conc.  $\times 10^{-7}/\text{ml}$	Mean particle dia. ( $\mu$ )	Geom. std. dev.	Particles per 1000 bubbles
(1)	(2)	(3)	(4)	(5)	(6)	(7)	(8)
50	1	G-50	1.1	2.8	6.8	2.01	267
50	2	G-100	1.1	2.8	7.5	1.80	344
50	3	G-150	1.1	2.8	8.8	1.98	268
51	1	G-50	2.2	2.8	5.7	2.46	404
51	2	G-100	2.2	2.8	8.4	2.32	482
51	3	G-150	2.2	2.8	8.4	2.48	472
52	1	G-50	3.7	2.8	5.1	1.71	184
52	2	G-100	3.7	2.8	6.5	1.77	211
53	1	DM	3.7	3.2	3.1	1.84	141
53	2	DA-100	3.7	3.2	2.6	2.46	205
53	3	A-100	3.7	3.2	3.0	1.70	322
54	1	DM	2.2	3.2	3.1	1.61	131
54	2	DA-100	2.2	3.2	5.0	2.36	146
54	3	A-100	2.2	3.2	2.9	1.65	238
55	1	DM	0.9	3.2	2.9	1.59	123
55	2	DA-100	0.9	3.2	16.5	2.12	106
55	3	A-100	0.9	3.2	4.8	1.59	90
56	1	DM	0.5	3.2	2.9	1.90	91
56	2	DA-100	0.5	3.2	5.5	1.96	103
56	3	A-100	0.5	3.2	5.8	1.78	116
57	1	G-150	0.5	0.82	7.4	1.26	283
57	2	G-150	0.5	1.2	7.2	1.28	446
57	3	G-150	0.5	1.6	7.2	1.28	428
57	4	G-150	0.5	2.4	7.1	1.30	580
57	5	G-150	0.5	3.2	7.2	1.28	605
57	6	G-150	0.5	4.0	7.0	1.31	625
58	1	G-150	0.9	0.41	9.6	1.36	161
58	2	G-150	0.9	0.61	9.6	1.36	221
58	3	G-150	0.9	0.82	9.8	1.41	261
58	4	G-150	0.9	1.2	9.4	1.47	268
58	5	G-150	0.9	1.6	9.4	1.54	290
58	6	G-150	0.9	2.0	9.1	1.56	292

Table 11. Summary of Data Computations (Continued)

Exp. no.	Run no.	Test liq.	Bubble dia.	Spore conc. $\times 10^{-7}/\text{ml}$	Mean particle dia. ( $\mu$ )	Geom. std. dev.	Particles per 1000 bubbles
(1)	(2)	(3)	(4)	(5)	(6)	(7)	(8)
59	1	G-150	1.1	0.2	12.3		223
59	2	G-150	1.1	0.3	10.6		335
59	3	G-150	1.1	0.41	10.7		383
59	4	G-150	1.1	0.61	10.6		407
59	5	G-150	1.1	0.82	10.0		436
59	6	G-150	1.1	1.2	10.5		457
60	1	G-150	2.2	0.05	10.6	1.75	103
60	2	G-150	2.2	0.1	10.5	1.79	193
60	3	G-150	2.2	0.15	10.5	1.86	285
60	4	G-150	2.2	0.2	10.1	1.86	351
60	5	G-150	2.2	0.41	10.2	1.97	389
60	6	G-150	2.2	0.82	9.6	2.14	440
61	2	DM	0.8	3.7	2.5	2.16	95
61	3	P-400	0.8	3.7	4.5	1.66	512
61	4	P-200	0.8	3.7	3.9	1.66	464
62	1	DM	2.2	3.7	3.2	2.19	116
62	3	P-200	2.2	3.7	5.0	1.84	538
62	4	P-400	2.2	3.7	5.7	1.70	646
63	1	DM	1.1	3.7	4.7	1.79	143
63	3	P-200	1.1	3.7	5.8	1.54	427
63	4	P-400	1.1	3.7	6.8	1.59	599
64	1	DM	0.5	3.7	3.2	2.03	75
64	3	P-200	0.5	3.7	4.2	1.62	270
64	4	P-400	0.5	3.7	5.1	1.48	241
65	1	DM	0.6	3.7	3.0	2.03	72
65	2	PH-400	0.6	3.7	4.3	2.28	69
66	1	DM	1.1	3.7	3.9	1.87	96
66	2	PH-400	1.1	3.7	3.5	1.77	229
67	1	DM	2.2	3.7	4.0	1.85	95
67	2	PH-400	2.2	3.7	3.8	1.79	243
68	1	PH-400	0.9	3.3	3.8	1.66	212
68	2	DM	0.9	3.3	2.8	1.93	128

Table 11. Summary of Data Computations (Continued)

Exp. no.	Run no.	Test liq.	Bubble dia.	Spore conc. $\times 10^{-7}/\text{ml}$	Mean particle dia. ( $\mu$ )	Geom. std. dev.	Particles per 1000 bubbles
(1)	(2)	(3)	(4)	(5)	(6)	(7)	(8)
69	1	P-400	1.1	0.08	8.2	1.67	84
69	2	P-400	1.1	0.17	7.8	1.73	165
69	3	P-400	1.1	0.33	8.5	1.74	243
69	4	P-400	1.1	0.66	7.0	1.50	322
69	5	P-400	1.1	0.99	6.9	1.59	384
69	6	P-400	1.1	2.0	6.3	1.56	430
70	1	P-400	2.2	0.08	7.9	1.57	137
70	2	P-400	2.2	0.17	7.4	1.57	279
70	3	P-400	2.2	0.33	7.2	1.56	353
70	4	P-400	2.2	0.66	7.2	1.60	389
70	5	P-400	2.2	0.99	6.4	1.56	407
70	6	P-400	2.2	2.0	6.0	1.60	502
71	1	P-400	0.5	0.17	4.4		28
71	2	P-400	0.5	0.33	4.3		83
71	3	P-400	0.5	0.66	4.7		146
71	4	P-400	0.5	0.99	5.5	1.36	229
71	5	P-400	0.5	2.0	5.5	1.46	356
71	6	P-400	0.5	3.3	5.2	1.46	392
72	1	P-400	0.9	0.17	6.1		26
72	2	P-400	0.9	0.33	5.7		73
72	3	P-400	0.9	0.66	6.5		93
72	4	P-400	0.9	0.99	5.5		132
72	5	P-400	0.9	2.0	5.4		183
72	6	P-400	0.9	3.3	5.4		233
74	1	A-25	0.9	3.3	4.1	1.78	117
74	2	DA-25	0.9	3.3	22.5	8.33	132
74	3	DM	0.9	3.3	3.2	1.60	121
75	1	DM	1.7	3.3	4.4	2.16	164
75	2	DA-25	1.7	3.3	6.6	1.97	335
75	3	A-25	1.7	3.3	3.4	1.71	278
76	1	DM	3.7	3.3	4.9	1.80	178
76	2	DA-25	3.7	3.3	4.2	2.10	179
76	3	A-25	3.7	3.3	4.4	1.86	358

Table 11. Summary of Data Computations (Continued)

Exp. no.	Run no.	Test liq.	Bubble dia.	Spore conc. $\times 10^{-7}/\text{ml}$	Mean particle dia. ( $\mu$ )	Geom. std. dev.	Particles per 1000 bubbles
(1)	(2)	(3)	(4)	(5)	(6)	(7)	(8)
77	1	DM	0.9	0.2	5.5	2.14	44
77	2	DM	0.9	0.4	5.2	2.06	89
77	3	DM	0.9	0.6	4.9	2.04	130
77	4	DM	0.9	0.8	4.6	1.87	142
77	5	DM	0.9	1.2	4.6	1.96	171
77	6	DM	0.9	1.8	4.1	1.95	201
78	1	DM	0.5	0.4	5.4	1.89	21
78	2	DM	0.5	0.8	5.4	1.89	70
78	3	DM	0.5	1.2	5.0	1.84	100
78	4	DM	0.5	1.8	5.0	1.72	114
78	5	DM	0.5	2.7	5.0	1.82	129
78	6	DM	0.5	3.6	4.6	1.85	131
79	1	S-400	0.9	0.2	7.3	2.17	32
79	2	S-400	0.9	0.4	7.3	2.35	62
79	3	S-400	0.9	0.6	7.5	2.27	93
79	4	S-400	0.9	0.8	8.0	2.30	96
79	5	S-400	0.9	1.2	8.0	2.42	126
79	6	S-400	0.9	1.8	7.4	2.32	151
80	1	S-400	0.5	0.4	7.8	2.39	19
80	2	S-400	0.5	0.8	8.0	2.25	40
80	3	S-400	0.5	1.2	7.8	2.31	63
80	4	S-400	0.5	1.8	7.5	2.48	80
80	5	S-400	0.5	2.7	7.6	2.63	81
80	6	S-400	0.5	3.6	6.7	2.50	106
81	1	S-400	2.2	0.05	5.9	1.98	116
81	2	S-400	2.2	0.1	5.3	1.82	225
81	3	S-400	2.2	0.2	4.6	1.83	313
81	4	S-400	2.2	0.4	4.4	1.86	332
81	5	S-400	2.2	0.6	4.0	1.98	380
81	6	S-400	2.2	0.8	3.8	1.95	397
82	1	DM	2.2	0.05	5.3	2.42	36
82	2	DM	2.2	0.1	4.1	2.32	55
82	3	DM	2.2	0.2	3.2	2.31	113
82	4	DM	2.2	0.4	3.0	2.33	130
82	5	DM	2.2	0.6	2.7	2.55	144
82	6	DM	2.2	0.8	2.6	2.50	149



Table 11. Summary of Data Computations (Continued)

Exp. no.	Run no.	Test liq.	Bubble dia.	Spore conc. $\times 10^{-7}/\text{ml}$	Mean particle dia. ( $\mu$ )	Geom. std. dev.	Particles per 1000 bubbles
(1)	(2)	(3)	(4)	(5)	(6)	(7)	(8)
83	1	DA-50	0.5	0.4	6.3		24
83	2	DA-50	0.5	0.8	6.3		50
83	3	DA-50	0.5	1.2	5.9		73
83	4	DA-50	0.5	1.8	5.4		94
83	5	DA-50	0.5	2.7	5.4		104
83	6	DA-50	0.5	3.6	5.0		116
84	1	DA-50	0.9	0.2	13.8		37
84	2	DA-50	0.9	0.4	13.2		75
84	3	DA-50	0.9	0.6	12.5		110
84	4	DA-50	0.9	0.8	12.0		125
84	5	DA-50	0.9	1.2	12.0		139
84	6	DA-50	0.9	1.8	11.3		147
85	1	DA-50	2.2	0.05	8.5	1.66	71
85	2	DA-50	2.2	0.1	7.4	1.82	104
85	3	DA-50	2.2	0.2	6.5	1.95	115
85	4	DA-50	2.2	0.4	5.8	2.09	149
85	5	DA-50	2.2	0.6	5.1	2.16	176
85	6	DA-50	2.2	0.8	4.7	2.22	184
86	1	A-50	0.5	0.4	6.2		20
86	2	A-50	0.5	0.8	5.4		35
86	3	A-50	0.5	1.2	5.3		49
86	4	A-50	0.5	1.8	5.2		59
86	5	A-50	0.5	2.7	5.0		66
86	6	A-50	0.5	3.6	4.8		71
87	1	A-50	0.9	0.2	7.0	1.89	28
87	2	A-50	0.9	0.4	6.0	1.82	51
87	3	A-50	0.9	0.6	5.8	1.81	66
87	4	A-50	0.9	0.8	5.5	1.75	76
87	5	A-50	0.9	1.2	5.2	1.73	86
87	6	A-50	0.9	1.8	4.8	1.81	99
88	1	A-50	2.2	0.05	5.1	1.57	61
88	2	A-50	2.2	0.1	4.6	1.52	111
88	3	A-50	2.2	0.2	4.3	1.56	137
88	4	A-50	2.2	0.4	3.9	1.62	154
88	5	A-50	2.2	0.6	3.8	1.60	162
88	6	A-50	2.2	0.8	3.5	1.66	182

Table 11. Summary of Data Computations (Continued)

Exp. no.	Run no.	Test liq.	Bubble dia.	Spore conc. $\times 10^{-7}/\text{ml}$	Mean particle dia. ( $\mu$ )	Geom. std. dev.	Particles per 1000 bubbles
(1)	(2)	(3)	(4)	(5)	(6)	(7)	(8)
89	1	PH-400	0.5	0.4	5.5	2.82	24
89	2	PH-400	0.5	0.8	5.9	2.41	48
89	3	PH-400	0.5	1.2	5.5	2.04	63
89	4	PH-400	0.5	1.8	4.6	2.46	76
89	5	PH-400	0.5	2.7	4.4	2.43	76
89	6	PH-400	0.5	3.6	4.2	2.45	88
90	1	PH-400	2.2	0.05	4.8	1.87	102
90	2	PH-400	2.2	0.1	4.2	1.90	147
90	3	PH-400	2.2	0.2	4.1	1.88	183
90	4	PH-400	2.2	0.4	3.7	1.95	207
90	5	PH-400	2.2	0.6	3.6	1.92	226
90	6	PH-400	2.2	0.8	3.6	1.92	246

## APPENDIX D

## BACKGROUND SAMPLE DATA

Table 12. Background Sample Data

Before Exp. no.	After Exp. no.	Date	Sampling time per sample (min)	Total Colonies per Sample		
				Dil. air only	Aeration w/o spores	Spores w/o aeration
(1)	(2)	(3)	(4)	(5)	(6)	(7)
1		8-19-65	20	0	0	
1		8-19-65	20	0	0	
	1	8-19-65	20	0	0	0
	4	8-26-65	5			0
	7	8-27-65	5			1
	8	9-8-65	5			2
	10	9-21-65	5			2
	11	9-22-65	5			0
	12	9-23-65	5			0
	13	9-24-65	5			2
	16	10-8-65	5			2
	17	10-8-65	5			0
18		10-9-65	10	0	0	0
	19	10-9-65	10			0
20		10-14-65	10	0	0	0
	21	10-14-65	10			1
22		10-15-65	10	0	0	0
	23	10-15-65	10			2
24		10-19-65	10	0	1	0
25		10-20-65	10	0	0	0
26		10-21-65	10	0	0	0
	27	10-21-65	10			1
28		11-16-65	10	1	0	0
	34	11-16-65	10			0
35		11-23-65	10	0	0	0
	36	11-23-65	10			2
37		11-24-65	10	0	0	0
	38	11-24-65	10			0
39		11-25-65	10	0	0	1
	42	11-25-65	10			0
47		12-4-65	10	0	0	0
	50	12-4-65	10			0
51		12-5-65	10	0	0	1
	52	12-5-65	10			0
53		12-6-65	10	1	0	0
	56	12-6-65	10			2
57		12-7-65	10	0	0	0
	60	12-7-65	10			0
61		1-26-66	10	0	0	0



Table 12. Background Sample Data (Continued)

Before Exp. no.	After Exp. no.	Date	Sampling time per sample (min)	Total Colonies per Sample		
				Dil. air only	Aeration w/o spores	Spores w/o aeration
(1)	(2)	(3)	(4)	(5)	(6)	(7)
	64	1-26-66	10			1
65		1-30-66	10	3	0	0
	67	1-30-66	10			0
68		2-3-66	10	0	2	2
	68	2-3-66	10			1
69		1-31-66	10	0	0	0
	70	1-31-66	10			0
71		2-3-66	10	0	0	0
	72	2-3-66	10			0
74		2-4-66	10	1	0	0
	76	2-4-66	10			0
77		2-5-66	10	1	0	1
	80	2-5-66	10			1
81		2-6-66	10	0	0	0
	84	2-6-66	10			1
85		2-7-66	10	0	0	0
	88	2-7-66	10			0
89		2-8-66	10	0	0	4
	90	2-8-66	10			0

APPENDIX E  
STATISTICAL COMPUTATIONS

### Verification of Poisson Distribution

All experimental sample data containing sufficient numbers of replicates were tested for randomness by chi square (75). A calculated chi square less than the critical chi square for a given degree of freedom and level of confidence indicates randomness at that level of confidence. The results presented in Table 13 below indicates randomness for the great majority of samples at the 95 per cent confidence limit ( $P=0.05$ ). That is, any observed differences in replicate sample data occurred by chance alone, accepting an error of five per cent. The Poisson distribution is thus verified.

$$\chi^2 = \sum (\bar{x} - x)^2 / \bar{x}$$

Where:

$$\chi^2 = \text{chi square}$$

$$x = \text{sample count}$$

$$\bar{x} = \text{mean sample count.}$$

Table 13. Chi Square Verification of Poisson Distribution

Exp. no.	Run no.	No. of Replicates	Average corrected no. of colonies per replicate	Degrees of freedom	Chi square	Critical values of chi square  P = 0.05
(1)	(2)	(3)	(4)	(5)	(6)	(7)
10	1	5	306	3	1.32	7.82
10	2	5	97	3	0.28	7.82
10	3	5	540	3	1.24	7.82
10	4	5	190	3	1.19	7.82
11	1	3	282	1	0.90	3.84
11	3	5	320	3	3.09	7.28
12	3	5	439	3	10.76	7.82
12	4	5	330	3	5.51	7.82
13	3	5	395	3	3.00	7.82
13	4	5	203	3	1.65	7.82
15	1	5	120	3	2.21	7.82
15	2	4	238	2	4.10	5.99
15	3	3	256	1	0.95	3.84
16	1	3	166	1	0.73	3.84
16	2	3	275	1	0.07	3.84
16	3	3	400	1	0.91	3.84
17	1	3	121	1	0.60	3.84
17	2	3	230	1	1.57	3.84
17	3	3	224	1	2.29	3.84
18	1	5	94	3	5.52	7.82
18	2	5	166	3	3.06	7.82
18	3	5	150	3	0.76	7.82
19	1	5	84	3	1.63	7.82
19	2	5	95	3	4.21	7.82
19	3	5	65	3	1.09	7.82
20	1	5	114	3	5.50	7.82
20	3	5	68	3	2.28	7.82



Table 13. Chi Square Verification of Poisson Distribution  
(Continued)

Exp. no.	Run no.	No. of Replicates	Average corrected no. of colonies per replicate	Degrees of freedom	Chi square	Critical values of chi square  P = 0.05
(1)	(2)	(3)	(4)	(5)	(6)	(7)
21	1	5	245	3	1.73	7.82
21	2	5	1250	3	1.05	7.82
21	3	5	251	3	7.71	7.82
23	1	5	165	3	0.30	7.82
23	2	5	183	3	3.36	7.82
24	1	5	846	3	3.70	7.82
24	2	5	1060	3	8.13	7.82
24	3	5	448	3	6.88	7.82
25	1	5	253	3	7.28	7.82
25	2	5	600	3	0.43	7.82
25	3	5	437	3	3.23	7.82
25	4	5	281	3	0.81	7.82
26	1	5	58	3	1.19	7.82
26	2	5	119	3	2.10	7.82
26	3	5	264	3	2.80	7.82
26	4	5	297	3	1.98	7.82
27	1	5	170	3	1.49	7.82
27	2	4	327	2	0.64	5.99
27	3	5	463	3	1.44	7.82
27	4	3	486	1	0.92	3.84
29	1	5	198	3	1.85	7.82
29	2	5	764	3	5.10	7.82
29	3	5	224	3	0.33	7.82
29	4	5	500	3	2.87	7.82
29	5	5	210	3	0.81	7.82

### Analysis of Variance

Analysis of Variance was performed on data used to prepare Figures 19, 20, and 21 in order to determine the significance of trends noted in the data and displayed in the Figures. The following symbols are utilized in presenting the analyses reported in the following three sections.

DF = Degrees of Freedom

F = Variance Ratio

MS = mean square (Variance Estimate)

N = total number of items

$N_m$  = number of items in a particular sample

SS = sum of squares =  $\sum x^2 - T^2/N$

T =  $\sum x$ , the grand total

$T_m$  =  $\sum x_m$ , the total for a particular sample

x = any item

#### Analysis of Variance: Ratio of Mean Bioparticle Size to Mean Size for 0.5 mm Bubbles versus Bubble Diameter (See Figure 19)

Applicable Experiments: 10-11, 15-27, 30-34, 39-42, 47-72, 77-90.

Table 14. Statistical Data:  $D_a/D_{a_{0.5}}$  vs.  $D_b$

$D_b$ (mm)	0.5	0.9	1.1	2.2	3.7	5.7
$N_m$	35	30	22	35	19	3
$\sum x^2$	35.0000	59.7958	32.4991	32.0636	12.7772	1.2062

Table 14. Statistical Data:  $D_a/D_{a_{0.5}}$  vs.  $D_b$  (Continued)

$D_b$ (mm)	0.5	0.9	1.1	2.2	3.7	5.7
$T_m$	35.00	37.62	25.83	32.00	14.96	1.88
$T_m^2$	1225.0000	1415.2644	667.1889	1024.0000	223.8016	3.5344
$T_m^2/N_m$	35.0000	47.1755	30.1755	29.2571	11.7790	1.1781

Note:  $x = D_a/D_{a_{0.5}}$

$$\begin{aligned}
 \Sigma N_m &= N = 144 \\
 \Sigma T_m &= T = 147.29 \\
 T^2 &= 21,694.3441 \\
 T^2/N &= 150.6552 \\
 \Sigma (T_m^2/N_m) &= 154.7165 \\
 \Sigma x^2 &= 173.3419
 \end{aligned}$$

Table 15. Analysis of Variance:  $D_a/D_{a_{0.5}}$  vs.  $D_b$ 

Source	SS	DF	MS
Bubble Size	$(\Sigma T_m^2/N_m) - (T^2/N) = 16.9259$	5	3.3852
Error	$(\Sigma x^2) - (\Sigma T_m^2/N_m) = 110.5692$	138	0.8012
Total	$(\Sigma x^2) - (T^2/N) = 127.4951$	143	

The Variance Ratio,  $F = 3.3852/0.8012 = 4.225$ .

The critical values of F for 5 and 138 degrees of freedom are 2.21 for  $P = 0.05$  and 3.02 for  $P = 0.01$ . A value of F as large as 4.225 will occur by chance less frequently than one per cent of the time. Therefore, for a confidence limit of 99 per cent, the variation with bubble size of the ratio of mean bioparticle size to mean size for 0.5 mm bubbles is significant.

Analysis of Variance: Ratio of Bioparticle Production Rate to  
Production Rate for 0.5 mm Bubbles versus Bubble Diameter  
 (See Figure 20)

Applicable Experiments: 10-11, 15-27, 30-34, 39-42, 47-72, 77-90.

Table 16. Statistical Data: (No. Bioparticles/Bubble)/  
 (No. Bioparticles/0.5 mm Bubble) vs.  $D_b$

$D_b$ (mm)	0.5	0.9	1.1	2.2	3.7	5.7
$N_m$	35	30	22	35	19	3
$\Sigma x^2$	35.0000	59.7958	32.4991	32.0636	12.7772	1.2062
$T_m$	35.0	37.62	35.83	32.00	14.96	1.88
$T_m^2$	1225.0000	1415.2644	667.1889	1024.0000	223.8016	3.5344
$T_m^2/N_m$	35.0000	47.1755	30.3268	29.2571	11.7790	1.1781

Note:  $x = (\text{No. Bioparticles/Bubble})/(\text{No. Bioparticles/0.5 mm Bubble})$

$$\begin{aligned}\Sigma N_m &= N = 144 \\ \Sigma T_m &= T = 147.2900 \\ T^2 &= 21,694.3441 \\ T^2/N &= 150.6552\end{aligned}$$



$$\Sigma (T_m^2/N_m) = 154.7165$$

$$\Sigma x^2 = 173.3419$$

Table 17. Analysis of Variance: (No. Bioparticles/Bubble)/  
(No. Bioparticles/0.5 mm Bubble) vs.  $D_b$

Source	SS	DF	MS
Bubble Size	$(\Sigma T_m^2/N_m) - (T^2/N) = 4.0613$	5	0.8123
Error	$(\Sigma x^2) - (\Sigma T_m^2/N_m) = 18.6254$	138	0.1350
Total	$(\Sigma x^2) - (T^2/N) = 22.6867$	143	

The Variance Ratio,  $F = 0.8123/0.1350 = 6.017$ .

The critical values of F for 5 and 138 degrees of freedom are 2.21 for  $P = 0.05$  and 3.02 for  $P = 0.01$ . A value of F as large as 6.017 will occur by chance less frequently than one per cent of the time. Therefore, for a confidence limit of 99 per cent, the observed variation with bubble size of the ratio of bioparticle production rate to production rate for 0.5 mm bubbles is significant.

Analysis of Variance: Ratio of Bioparticle Dispersion  
to Dispersion for 0.5 mm Bubbles versus Bubble Diameter  
(See Figure 21)

Applicable Experiments: 10-11, 15-27, 30-34, 39-42, 47-72, 77-90.

Table 18. Statistical Data:  $\sigma_g/\sigma_{g_{0.5}}$  vs.  $D_b$ 

$D_b$ (mm)	0.5	0.9	1.1	2.2	3.7	5.7
$N_m$	35	26	20	33	19	3
$\Sigma x^2$	35.0000	45.1682	42.3484	51.4911	30.5877	3.7606
$T_m$	35.00	30.52	25.36	38.77	22.01	3.32
$T_m^2$	1225.0000	931.4704	643.1296	1503.1129	484.4401	11.0224
$T_m^2/N_m$	35.0000	35.8258	32.1565	45.5489	25.4968	3.6741

Note:  $x = \sigma_g/\sigma_{g_{0.5}}$

$$\begin{aligned}
 \Sigma N_m &= N = 136 \\
 \Sigma T_m &= T = 154.98 \\
 T^2 &= 24,018.8004 \\
 T^2/N &= 176.6088 \\
 \Sigma (T_m^2/N_m) &= 177.7021 \\
 \Sigma x^2 &= 208.3560
 \end{aligned}$$

Table 19. Analysis of Variance:  $\sigma_g/\sigma_{g_{0.5}}$  vs.  $D_b$ 

Source	SS	DF	MS
Bubble Size	$(\Sigma T_m^2/N_m) - (T^2/N) = 1.0133$	5	0.2027
Error	$(\Sigma x^2) - (\Sigma T_m^2/N_m) = 30.6539$	130	0.2358
Total	$(\Sigma x^2) - (T^2/N) = 31.6672$	135	

The Variance Ratio,  $F = 0.2027/0.2358 = 0.860$ .

The critical value of  $F$  for 5 and 130 degrees of freedom is 2.21 for  $P = 0.05$ . A value of  $F$  as small as 0.860 will occur by chance more frequently than five per cent of the time. Therefore, for a confidence limit of 95 per cent, the observed variation with bubble size of the ratio of bioparticle dispersion to dispersion for 0.5 mm bubbles represents a trend only. However, the bioparticle dispersion for 1.1 mm bubbles was observed to be significantly different from that for 0.5 mm bubbles at the 95 per cent confidence level as shown below.

For  $D_b$  (mm) = 0.5 and 1.1:

$$\begin{aligned}
 \sum N_m &= N = 50 \\
 \sum T_m &= T = 60.36 \\
 T^2 &= 3643.3296 \\
 T^2/N &= 66.2424 \\
 \sum (T_m^2/N_m) &= 67.1565 \\
 \sum x^2 &= 77.3484
 \end{aligned}$$

Table 20. Analysis of Variance:  $\sigma_g/\sigma_{g_{0.5}}$  vs.  $D_b$

for  $D_b$  = 1.1 mm and 0.5 mm

Source	SS	DF	MS
Bubble Size	$(\sum T_m^2/N_m) - (T^2/N) = 0.9141$	1	0.9141
Error	$(\sum x^2) - (\sum T_m^2/N_m) = 10.1919$	53	0.1923
Total	$(\sum x^2) - (T^2/N) = 11.1060$	54	

The Variance Ratio,  $F = 0.9141/0.1923 = 4.754$ .

The critical value of  $F$  for 1 and 53 degrees of freedom is 4.02 for  $P = 0.05$ . A value of  $F$  as large as 4.754 will occur by chance less frequently than one per cent of the time. Therefore, for a confidence limit of 95 per cent, the observed variation with bubble size of the ratio of bioparticle dispersion to dispersion for 0.5 mm bubbles is significant for 0.5 mm and 1.1 mm bubbles.



## APPENDIX F

## MISCELLANEOUS DATA AND COMPUTATIONS

Test Liquid Surface Tension and Viscosity

Table 21. Surface Tension and Viscosity Measurements

Test liquid*	Temperature (°C)	Surface Tension *** (dynes/cm)	Viscosity**** (centipoise)
DM**	23	72.3	0.944
DM	23	70.9	0.935
S-100	23	71.6	0.933
S-400	23	72.3	0.930
S-1600	23	72.3	0.930
G-50	23	69.5	0.954
G-75	23	69.5	0.965
G-100	23	68.8	0.970
G-150	23	68.1	0.980
G-200	23	67.4	0.991
G-250	23	66.7	0.998
G-300	23	66.0	1.006
DA-25	23	71.6	0.945
DA-50	23	70.9	0.947
DA-100	23	69.5	0.948
A-25	23	72.3	0.958
A-50	23	71.6	0.964
A-100	23	70.9	0.970
P-200	23	69.5	0.964
P-400	23	67.4	0.972
PH-400	23	72.3	0.933

\*Spore concentration in aeration liquid was approximately  $7 \times 10^7$  per ml.

\*\*Contained no spores (reference).

\*\*\*Capillary - four determinations each.

\*\*\*\*Ostwald - four determinations each.

Table 22. Calculation of Initial Droplet Size Distribution

Stage no.	Mean biopart size( $D_a$ ) ( $\mu$ )	Solids ratio*	$D_{d_o}$ (2)X(3) ( $\mu$ )	$C_{spr}$ $\times 10^7$ /ml	$\frac{C_{spr}}{C_{sp}}$	Observed no. of biopart's per stage	Calc. no. of biopart's per stage (6)X(7)
(1)	(2)	(3)	(4)	(5)	(6)	(7)	(8)
E-57-3: Test liquid spore conc. = $1.6 \times 10^7$ /ml = $C_{sp}$							
5	2.2	6.95	15.3	53.3	33.3	7	233
4	3.8	6.95	26.4	10.4	6.5	9	59
3	6.2	6.95	43.1	2.38	1.49	415	618
2	9.8	6.95	68.1	0.60	1.00	1083	1083
1					1.00	167	167
E-26-2: Test liquid spore conc. = $3.0 \times 10^6$ /ml = $C_{sp}$							
5	2.2	6.95	15.3	53.3	178	5	890
4	3.8	6.95	26.4	10.4	34.6	6	208
3	6.2	6.95	43.1	2.38	7.93	26	206
2	9.8	6.95	68.1	0.60	2.00	306	712
1					1.00	249	249
E-59-3: Test liquid spore conc. = $4.1 \times 10^6$ /ml = $C_{sp}$							
5	2.2	7.66	16.9	39.5	96.4	39	3750
4	3.8	7.66	29.1	7.75	18.9	40	756
3	6.2	7.66	47.5	1.78	4.35	83	361
2	9.8	7.66	75.0	0.45	1.10	511	563
1					1.00	859	859
E-60-4: Test liquid spore conc. = $2.0 \times 10^6$ /ml = $C_{sp}$							
5	2.2	9.60	21.2	20.0	100	27	2700
4	3.8	9.60	36.5	3.93	19.7	32	630
3	6.2	9.60	59.5	0.91	4.55	165	750
2	9.8	9.60	94.0	0.23	1.15	433	499
1					1.00	742	742

\*Solids ratio = observed initial droplet CMD/observed bioparticle CMD:  
See column (7) Table 6.

Symbols used in Table 22 are as follows:

$D_{d_o}$  = initial droplet diameter

$C_{spr}$  = test liquid spore concentration required to provide one spore per droplet size  $D_{d_o}$  :  $C_{spr} = 6/\pi D_a^3$

$C_{sp}$  = Test liquid spore concentration.



## LITERATURE CITED

- (1) Wells, W.F., Airborne Contagion and Air Hygiene, Harvard University Press, Cambridge, Massachusetts (1955).
- (2) Gregory, P.H., The Microbiology of the Atmosphere, Interscience Publishers, New York (1961).
- (3) Langmuir, A.D., "Airborne Infection: How Important for Public Health? I. A. Historical Review" American Journal of Public Health, 54, 1666-1668 (1964).
- (4) Wells, W.F., "Apparatus for the Study of the Bacterial Behavior of Air", American Journal of Public Health, 23, 58-59 (1933).
- (5) Wells, W.F., "On Air-borne Infection: Study II. Droplets and Droplet Nuclei," American Journal of Hygiene, 20, 611-618 (1934).
- (6) Wells, W.F., and Stone, W.R., "On Air-borne Infection: Study III. Viability of Droplet Nuclei Infection," American Journal of Hygiene, 20, 619-627 (1934).
- (7) Wells, W.F., "Air-borne Infection and Sanitary Air Control," Journal of Industrial Hygiene, 17, 253-257 (1935).
- (8) Wells, W.F., and Fair, G.M., "Viability of B. Coli Exposed to Ultra-Violet Radiation in Air," Science, 82, 280-281 (1935).
- (9) Wells, W.F., and Brown, H.W., "Recovery of Influenza Virus Suspended in Air and Its Destruction by Ultra-Violet Radiation," American Journal of Hygiene, 24, 407-413 (1936).
- (10) Wells, W.F., and Riley, E.C., "An Investigation of the Bacterial Contamination of the Air of Textile Mills with Special Reference to the Influence of Artificial Humidification," Journal of Industrial Hygiene and Toxicology, 19, 513-561 (1937).
- (11) Wells, W.F., and Zappososid, P., "The Effect of Humidity on Beta Streptococci (Group C) Atomized into Air," Science, 96, 277-278 (1942).
- (12) Langmuir, A.D., "Epidemiology of Airborne Infection," Bacteriological Reviews, 25, 173-181 (1961).
- (13) Steere, N.V., Handbook of Laboratory Safety, The Chemical Rubber Co., (1967).

- (14) Tyndall, J., Floating Matter of the Air, 2nd. Edition, Longmans, Green and Co., London (1883).
- (15) Horrocks, W.H., "Experiments to Determine the Conditions Under Which Specific Bacteria Derived from Sewage may be Present in the Air of Ventilating Pipes, Drains, Inspection Chambers and Sewers," Proceedings of the Royal Society of London, Series B, 79, 236 (1907).
- (16) Riley, R.L., and O'Grady, F., Airborne Infection, McMillan, New York (1961).
- (17) Fair, G.M., and Wells, W.F., "Measurement of Atmospheric Pollution and Contamination by Sewage Treatment Works, " Proceedings of the Nineteenth Annual Meeting of the New Jersey Sewage Works Association (1934).
- (18) Albrecht, C.R., Bacterial Air Pollution Associated with the Sewage Treatment Process, M.S. Thesis, University of Florida (1958).
- (19) Jensen, K.E., "Presence and Destruction of Tubercle Bacilli in Sewage," Bulletin of World Health Organization, 10, 171 (1954).
- (20) Gravelle, C.R., and Chin, T.D.Y., "Enterovirus Isolations from Sewage: A Comparison of Three Methods," Journal of Infectious Diseases, 109, 205-209 (1961).
- (21) Kabler, P., "Removal of Pathogenic Microorganisms by Sewage Treatment Processes," Sewage and Industrial Wastes, 31, 1373-1382 (1959).
- (22) Dixon, F.R., and McCabe, L.J., "Health Aspects of Wastewater Treatment," Journal Water Pollution Control Federation, 36, 984-989, (1964).
- (23) Woodcock, A.H., "Bursting Bubbles and Air Pollution," Sewage and Industrial Wastes, 27, 1189 (1955).
- (24) Higgins, F.B., Jr., Bacterial Aerosols from Bursting Bubbles, PhD Thesis, Georgia Institute of Technology (1964).
- (25) Ledbetter, J.O., and Randall, C.W., "Bacterial Emissions from Activated Sludge Units," Industrial Medicine and Surgery, 34, 130-133 (1965).
- (26) Randall, C.W., and Ledbetter, J.O., "Bacterial Air Pollution from Activated Sludge Units," American Industrial Hygiene Conference, Pittsburgh, May 16-20 (1966).
- (27) Ledbetter, J.O., "Air Pollution from Wastewater Treatment," Water and Sewage Works, No. 2 (1966).

- (28) Randall, C.W., and Ledbetter, J.O., "Bacterial Air Pollution from Activated Sludge Units," American Industrial Hygiene Association Journal, 27, 506-519 (1966).
- (29) Decker, H.M., and Wilson, M.E., "A Slit Sampler for Collecting Airborne Microorganisms," Applied Microbiology, 2, 267-269 (1954).
- (30) Sampling Microbiological Aerosols, Public Health Monograph No. 60, U.S. Public Health Service, U.S. Government Printing Office (1959).
- (31) Andersen, A.A., "New Sampler for the Collection, Sizing, and Enumeration of Viable Airborne Particles," Journal of Bacteriology, 76, 471-484 (1958).
- (32) Stuhlman, O., "The Mechanics of Effervescence," Physics, 2, 457-466 (1932).
- (33) Newitt, D.M., Dombrowski, N., and Knelman, F.H., "Liquid Entrainment, 1. The Mechanism of Drop Formation from Gas or Vapour Bubbles," Transactions of Institute of Chemical Engineers, 32, 244-261 (1954).
- (34) Laplace, P.S., Mecanique Celeste, supplement 10 Vol. (1806).
- (35) Kientzler, C.F., Arons, A.B., Blanchard, A.H., Woodcock, A.H., "Photographic Investigation of the Projection of Droplets by Bubbles Bursting at a Water Surface," Tellus, 6, 1-7 (1954).
- (36) Facy, L., "Embruns et Noyqun de Condensation," Journal Scientifique de la Meteorologic, 3, 62-68 (1951).
- (37) Facy, L., "Eclatement des Lames Mincer et Noyaux de Condensation," Journal Scientifique de la Meteorologic, 3, 86-98 (1951).
- (38) Worthington, A.M., Study of Splashes, Longmans (1908).
- (39) Worthington, A.M., and Cole, R.S., "Impact with a Liquid Surface Studied by the Aid of Instantaneous Photography," Philosophical Transactions of the Royal Society, A, 194, 175-200 (1900).
- (40) Worthington, A.M., A Study of Splashes, MacMillan Co. (1963).
- (41) Plateau, J., "Statique, Experimentale et Theorique des Liquids Sournies aux Seules Forces Molecularies," Gent (1873).
- (42) Rayleigh, Lord, "On the Instability of Jets," Proceedings of the London Mathematical Society, 10, 4-13 (1878).
- (43) Orr, Clyde, Jr., Particulate Technology, MacMillan, New York (1966).



- (44) Dombrowski, N., and Frazer, R.P., "A Photographic Investigation into the Disintegration of Liquid Sheets," Philosophical Transactions of the Royal Society, 247, 101-130 (1954).
- (45) Moore, D.J., and Mason, B.J., "The Concentration, Size Distribution and Production Rate of Large Salt Nuclei Over the Oceans," Journal of the Royal Meteorological Society, 80, 583 (1954).
- (46) Mason, B.J., "Bursting of Bubbles at the Surface of Sea Water," Nature, 174, 470 (1954).
- (47) DeOme, K.B., "The Effect of Temperature, Humidity, and Glycol Vapor on the Viability of Airborne Bacteria," American Journal of Hygiene, 40, 239-250 (1944).
- (48) Kethley, T.W., Fincher, E.L., and Cown, W.B., "A System for the Evaluation of Aerial Disinfectants," Applied Microbiology, 4, 237-243 (1956).
- (49) Kethley, T.W., Cown, W.B., and Fincher, E.L., "The Nature and Composition of Experimental Bacterial Aerosols," Applied Microbiology 5, 1-8 (1957).
- (50) Fincher, E.L., Kethley, T.W., and Cown, W.B., "Variations in the Aerial Viability Associated with Variation in Morphology of Color Variants of Serratia marcescens," Applied Microbiology, 5, 131-135 (1957).
- (51) Irani, R.R., and Callis, C.F., Particle Size: Measurement, Interpretation, and Application, John Wiley and Sons, Inc., New York (1963).
- (52) Perry, J.H., Chemical Engineers Handbook, McGraw-Hill Book Co., Inc., New York (1963).
- (53) Rouse, H., Engineering Hydraulics, John Wiley and Sons, Inc., New York (1964).
- (54) Houghton, H.G., "A Study of the Evaporation of Small Water Drops," Physics, 4, 419-424 (1933).
- (55) Goldstein, S., Modern Developments in Fluid Dynamics, Oxford Press, London, 1 (1950).
- (56) Smail, L.L., Calculus, Appleton-Century-Crofts, Inc., New York (1949).
- (57) List, R.J., Smithsonian Meteorological Tables, 6th ed., Smithsonian Institution, Washington, D.C., 394-399 (1951).



- (58) Kinzer, G.D., and Gunn, R., "The Evaporation, Temperature and Thermal Relaxation - Time of Freely Falling Water Drops," Journal of Meteorology, 8, 71-83 (1951).
- (59) Van Zoonen, D., "Measurements of Diffusional Phenomena and Velocity Profiles in a Vertical Riser," Proceedings of the Symposium on the Interaction Between Fluids and Particles, Institution of Chemical Engineers, London (1962).
- (60) Bikerman, J.J., Foams: Theory and Industrial Applications, Reinhold Publishing Corp., New York (1953).
- (61) Brown, J.H., Cook, K.M., Ney, F.G., and Hatch, T., "Influence of Particle Size Upon the Retention of Particulate Matter in the Human Lung," American Journal of Public Health, 40, 450-459 (1950).
- (62) Kethley, T.W., Personal Communication (1965).
- (63) Miller, W.S., Scherff, R.A., Piepoli, C.R., and Idoine, L.S., "Physical Tracers for Bacterial Aerosols," Journal of Applied Microbiology, 9, 248-251 (1961).
- (64) Kethley, T.W., "Effect of Ventilation on Distribution of Airborne Microbial Contamination - Laboratory Studies," Surface Contamination, Pergamon Press, New York, N.Y., 271-278 (1967).
- (65) Bradley, D.E., and Franklin, J.G., "Electron Microscope Survey of the Surface Configuration of Spores of the Genus Bacillus," Journal of Bacteriology, 76, 618-630 (1958).
- (66) Fitz-James, P.C., and Young, I.E., "Comparison of Species and Varieties of the Genus Bacillus: Structure and Nucleic Acid Content of Spores," Journal of Bacteriology, 78, 743-754 (1959).
- (67) Harden, V.P., and Harris, J.O., "The Isoelectric Point of Bacterial Cells," Journal of Bacteriology, 65, 198-200 (1953).
- (68) Salle, A.J., Fundamental Principles of Bacteriology, 4th ed., McGraw-Hill Book Co., Inc., New York (1954).
- (69) Evans, F.R., and Curran, H.R., "Influence of Preheating, pH and Holding Temperature Upon Viability of Bacterial Spores Stored for Long Periods," Journal of Bacteriology, 79, 361-368 (1960).
- (70) Fleming, H.P., and Ordal, Z.J., "Responses of Bacillus subtilis Spores to Ionic Environments During Sporulation and Germination," Journal of Bacteriology, 88, 1529-1537 (1964).
- (71) Gaudin, A.M., Malar, A.L., and O'Conner, R.F., "Separation of Microorganisms by Flotation: II. Flotation of Spores of Bacillus subtilis var. niger," Journal of Applied Microbiology, 8, 91-97 (1960).

- (72) Weiser, H.B., Colloid Chemistry, John Wiley and Sons, Inc., New York, N.Y. (1949).
- (73) Harkins, W.D., and McLaughlin, "Dilute Electrolyte Solutions," Journal American Chemical Society, 47, 2083 (1925).
- (74) Findlay, A., Practical Physical Chemistry, Longmans, Green, and Co., New York, 72-88 (1937).
- (75) Goldstein, A., Biostatistics, The McMillan Co., New York, 117-125 (1964).
- (76) Kethley, T.W., Cown, W.B., and Fincher, E.L., "Adequate Expression for Average Particle Size of Microbiological Aerosols," Applied Microbiology, 11, 188-189 (1963).
- (77) Hatch, T.F., "Distribution and Deposition of Inhaled Particles in Respiratory Tract," Bacteriological Reviews, 25, 237-240 (1961).
- (78) Fair, G.M., and Geyer, J.C., Water Supply and Waste-Water Disposal, John Wiley and Sons, Inc., New York, N.Y. (1956).
- (79) Babbitt, H.E., and Baumann, E.R., Sewerage and Sewage Treatment, John Wiley and Sons, Inc., New York, N.Y. (1958).

## OTHER REFERENCES

1. Andersen, A.A., and Andersen, M.R., "A Monitor for Airborne Bacteria," Applied Microbiology, 10, 181-184 (1962).
2. Batchelor, H.W., "Aerosol Samplers," Advanced Applied Microbiology, 2, 31-64 (1960).
3. Bateman, J.B., McCaffrey, A., O'Conner, R.J., and Monk, G.W., "Relative Humidity and the Killing of Bacteria: The Survival of Damp Serratia marcescens in Air," Applied Microbiology, 9, 567-571 (1961).
4. Blanchard, D.C., "Bursting of Bubbles at an Air-Water Interface," Nature, 173, 1048 (1954).
5. Blanchard, C., "Electrified Droplets From the Bursting of Bubbles at an Air-Sea Water Interface," Nature, 175, 334 (1955).
6. Bourdillion, R.B., Lidwell, O.M., and Schuster, E., Studies in Air Hygiene, Medical Research Council Report No. 262 (1948).
7. Boyce, S.G., "Source of Atmospheric Salts," Science, 113, 620-621 (1951).
8. Boyles, W.A., and Lincoln, R.E., "Separation and Concentration of Bacterial Spores and Vegetative Cells by Flotation," Applied Microbiology, 6, 327-334 (1958).
9. Clarke, N.A., and Kabler, P.W., "Human Enteric Viruses in Sewage," Health Laboratory Science, 1, 44-50 (1964).
10. Cown, W.B., Kethley, T.W., and Fincher, E.L., "The Critical-Orifice Liquid Impinger as a Sampler for Bacterial Aerosols," Applied Microbiology, 5, 119-124 (1957).
11. Cox, C.S., "Protecting Agents and Their Mode of Action," Proceedings of the First International Symposium on Aerobiology, Berkley, California, 345-367 (1963).
12. Defay, R., and Prigogine, I., Surface Tension and Adsorption, John Wiley and Sons, New York (1966).
13. Dallaville, J.M., Micromeritics, 2 ed. Pitman Publishing Corp., New York (1948).



14. Dallavalle, J.M., Kethley, T.W., Cown, W.B., and Fincher, E.L., The Effect of Relative Humidity on Airborne Bacteria, Engineering Experiment Station, Georgia Institute of Technology, Atlanta, Georgia (1957).
15. Davis, C.N., Recent Advances in Aerosol Research, The MacMillan Co., New York (1964).
16. Davis, C.N., Aerosol Science, Academic Press, New York (1966).
17. Dimmick, R.L., "Factors Affecting Survival of Airborne Organisms: Effects of Buffer Concentration of Original Suspension of Bacteria and the Aerosol Chamber Temperature and Relative Humidity," Naval Biological Laboratory Twenty-Sixth Technical Progress Report, School of Public Health, University of California, Berkeley (1959).
18. Doyle, A.W., Smith, W.J., and Wiederhorn, N.M., The Collection, Monitoring and Identification of Particles in Gas Distribution Systems, American Gas Association, Inc., New York (1959).
19. DuBuy, H.G., Hollaender, A., and Lackey, M.D., "A Comparative Study of Sampling Devices for Air-Borne Micro-organisms," Public Health Reports, Supplement No. 184 (1945).
20. Dunkin, E.W., and Puck, T.T., "The Lethal Effect of Relative Humidity on Air-Borne Bacteria," Journal of Experimental Medicine, 87, 87-101 (1948).
21. Edward, D.B., Elford, W.J., and Laidlaw, P.P., "Air Borne Virus Infections," Journal of Hygiene, 1-10 (1943).
22. Fletcher, N.H., The Physics of Rainclouds, The University Press, Cambridge (1962).
23. Friedman, C.A., and Henry, B.S., "Bound Water Content of Vegetative and Spore Forms of Bacteria," Journal of Bacteriology, 65, 75 (1953).
24. Fuchs, N.A., Evaporation and Droplet Growth in Gaseous Media, Pergamon Press, New York (1959).
25. Gaudin, A.M., Flotation, 2nd ed., McGraw-Hill Book Co., Inc., New York (1957).
26. Gaudin, A.M., Nular, A.L., and O'Connor, R.F., "Separation of Microorganisms by Flotation: I. Development and Evaluation of Assay Procedures," Applied Microbiology, 8, 84-90 (1960).
27. Gregory, P.H., The Microbiology of the Atmosphere, Interscience Publishers, Inc., New York (1961).



28. Harper, G.J., Hood, A.M., and Morton, J.D., "Airborne Microorganisms: A Technique for Studying Their Survival," Journal of Hygiene, 56, 364-370 (1958).
29. Harper, G.J., "Airborne Microorganisms: Survival Tests with Four Viruses," Journal of Hygiene, 59, 479-486 (1961).
30. Henderson, D.W., "An Apparatus for the Study of Air-borne Infection," Journal of Hygiene, 50, 53-58 (1952).
31. Henry, B.S., and Friedman, C.A., "The Water Content of Bacterial Spores," Journal of Bacteriology, 33, 323 (1937).
32. Herdan, G., Small Particle Statistics, Elsevier Publishing Co., New York (1953).
33. Hill, W.F., and Cox, C.M., Bacterial Aerosol Sampler Evaluation, Wright Air Development Center, Technical Report, No. 59/27 (1959).
34. Hughes, R.R., and Gilliland, E.R., "The Mechanics of Drops," Chemical Engineering Progress, 48, 497-504 (1952).
35. Kethley, T.W., Fincher, E.L., and Cown, W.B., "The Effect of Sampling Method Upon the Apparent Response of Airborne Bacteria to Temperature and Relative Humidity," Journal of Infectious Diseases, 100, 97-102 (1957).
36. Knelman, F., Dombrowski, N., and Newitt, D.M., "Mechanism of the Bursting of Bubbles," Nature, 173 (1954).
37. Langmuir, I., "The Evaporation of Small Spheres," Physics Review, 12, 368-370 (1918).
38. Langmuir, I., "The Mechanism of the Surface Phenomena of Flotation," Transactions of the Faraday Society, 15, 62-74 (1920).
39. Lapple, C.E., and Shepherd, C.B., "Calculation of Particle Trajectories," Industrial and Engineering Chemistry, 32, 605-617 (1940).
40. Lepper, M.H., "Airborne Infection: How Important for Public Health? IV. Research Needed to Learn How to Cope with Airborne Infection," Journal of Public Health, 54, 1683-1688 (1964).
41. Levin, V., Clendenning, J.R., Gibor, A., and Bogar, F.D., "Harvesting of Algae by Froth Flotation," Applied Microbiology, 10, 169-175 (1962).
42. Lidwell, O.M., "Impaction Sampler for Size Grading Air-Borne Bacteria Carrying Particles," Journal of Scientific Instruments, 36, 3-8 (1959).

43. Loosli, C.G., Lemon, H.M., Robertson, O.H., and Appel, E., Experimental Air Borne Infection: II. Influence of Humidity on Survival of Virus in Air," Proceedings of Society of Experimental Biology and Medicine, 53, 205-206 (1943).
44. Malligo, J.E., and Idoine, L.S., "Single Stage Impaction Device for Particle Sizing Biological Aerosols," Applied Microbiology, 12, 32-26 (1964).
45. May, K.R., "The Cascade Impactor; An Instrument for Sampling Coarse Aerosols," Journal of Scientific Instruments, 22, 187-195
46. May, K.R., "Calibration of a Modified Andersen Bacterial Aerosol Sampler," Applied Microbiology, 12, 37-43 (1964).
47. Mudd, S., and Mudd, E.B.H., "Certain Interfacial Tension Relations and the Behavior of Bacteria in Films," Journal of Experimental Medicine, 40, 647-660 (1924).
48. National Academy of Sciences, "Conference on Airborne Infection," Bacteriological Review, 25, 173-382 (1961).
49. Nelson, R.Y., and Ledbetter, J.O., "Atmospheric Emissions from Oxidation Ponds," Journal of Air Pollution Control Association, 14, 50-52 (1964).
50. Nutt, C.W., "Froth Flotation: The Adhesion of Solid Particles to Flat Interfaces and Bubbles," Chemical Engineering Science, 12, 133-141 (1960).
51. Orr, C., and Dallavalle, J.M., Fine Particle Measurement, The MacMillan Co., New York (1959).
52. Ranz, W.E., and Wong, J.B., "Jet Impactors for Determining the Particle Size Distribution of Aerosols," AMA Archives of Industrial Hygiene and Occupational Medicine, 5, 364-477 (1952).
53. Richardson, E.G., (ed.), Aerodynamic Capture of Particles, Pergamon Press, New York (1960).
54. Rittenberg, S.C., "Investigations on the Microbiology of Marine Air," Journal of Marine Research, 2, 208 (1939).
55. Robertson, O.H., "Air-borne Infection," Science, 97, 495-502 (1943).
56. Rosebury, T., Experimental Air-borne Infection, The Williams and Wilkins Company (1947).
57. Ross, S., Chemistry and Physics of Interfaces, American Chemical Society, Washington, D.C., (1965).

58. Schweyer, H.E., and Work, L.T., "Methods for Determining Particle Size Distribution," Symposium on New Methods for Particle Size Determination in the Subsieve Range, ASTM, 1-22 (1941).
59. Shaffer, J.G., "Air-borne Infection: How Important for Public Health? III. Air-borne Infection in Hospitals," Journal of Public Health, 54, 1674-1682 (1964).
60. Sonkin, L.S., "Role of Particle Size in Experimental Air-borne Infection," American Journal of Hygiene, 53, 337-354 (1951).
61. Spendlove, C., "Utilization of Lung Clearance Rates to Determine Bacterial Aerosol Particle Deposition Patterns," Aerosols, Czechoslovak Academy of Sciences, Prague (1965).
62. Tyler, M.E., Shipe, E.L., and Painter, R.B., "Bacterial Aerosol Samplers: III. Comparison of Biological and Physical Effects in Liquid Impinger Samplers," Applied Microbiology, 7, 355-362 (1959).
63. U.S. Navy Laboratory Research Unit No. 1, "Air-borne Infections, A Review," War Medicine, 4, 1-30 (1943).
64. Webb, S.J., "Factors Affecting the Viability of Air-borne Bacteria: I. Bacteria Aerosolized from Distilled Water," Canadian Journal of Microbiology, 5, 649-669 (1959).
65. Wedum, A.G., "Air-borne Infection: How Important for Public Health? II. Air-borne Infection in the Laboratory," Journal of Public Health, 54, 1669-1673 (1964).
66. Wells, W.F., and Stone, W.R., "On Air-borne Infection: Study III. Viability of Droplet Nuclei Infection," American Journal of Hygiene, 20, 619-627 (1934).
67. Wells, W.F., "Air-borne Infection and Sanitary Air Control," Journal of Industrial Hygiene, 17, 253-257 (1935).
68. Wells, W.F., "An Apparatus for the Study of Experimental Air-borne Disease," Science, 91, 172-174 (1941).
69. Wells, W.F., Winslow, C.E.A., and Robertson, E.C., "Bacteriological Procedures in the Evaluation of Methods for Control of Airborne Infection," American Journal of Public Health, 36, 324 (1946).
70. Wolf, H.W., Skaliy, P., Hall, L.B., Harris, M.M., Decker, H.M., Buchanan, L.E., and Dahlgren, C.M., Sampling Microbiology Aerosols, U.S. Dept. of Health, Education, and Welfare, Public Health Monograph No. 60 (1959).
71. Wolfe, E.K., Jr., "Quantitative Characterization of Aerosols," Bacteriological Review, 25, 194-202 (1961).

72. Woodcock, A.H., "Note Concerning Human Respiratory Irritation Associated with High Concentrations of Plankton and Mass Mortality of Marine Organisms," Journal of Marine Research, 7, 56-62 (1948).
73. Woodcock, A.H., "Atmospheric Salt Particles and Raindrops," Journal of Meteorology, 9, 200-212 (1952).
74. Woodcock, A.H., Kientzler, C.F., Arons, A.B., and Blanchard, "Giant Condensation Nuclei from Bursting Bubbles," Nature, 172, 1144 (1953).



## VITA

Benjamin Michael Smith was born on August 26, 1936, in Gainesville, Georgia, where he subsequently received his primary and secondary education, and was granted a diploma from Gainesville High School in 1954. He enrolled at the Georgia Institute of Technology in 1954 and received the degrees Bachelor of Civil Engineering in 1958, and Master of Science in Sanitary Engineering in 1960. After serving three years with the U.S. Public Health Service, he returned to Georgia Tech in 1964 to complete his Doctoral studies. He is currently employed as a Research Sanitary Engineer with the National Center for Air Pollution Control, U.S. Public Health Service, and is conducting a joint U.S. Public Health Service - Atomic Energy Commission air pollution research project at the Oak Ridge National Laboratory, Oak Ridge, Tennessee. He is a member of the Society of Sigma Xi as well as Civil Engineering, Sanitary Engineering, and Health Physics professional organizations, and has authored papers on radiation contamination of water, x-radiation control, water pollution control, and gas-particle interactions.